CCI+ PHASE 1 – NEW ECVS
PERMAFROST

CCN1 & CCN2
ROCK GLACIER KINEMATICS AS NEW ASSOCIATED PARAMETER OF ECV PERMAFROST

D4.2 Climate Research Data Package

VERSION 1.0

22 DECEMBER 2020

PREPARED BY

b·geos
GAMMA REMOTE SENSING
West University of Timisoara
TERRASIGNA
NORCE
UNI FR
UNIVERSITÉ DE FRIBOURG
UNIVERSITÄT FREIBURG
UiO : University of Oslo
UNIS
The University Centre in Svalbard
AWI
Stockholm University

Document Status Sheet

Issue	Date	Details	Authors
1.0	22.12.2020	1st version for submission, includes version 1.0 of CCN1	A. Bertone, L. Rouyet, T. Strozzi, A. Kääb, R. Delaloye, A. Bartsch

Author team

Aldo Bertone, Chloé Barboux and Reynald Delaloye, UNIFR

Line Rouyet and Tom Rune Lauknes, NORCE

Andreas Kääb, GUIO

Hanne H. Christiansen, UNIS

Alexandru Onaca and Flavius Sirbu, WUT

Valentin Poncos, TERRASIGNA

Tazio Strozzi and Rafael Caduff, GAMMA

Annett Bartsch, B.GEOS

ESA Technical Officer:

Frank Martin Seifert

EUROPEAN SPACE AGENCY CONTRACT REPORT

The work described in this report was done under ESA contract. Responsibility for the contents resides in the authors or organizations that prepared it.

TABLE OF CONTENTS

Executive summary

The European Space Agency (ESA) Climate Change Initiative (CCI) is a global monitoring program that aims to provide long-term satellite-based products to serve the climate modelling and climate data user community. Permafrost has been selected as one of the Essential Climate Variables (ECVs) that are elaborated during Phase 1 of CCI+ (2018-2021). As part of the Permafrost_cci baseline project, ground temperature and active layer thickness were considered to be the primary variables that require climate-standard continuity as defined by the Global Climate Observing System (GCOS). Permafrost extent and zonation are secondary parameters, but of high interest to users. The ultimate objective of Permafrost_cci is to develop and deliver permafrost maps as ECV products primarily derived from satellite measurements. Algorithms have been identified, which can provide these parameters by ingesting a set of global satellite data products (Land Surface Temperature LST, Snow Water Equivalent SWE, and Landcover) in a permafrost model scheme that computes the ground thermal regime. Annual averages of ground temperature and annual maxima of thaw depth (active layer thickness) were provided at 1 km spatial resolution during Year 1&2 of Permafrost_cci. The data sets were created from the analysis of lower level data, resulting in gridded, gap-free products.

In periglacial mountain environments, the permafrost occurrence is patchy, and the preservation of permafrost is controlled by site-specific conditions. Three options of Permafrost_cci initiated within CCN1 and CCN2 address the need for additional regional cases in cooperation with dedicated users in characterizing mountain permafrost as local indicator for climate change and direct impact on the society in mountainous areas. CCN1 started in October 2018 and is led by a Romanian team focusing on case studies in the Carpathians. The specific objective of CCN1 is to develop and deliver maps and products for mountain permafrost, such as (i) rock glacier inventories, (ii) kinematic time series of selected rock glaciers and (iii) a permafrost distribution model, primarily derived from satellite measurements. CCN2 started in September 2019 and consists of two options led by Swiss and Norwegian teams focusing on the investigation and definition of a new associated ECV Permafrost product related to rock glacier kinematics. Early 2020, Rock Glacier Kinematics (RGK) has been proposed as a new product to the ECV Permafrost for the next GCOS Implementation Plan (IP). It would consist of a global dataset of surface velocity time series measured/computed on single rock glacier units. A proper rock glacier kinematics monitoring network, adapted to climate research needs, builds up a unique validation dataset of climate models for mountain regions, where direct permafrost (thermal state) measurements are very scarce or even lacking totally. CCN2 is working closely with the IPA (International Permafrost Association) Action Group Rock glacier inventories and kinematics, gathering about one hundred fifty members [RD-10 to RD-13]. Following the recommendations of this IPA Action Group, the overall goal of CCN2 is achieved through the development of two products: (i) regional kinematics-based rock glacier inventories and (ii) kinematic time series of selected rock glacier. User Requirements, Product Specifications and Data Access Requirements are described in D1.1-1.3 of CCN1-2 [RD-20 to RD-22]. Product Validation and Algorithm Selection, Algorithm Theoretical Basis, End-to-End ECV Uncertainty Budget, Algorithm Development Plan and Product Validation Plan are described in D2.1-2.5 of CCN1-2 [RD-23 to RD-27]. System Requirement, System Specification and the System Verification are described in D3.1-3.3 of CCN1-2 [RD-28].

The products required within CCN1 & CCN2 of the ESA CCI project for mountain permafrost regions include (i) regional rock glaciers inventories (RGI), (ii) selected rock glacier kinematic time series (RGK), and (iii) a mountain permafrost distribution model (MPDM) in the Romanian Carpathians.

Kinematics-based rock glacier inventories were generated by different CCI groups and external providers. Entirely new kinematics-based rock glacier inventories or updates / upgrades of existing inventories have been generated according to the standards defined by the IPA Action Group Rock glacier inventories and kinematics [RD-31 and RD-32] in different climatic regions:

- European Alpine sites: Western Alps (Switzerland), Ultental (Italy), Vanoise Massif (France);
- European subarctic/arctic sites: Troms, Finnmark (Northern Norway), Nordenskiöld Land (Svalbard);
- Extra-European sites: Disko Island (Greenland), Tien Shan (Kazakhstan-Kyrgyzstan), Brookes Range (Alaska), Central Andes (Argentina), Southern Alps (New Zeeland).

Kinematic time series (RGK) on selected rock glaciers in the Swiss Alps, Norway, Svalbard and Disko Island (Greenland) were produced mainly based on SAR data. In addition, trends in rock glaciers velocity from ALOS-2 PALSAR-2 and Sentinel-1 SAR interferometry were computed in the Romanian Carpathians.

The mountain permafrost distribution model (MPDM) product from CCN1 shows that permafrost distribution in the Southern Carpathians is patchy, being able to exist only under certain topographical conditions. It has an extent of, most likely, 3 km^2 (possibly between 0.1 km^2 to 7.74 km^2).

1 Introduction

1.1 Purpose of the document

The products required within CCN1 and CCN2 of the ESA CCI project for mountain permafrost regions include (i) regional kinematics-based rock glaciers inventories (RGI), (ii) kinematic time series (RGK) on selected rock glaciers, and (iii) a mountain permafrost distribution model (MPDM) in the Carpathians. The Climate Research Data Package (CRDP) describes the generated products in compliance with CCI Data standards.

1.2 Structure of the document

Section 2 provides an overview of the kinematics-based rock glaciers inventories generated by different CCI groups and external providers in different climatic regions.

Section 3 describes the kinematic time series (RGK) on selected rock glaciers, including the trends in rock glaciers velocity in the Romanian Carpathians.

Section 4 introduces the outcome of the permafrost distribution model at regional scale in the Romanian Carpathians.

1.3 Applicable documents

[AD-1] ESA 2017: Climate Change Initiative Extension (CCI+) Phase 1 – New Essential Climate Variables - Statement of Work. ESA-CCI-PRGM-EOPS-SW-17-0032

[AD-2] Requirements for monitoring of permafrost in polar regions - A community white paper in response to the WMO Polar Space Task Group (PSTG), Version 4, 2014-10-09. Austrian Polar Research Institute, Vienna, Austria, 20 pp

[AD-3] ECV 9 Permafrost: assessment report on available methodological standards and guides, 1 Nov 2009, GTOS-62

[AD-4] GCOS-200. 2016. The Global Observing System for Climate: Implementation Needs. GCOS Implementation Plan, WMO

[AD-5] GEO/CEOS Quality Assurance framework for Earth Observation (QA4EO) protocols 3-4

[AD-6] ESA Climate Change Initiative. CCI Project Guidelines. EOP-DTEX-EOPS-SW-10-0002

[AD-7] National Research Council. 2014. Opportunities to Use Remote Sensing in Understanding Permafrost and Related Ecological Characteristics: Report of a Workshop. Washington, DC: The National Academies Press. https://doi.org/10.17226/18711.

[AD-8] IPA Action Group "Specification of a Permafrost Reference Product in Succession of the IPA Map" (2016): Final report. https://ipa.arcticportal.org/images/stories/AG_reports/IPA_AG_SucessorMap_Final_2016.pdf

[AD-9] GlobPermafrost team (2017): Summary report from 3rd user Workshop. ESA DUE GlobPermafrost project. ZAMG, Vienna.

https://www.globpermafrost.info/cms/documents/reports/ESA_DUE_GlobPermafrost_workshop_summary_ACOP_v1_public.pdf

1.4 Reference Documents

[RD-1] A. Bartsch, H. Matthes, S. Westermann, B. Heim, C. Pellet, A. Onaca, C. Kroisleitner, T. Strozzi: ESA CCI+ Permafrost User Requirements Document (URD), v1.1 12 February 2019

[RD-2] A. Bartsch, S. Westermann, T. Strozzi, A. Wiesmann, C. Kroisleitner: ESA CCI+ Permafrost Product Specifications Document (PSD), v2.0 30 November 2019

[RD-3] A. Bartsch, S. Westermann, B. Heim, M. Wieczorek, C. Pellet, C. Barboux, C. Kroisleitner, T. Strozzi: ESA CCI+ Permafrost Data Access Requirements Document (DARD), v1.0 15 January 2019

[RD-4] A. Bartsch, S. Westermann, T. Strozzi: ESA CCI+ Permafrost Product Validation and Algorithm Selection Report (PVASR), v2.0 30 November 2019

[RD-5] S. Westermann, A. Bartsch, T. Strozzi: ESA CCI+ Permafrost Algorithm Theoretical Basis Document (ATBD), v2.0 30 November 2019

[RD-6] S. Westermann, A. Bartsch, B. A. Heim, T. Strozzi: ESA CCI+ Permafrost End-to-End ECV Uncertainty Budget (E3UB), v2.0 30 November 2019

[RD-7] S. Westermann, A. Bartsch, B. A. Heim, T. Strozzi: ESA CCI+ Permafrost Algorithm Development Plan (ADP), v2.0 30 November 2019

[RD-8] B. Heim, M. Wieczorek, C. Pellet, R. Delaloye, C. Barboux, S. Westermann, A. Bartsch, T. Strozzi: ESA CCI+ Permafrost Product Validation Plan (PVP), v2.0 30 November 2019

[RD-9] A. Wiesmann, A. Bartsch, S. Westermann, T. Strozzi: ESA CCI+ Permafrost System Requirement Document (SRD), v2.0 29 February 2020

[RD-10] A. Wiesmann, A. Bartsch, S. Westermann, T. Strozzi: ESA CCI+ Permafrost System Specification Document (SSD), v2.0 29 February 2020

[RD-11] A. Wiesmann, A. Bartsch, S. Westermann, T. Strozzi: ESA CCI+ Permafrost System Verification Report (SVR), v2.0 31 May 2020

[RD-12] B. Heim, M. Wieczorek, C. Pellet, R. Delaloye, A. Bartsch, D. Jakober, G. Pointner, T. Strozzi, GAMMA: ESA CCI+ Permafrost Product Validation and Intercomparison Rerport (PVIR), v2.0 30 September 2020

[RD-13] J. Obu, S. Westermann, T. Strozzi, A. Bartsch.: ESA CCI+ Permafrost Climate Research Data Package Version 1 (CRDPv1), v2.0 31 May 2020

[RD-14] A. Bartsch, J. Obu, S. Westermann, T. Strozzi: ESA CCI+ Permafrost Product User Guide (PUG), v2.0 27 May 2020

[RD-15] I. Nitze, G. Grosse, B. Heim, M. Wieczorek, H. Matthes, A. Bartsch, T. Strozzi: ESA CCI+ Permafrost Climate Assessment Report (CAR), v2.1 16 October 2020

[RD-16] T. Strozzi, A. Onaca, V. Poncos, F. Ardelean, A. Bartsch: ESA CCI+ Permafrost CCN1 D1. User Requirement, Product Specifications and Data Access Requirements Document, v1.0 15 February 2019

[RD-17] A. Onaca, F. Ardelean, F. Sirbu,V. Poncos, T. Strozzi, A. Bartsch: ESA CCI+ Permafrost CCN1 D2. Algorithm Development Document, v1.0 31 May 2019

[RD-18] A. Wiesmann, T. Strozzi, A. Onaca, F. Sîrbu, A. Bartsch: ESA CCI+ Permafrost CCN1 D3. System Development Document, v1.0 30 September 2019

[RD-19] F. Sîrbu, A. Onaca, V. Poncos, T. Strozzi, A. Bartsch: ESA CCI+ Permafrost CCN1 D3. Product Generation and Validation Document, v1.0 30 April 2020

[RD-20] C. Barboux, A. Bertone, R. Delaloye, A. Onaca, F. Ardelean, V. Poncos, A. Kääb, L. Rouyet, H. H. Christiansen, T. Strozzi, A. Bartsch: ESA CCI+ Permafrost. CCN1 & CCN2 Rock Glacier Kinematics as New Associated Parameter of ECV Permafrost. D1.1 User Requirement Document (URD), v1.0 30 November 2019

[RD-21] C. Barboux, A. Bertone, R. Delaloye, A. Onaca, F. Ardelean, V. Poncos, A. Kääb, L. Rouyet, H. H. Christiansen, T. Strozzi, A. Bartsch: ESA CCI+ Permafrost. CCN1 & CCN2 Rock Glacier Kinematics as New Associated Parameter of ECV Permafrost. D1.2 Product Specification Document (PSD), v1.0 30 November 2019

[RD-22] C. Barboux, A. Bertone, R. Delaloye, A. Onaca, F. Ardelean, V. Poncos, A. Kääb, L. Rouyet, H. H. Christiansen, T. Strozzi, A. Bartsch: ESA CCI+ Permafrost. CCN1 & CCN2 Rock Glacier Kinematics as New Associated Parameter of ECV Permafrost. D1.3 Data Access Requirement Document (DARD), v1.0 30 November 2019

[RD-23] L. Rouyet, T. R. Lauknes, C. Barboux, A. Bertone, R. Delaloye, A. Kääb, H. H. Christiansen, A. Onaca, F. Sirbu, V. Poncos, T. Strozzi, A, Bartsch: ESA CCI+ Permafrost. CCN1 & CCN2 Rock Glacier Kinematics as New Associated Parameter of ECV Permafrost. D2.1 Product Validation and Algorithm Selection Report (PVASR), v1.0 April 30, 2020

[RD-24] L. Rouyet, T. R. Lauknes, C. Barboux, A. Bertone, R. Delaloye, A. Kääb, H. H. Christiansen, A. Onaca, F. Sirbu, V. Poncos, T. Strozzi, A, Bartsch: ESA CCI+ Permafrost. CCN1 & CCN2 Rock Glacier Kinematics as New Associated Parameter of ECV Permafrost. D2.2 Algorithm Theoretical Basis Document (ATBD), v1.0 April 30, 2020

[RD-25] L. Rouyet, T. R. Lauknes, C. Barboux, A. Bertone, R. Delaloye, A. Kääb, H. H. Christiansen, A. Onaca, F. Sirbu, V. Poncos, T. Strozzi, A, Bartsch: ESA CCI+ Permafrost. CCN1 & CCN2 Rock Glacier Kinematics as New Associated Parameter of ECV Permafrost. D2.3 End-to-End ECV Uncertainty Budget (E3UB), v1.0 April 30, 2020

[RD-26] L. Rouyet, T. R. Lauknes, C. Barboux, A. Bertone, R. Delaloye, A. Kääb, H. H. Christiansen, A. Onaca, F. Sirbu, V. Poncos, T. Strozzi, A, Bartsch: ESA CCI+ Permafrost. CCN1 & CCN2 Rock Glacier Kinematics as New Associated Parameter of ECV Permafrost. D2.4 Algorithm Development Plan (ADP), v1.0 April 30, 2020

[RD-27] L. Rouyet , T. R. Lauknes, C. Barboux, A. Bertone, R. Delaloye, A. Kääb, H. H. Christiansen, A. Onaca, F. Sirbu, V. Poncos, T. Strozzi, A, Bartsch: ESA CCI+ Permafrost. CCN1 & CCN2 Rock Glacier Kinematics as New Associated Parameter of ECV Permafrost. D2.5 Product Validation Plan (PVP), v1.0 April 30, 2020

[RD-28] A. Wiesmann, R. Carduff, T. Strozzi, A. Onaca, F. Sirbu, V. Poncos and A. Bartsch, 2020: ESA CCI+ Permafrost. CCN1 & CCN2 Rock Glacier Kinematics as New Associated Parameter of ECV Permafrost. D3 System Development Document (SSD), v1.0 30 November 2020

[RD-29] IPA Action Group Rock glacier inventories and kinematics, 2020. Towards standard guidelines for inventorying rock glaciers. Baseline concepts. Last version available on https://bigweb.unifr.ch/Science/Geosciences/Geomorphology/Pub/Website/IPA/CurrentVersion/Current_Baseline_Concepts_Inventorying_Rock_Glaciers.pdf

[RD-30] IPA Action Group Rock glacier inventories and kinematics, 2020. Kinematics as an optional attribute of standardized rock glacier inventories. Last version available on: https://bigweb.unifr.ch/Science/Geosciences/Geomorphology/Pub/Website/IPA/CurrentVersion/Current_KinematicalAttribute.pdf

[RD-31] IPA Action Group Rock glacier inventories and kinematics, 2020. Rock glaciers kinematics as an associated parameter of ECV Permafrost. Last version available on: https://bigweb.unifr.ch/Science/Geosciences/Geomorphology/Pub/Website/IPA/CurrentVersion/Current_RockGlacierKinematics.pdf

[RD-32] IPA Action Group Rock glacier inventories and kinematics, 2020. Response to GCOS ECV review – ECV Permafrost. ECV Product: Rock Glacier Kinematics. Available on: https://gcos.wmo.int/en/ecv-review-2020.

1.5 Bibliography

A complete bibliographic list that supports arguments or statements made within the current document is provided in Section 5.1.

1.6 Acronyms

A list of acronyms is provided in Section 5.2.

1.7 Glossary

A comprehensive glossary of terms relevant for the parameters addressed in Permafrost_cci is available as part of the User Requirement Documents of the baseline project [RD-1] and of CCN 1-2 [RD-16].

2 Regional Kinematics-based Rock Glaciers Inventories

2.1 Introduction

Entirely new kinematics-based rock glacier inventories or updates / upgrades of existing inventories were generated by different Permafrost_cci team members and external providers in different climatic regions. The tasks were carried out according to the standards defined by the IPA Action Group Rock glacier inventories and kinematics [RD-29 and RD-30]. These standards are described in the Algorithm Theoretical Basis Document (ATBD) [RD-24], including the theoretical background of the methods used to develop the products described in the CCN, and according to the Product Specification Document (PSD) [RD-21].

The climatic regions where entirely new rock glacier inventories were generated are listed below:

- European subarctic/arctic sites: Nordenskiöld Land (Svalbard);
- Extra-European sites: Southern Alps (New Zealand).

The climatic regions where the existing rock glacier inventories were updated/upgraded are listed below:

- European Alpine sites: Western Alps (Switzerland), Ultental (Italy), Vanoise Massif (France);
- European subarctic/arctic sites: Troms and Finnmark (Northern Norway);
- Extra-European sites: Disko Island (Greenland), Tien Shan (Kazakhstan-Kyrgyzstan), Brookes Range (Alaska), Central Andes (Argentina).

The rock glacier inventories of each climatic region are described below.

2.2 Regional rock glaciers inventories

2.2.1 Western Alps (Switzerland)

The Western Swiss Alps (Fig. 2.2.1.1) inventory covers an area of around 1500 km^2, and the region is called Bas-Valais. This mountain region is characterised by reliefs higher than 4000 meters, with five main valleys North-South oriented.

The latest geomorphological inventory covering the Western Swiss Alps relates to the GlobPermafrost project, completed in 2018. It includes several kinds of geomorphological landforms, such as rock glaciers, debris-covered glaciers, push-moraine, landslides, debris-mantled slopes and solifluction areas. This inventory was used to identify the rock glacier locations, and to collect the previous kinematic state of each rock glacier.

Interferograms from Sentinel-1 were computed from both Track 160 ASC and Track 138 DSC, between 2018 and 2019. Since the Western Swiss Alps are located in the northern hemisphere, only the images acquired between June and October (i.e. in the unfrozen summer periods) were used, in order to avoid the presence of snow cover. In detail, 17 interferograms were computed for the Track 160 ASC, 15 interferograms for the Track 138 ASC, using time intervals of 6, 12, 24, 48, 354 and 366 days.

The rock glacier identification was conducted using the Digital Terrain Model (DTM) and the Orthoimages of the Western Swiss Alps, both acquired in the period between 2017 and 2018, with a spatial resolution of 0.5 and 0.25 meters, respectively.
Based on InSAR, 677 moving areas related to rock glaciers were detected. Figure 2.2.1.2 contains the number of identified moving areas for each velocity class.
The identified rock glacier units with available kinematic information extracted from the previous moving areas are 619; 337 are simple units and 103 are composite landforms composed of 282 units. Figure 2.2.1.3 contains the number of the classified rock glacier units for each kinematic class.
Figure 2.2.1.1 shows the entire investigated region, with a focus on selected representative areas.
No particular problem related to the interferograms quality was detected, because the interferograms have been appropriately selected with the minimum noise level. However, some problems related to the properties of the investigated landforms (such as the dimensions, the location, and the kinematic behaviour) were identified. For some rock glaciers characterized by small size, it was difficult to identify the moving areas and assign velocity/kinematic attributes. Many rock glaciers were located in areas of foreshortening, layover or shadow for both acquisition geometries, and therefore it was not possible to assign a kinematic attribute for these rock glaciers (category “undefined”). Some rock glaciers characterised by a low velocity rate – around few centimetres per year – have been difficult to classify, because sometimes the annual interferograms were characterised by decorrelation around the rock glacier. For other rock glacier systems, the complexity of the detected moving areas – related to the same rock glacier system/unit – made it difficult to assign a reliable kinematic attribute.
The work on this climatic region was conducted by Aldo Bertone and Tania Monier.

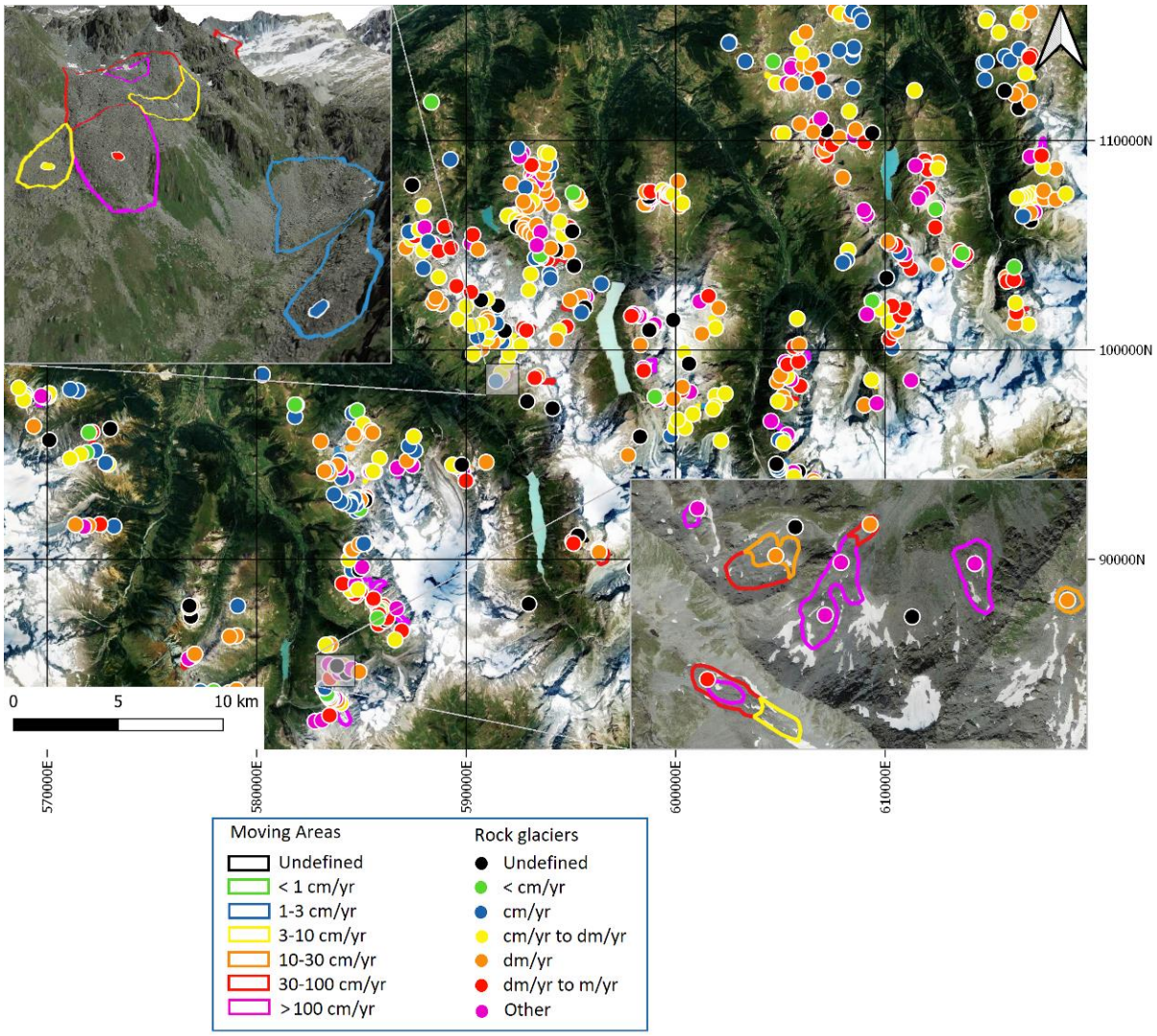

Figure 2.2.1.1: Example of the Western Swiss Alps inventory, with two panels zooming into representative detail areas.

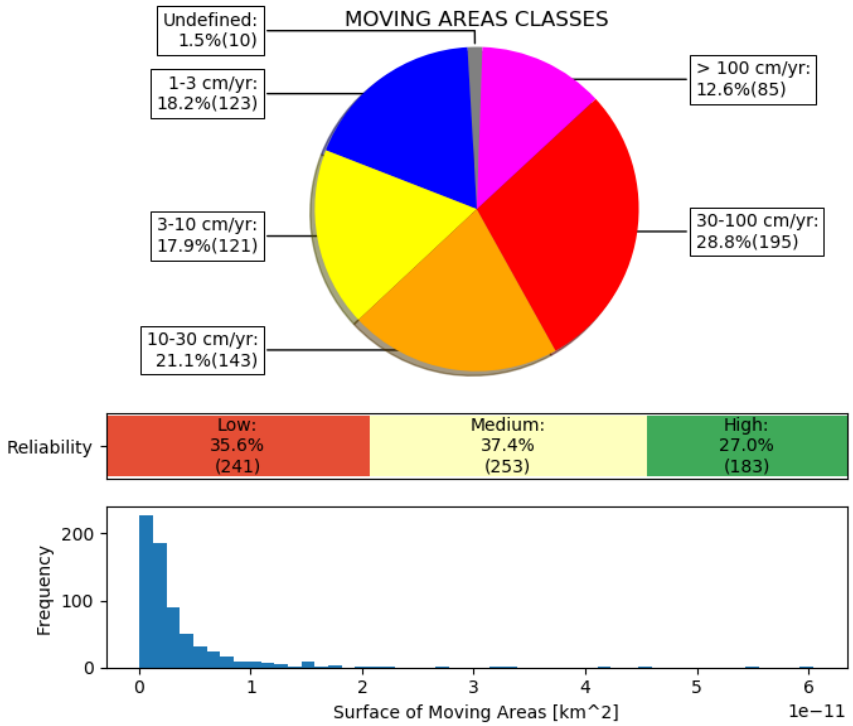

Figure 2.2.1.2: Western Alps (Switzerland) pie chart of the velocity classes of moving areas (upper part), horizontal bar of reliability of classified moving areas (central part), and histogram of the surface covered by moving areas (lower part).

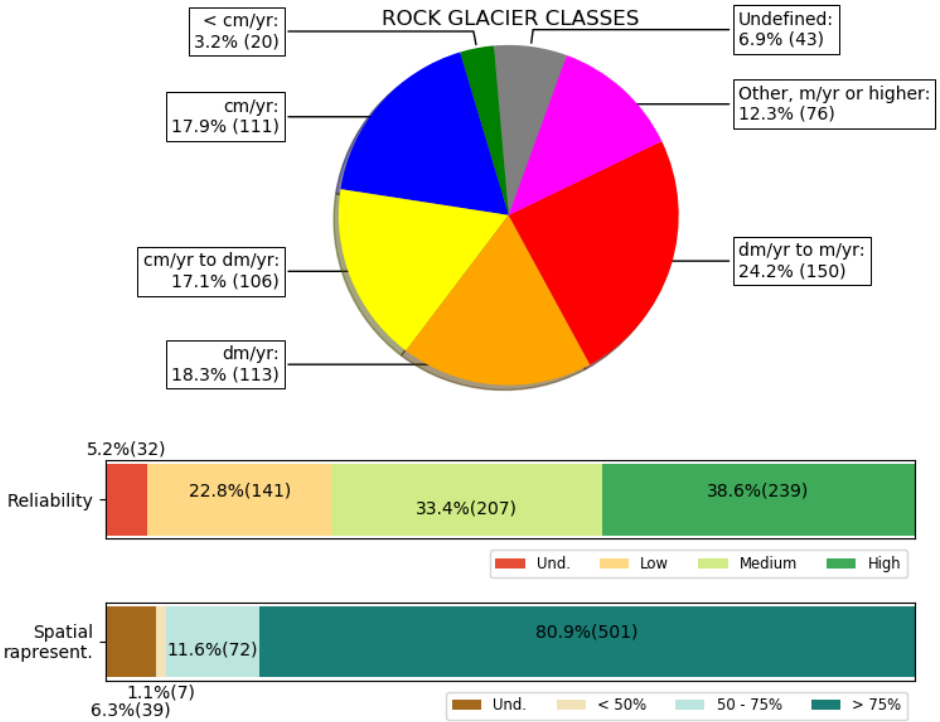

Figure. 2.2.1.3: Western Alps (Switzerland) pie chart of the kinematic classes of rock glaciers (upper part), horizontal bar of reliability of classified rock glaciers (central part), and horizontal bar of the spatial representativeness of classified rock glaciers (lower part).

2.2.2 Ultental (Italy)

The study area (Fig. 2.2.2.1) occupies the north-eastern portion of the Ortles-Cevedale massif in South Tyrol, Central-Eastern Italian Alps (46°31' N, 10°50' E). It covers about 970 km^2 and includes the southern side of lower Vinschgau (Val Venosta) as well as five tributary valleys: Ultental (Val d'Ultimo), Martelltal (Val Martello), Laasertal (Val di Lasa), and Suldental (Val di Solda). Elevation ranges from 3905 m on Mount Ortles, down to about 500 m at the Ultental outlet. Bedrock geology is dominated by metamorphic lithologies (chiefly paragneiss, micaschists, and orthogneiss), with granite outcropping locally in lower Martelltal, and limestones and dolostones in upper Suldental. Climate is dry, with mean annual precipitation ranging from less than 600 mm at the Vinschgau valley floor (Schlanders station) to more than 1200 mm in upland cirque valleys (Weissbrunn station). According to Permanet modelling (www.permanet.eu) and field-based evidence, discontinuous mountain permafrost roughly occurs above threshold elevations varying between 2300 and 2700 m a.s.l., depending on topographic (e.g., aspect) and microclimatic (site specific) conditions (Boeckli et al., 2012). In this context, rock glaciers are dominant geomorphic features above the present treeline. According to an unpublished regional inventory completed in September 2019 (publication under preparation), the study area hosts 781 rock glaciers, including 166 classified morphologically active, 152 inactive and 463 relicts.

Interferograms from Sentinel-1 were computed from both Tracks 117 ASC and 168 DSC between 2018 and 2019 as well as interferograms from ALOS-1 PALSAR-1 from Track ASC between 2007 and 2010. Since the study area is located in the Northern hemisphere, only images acquired between August and October (i.e., in the unfrozen summer periods) were used, in order to avoid snow cover at elevations below about 2900 m a.s.l. In particular, we processed respectively: (i) 14 interferograms for Track Sentinel-1 117 ASC, using time intervals of 6, 12, 24, 30, 42, 330 and 342 days; (ii) 18 interferograms for Track Sentinel-1 168 DSC using time intervals of 6, 12, 24, 36 and 342 days; and (iii) 3 interferograms for ALOS-1 PALSAR-1 using time intervals of 46, 966 and 1012 days.

The rock glacier identification was conducted using the LiDAR Digital Terrain Model (DTM) of the Autonomous Province of Bolzano/Bozen acquired in 2005 with a spatial resolution of 2.5 m and using orthoimages of the Italian Ministry of Environment, Land and Sea Orthoimages and of the Autonomous Province of Bolzano/Bozen acquired in July-September 2014 and July-October, respectively, both with a spatial resolution of 0.2 m.

Based on InSAR, 614 moving areas related to rock glaciers were detected. Figure 2.2.2.1 shows the entire study area, with close-up views on selected representative areas. Figure 2.2.2.2 shows the number of identified moving areas for each velocity class. The identified rock glacier units with available kinematic information extracted from the previous moving areas are 330; 212 are simple units and 118 are composite landforms. Figure 2.2.2.3 shows the number of the classified rock glacier units for each kinematic class.

In terms of interferogram quality, no major issue was experienced that could prevent the delineation of moving areas. Decorrelation due to snow cover was observed at elevations above 2600 m a.s.l. in interferograms composed by the first image of Sentinel-1 Track 168 DSC. Nevertheless, delineation of the moving areas was possible on other acquisitions. Decorrelation in ALOS-1 PALSAR-1 interferograms with time interval equal to 3 years prevented the delineation of moving areas within rock glaciers, thus only one ALOS-1 PALSAR-1 interferogram with time interval of 46 days was used. Sentinel-1 Interferograms with time intervals of 330 and 342 days show more decorrelation than shorter interferograms. Decorrelation, together with the limited number of available interferograms,

caused less reliable identification and delineation of moving areas with velocity in the order of few centimetres per year. When there was extended decorrelation around rock glaciers, it was difficult to assign a reliable velocity class. This is especially the case for rock glaciers characterised by a low displacement rate. Small moving areas have low reliability because they are composed by a limited number of cells. For other rock glacier systems, the complexity of the detected moving areas – related to the same rock glacier system/unit – made it difficult to assign a reliable kinematic attribute.
The work on this climatic region was conducted by Francesco Brardinoni and Gabriel Pellegrinon.

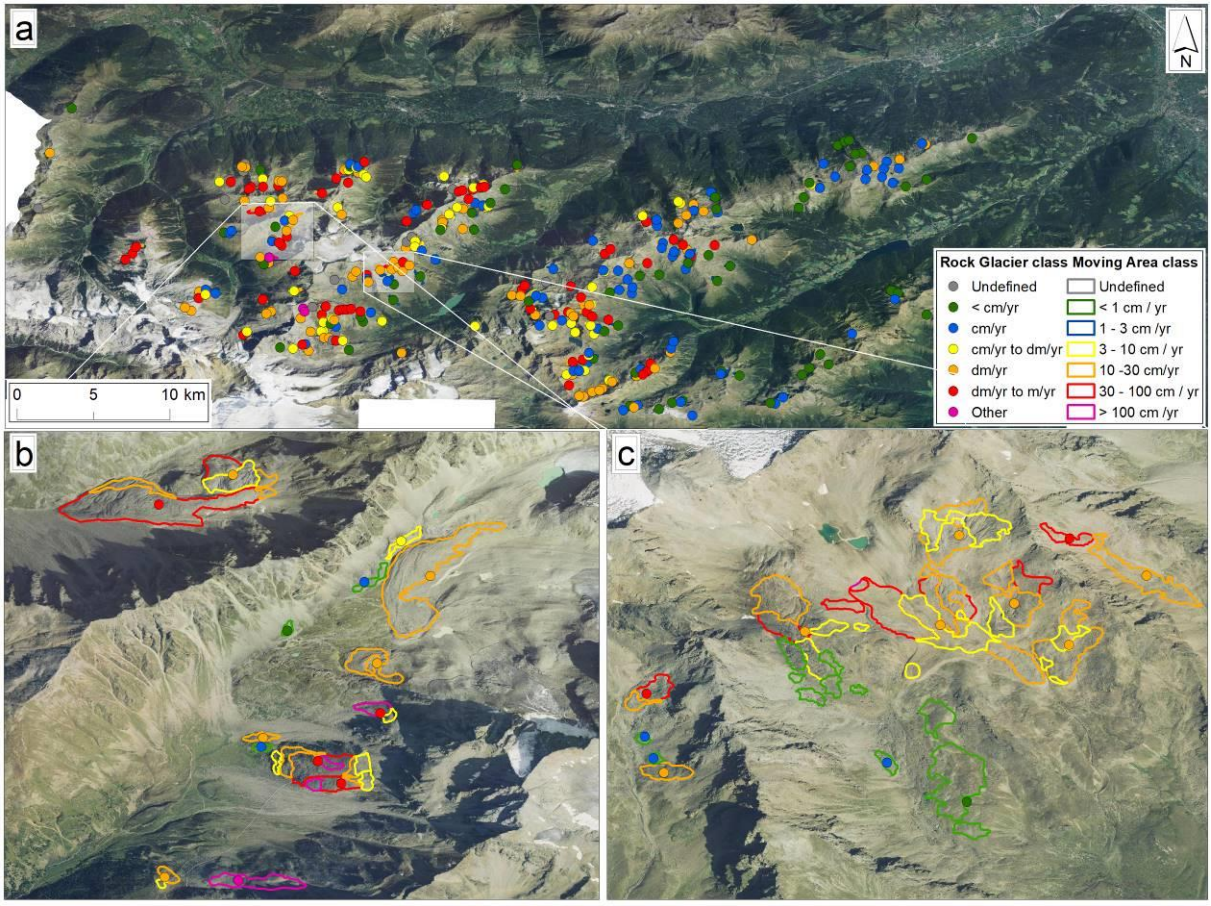

Figure 2.2.2.1: Rock glacier inventory of Vinschgau/Val Venosta with close-up views of selected areas in Suldental and Martelltal.

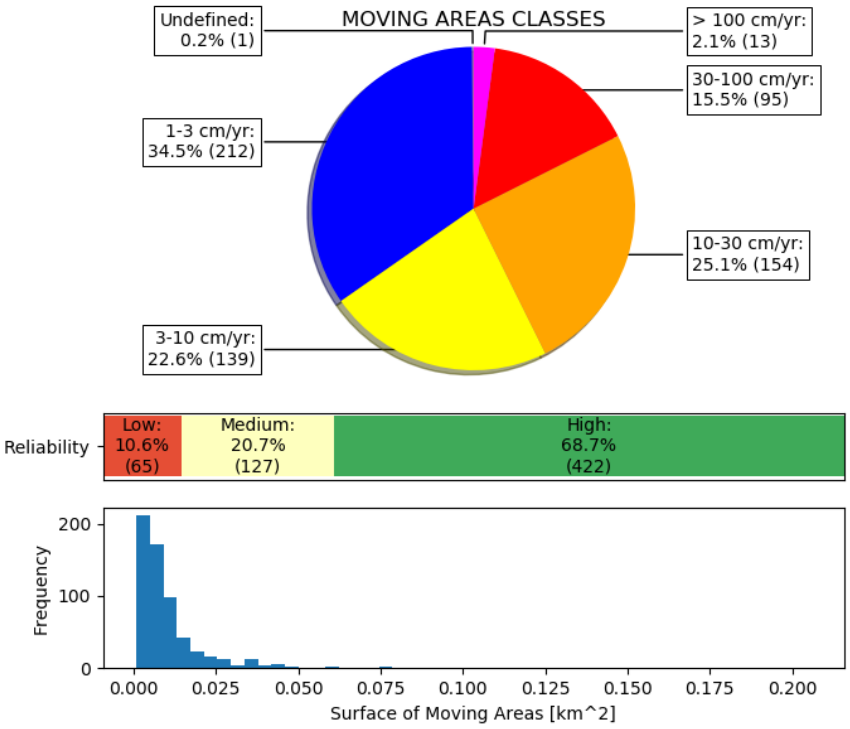

Figure. 2.2.2.2: Ultental (Italy) pie chart of the velocity classes of moving areas (upper part), horizontal bar of reliability of classified moving areas (central part), and histogram of the surface covered by moving areas (lower part).

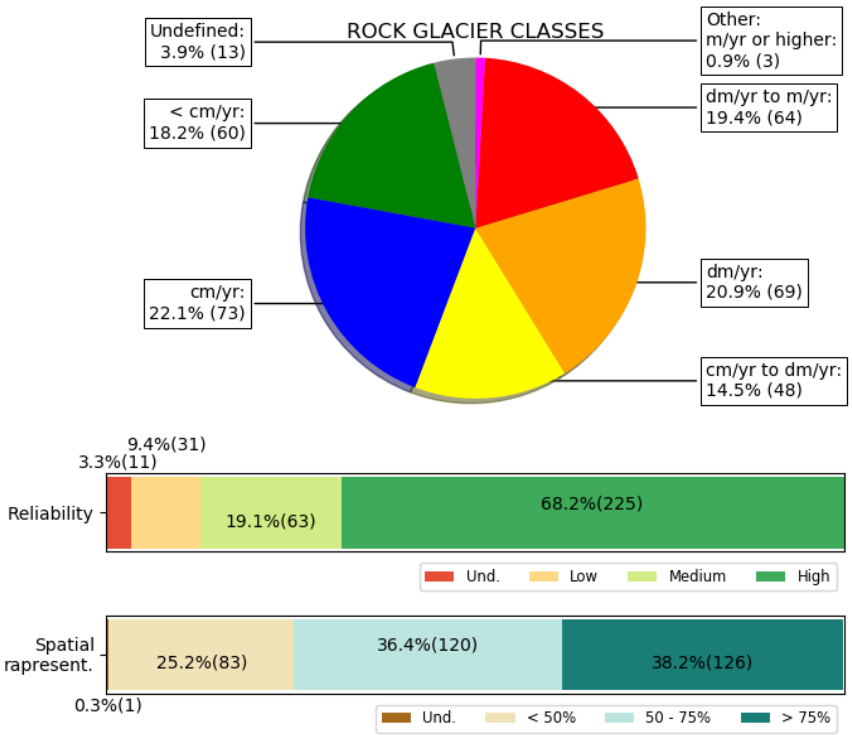

Figure. 2.2.2.3: Ultental (Italy) pie chart of the kinematic classes of rock glaciers (upper part), horizontal bar of reliability of classified rock glaciers (central part), and horizontal bar of the spatial representativeness of classified rock glaciers (lower part).

2.2.3 Vanoise Massif (France)

The study area Vanoise massif (figure 2.2.3.1) is a a mountain region located between N 45.6° and N 45.2° in the French Alps, covering approximately 2000 km², and reaching 3855 m a.s.l. at its highest point (la Grande Casse). Though it has no strictly delimited boundaries, the massif is here confounded with the territory of the "Parc national de la Vanoise" and it mostly includes the highest parts of the Arc and Isère rivers watersheds. The mean elevation of the massif is 2325 m a.s.l., and about 60 % of the terrain are above 2500 m a.s.l., and about 4 % are covered with glaciers (Gardent et al., 2015). Because of its topographical and climatic settings, permafrost is largely present (Marcer et al., 2017) in the region, as testified by abundant rock glaciers (n = 537, 41 km²). These landforms are mostly located in valleys above 2400 m a.s.l. (Monnier, 2004), and more than half of them (n = 363) most probably contain ice (Marcer et al., 2017). Among the actively creeping rock glaciers of the Vanoise massif, 24 landforms presently show evidence of destabilization, such as extensional cracks, crevasses and scarps (Marcer et al., 2019).

The geomorphological mapping of rock glaciers of the Vanoise was made by Roudnitska et al. (2016), as part of the effort made since 2008 by RTM-ONF (French office in charge of mitigating the natural hazard in mountain regions) and PACTE/UGA EDYTEM/CNRS-USMB laboratories for inventorying rock glaciers in France. The inventorying relies on a combination of photo-interpretation with stereoscopic lenses of printed IGN (French institute of geographic information) air photographs (generally dating from late 90's), observation of recent IGN ortho-photographs (generally dating from 2013, 2014 of 2015, and with a resolution of 0.5 and 0.2 m, accessible on www.geoportail.gouv.fr) and 1:25000 topographic maps, and field inspections.

Interferograms from Sentinel-1 were computed from both ascending and descending tracks, between 2016 and 2019. Since the French Alps are located in the Northern hemisphere, only the images acquired between June and October (i.e. in the unfrozen summer periods) were used, in order to avoid the presence of snow cover, with an exception for a pair of images in February 2019 (with cold snow on most the high elevation terrain, allowing coherent InSAR signal). In detail, 16 interferograms were computed for the ascending track, 18 interferograms for the descending, using time intervals of 6, 12, 18, 24, 48, 54, 354 and 366 days.

Based on InSAR, 338 moving areas related to rock glaciers were detected. Figure 2.2.3.2 contains the number of identified moving areas for each velocity class. The identified rock glacier units with available kinematic information extracted from the previous moving areas are 275. Of those, only 126 RGs were classified, for which external information on surface velocity was available (figure 2.2.3.3).

The work on this climatic region was conducted by Xavier Bodin.

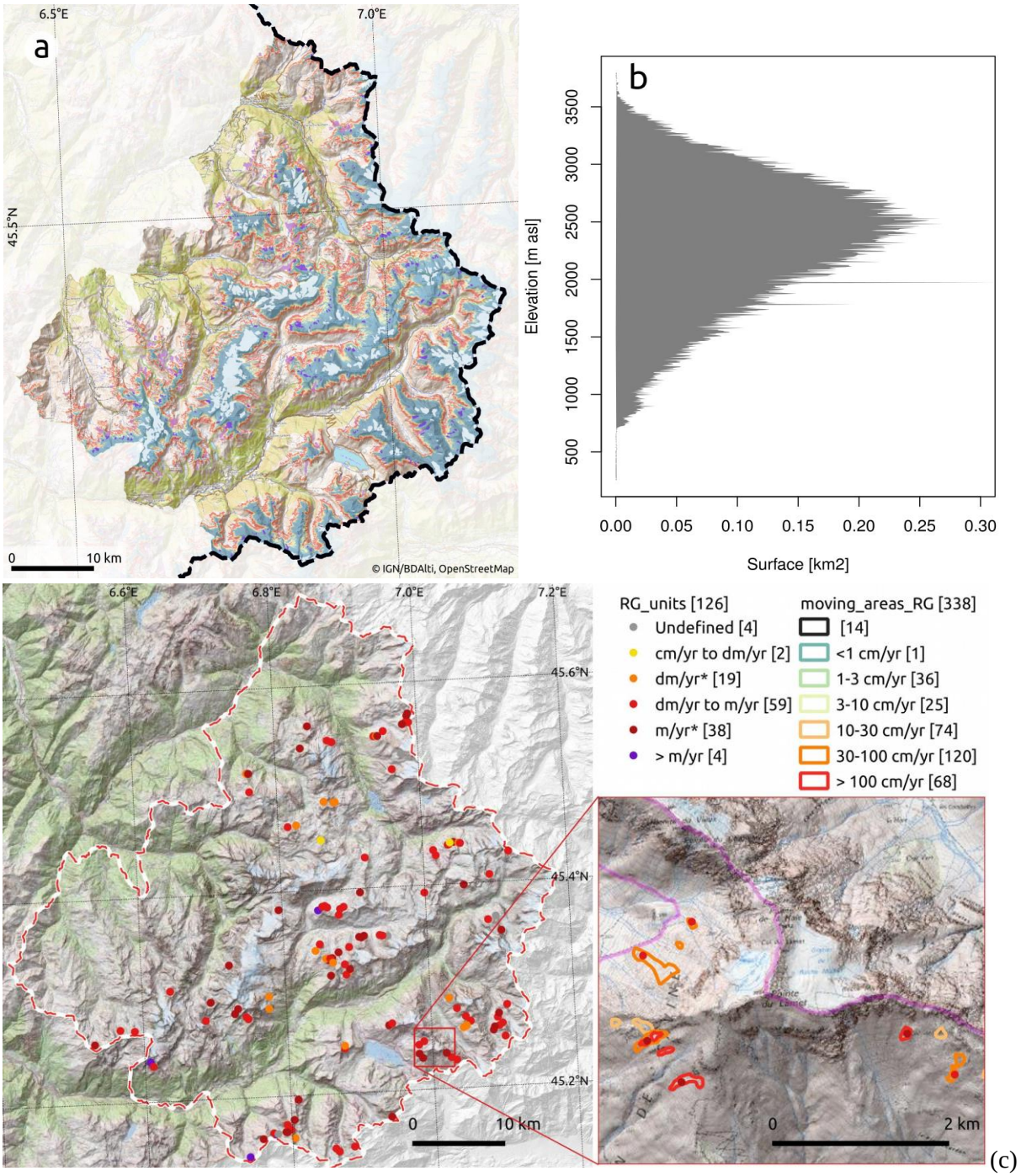

Figure 2.2.3.1: Geographical context (a) and hypsometry (b) of the Vanoise massif. (c) InSAR inventory in the Vanoise massif, showing both the moving areas and the classified rock glaciers.

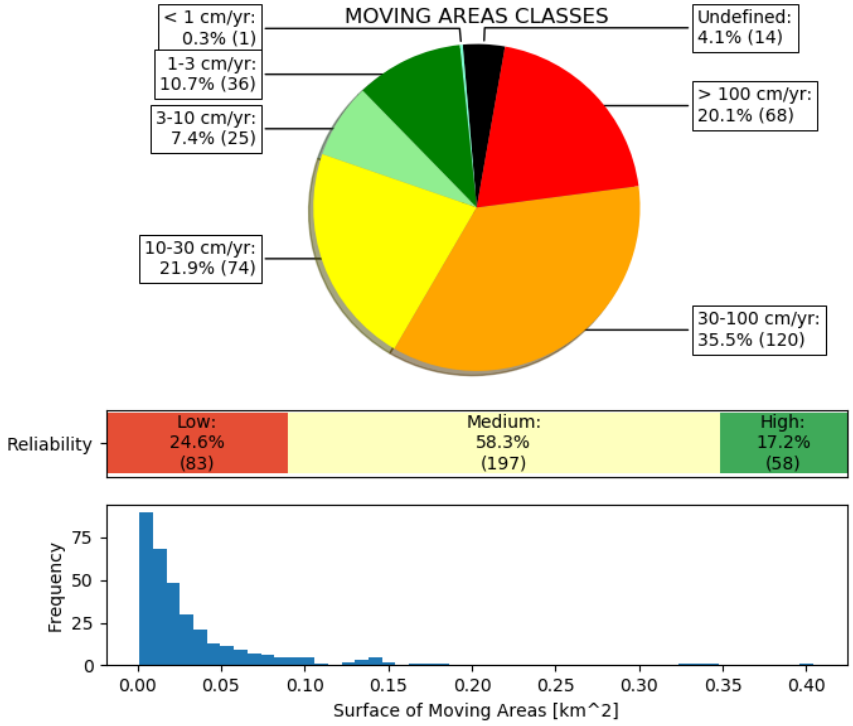

Figure 2.2.3.2: Vanoise Massif (France) pie chart of the velocity classes of moving areas (upper part), horizontal bar of reliability of classified moving areas (central part), and histogram of the surface covered by moving areas (lower part).

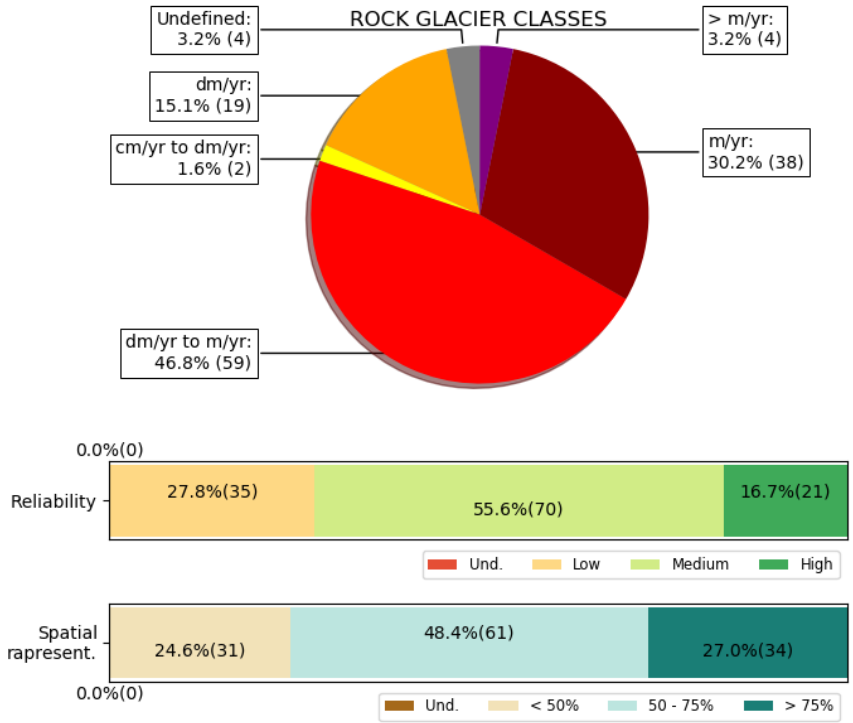

Figure 2.2.3.3: Vanoise Massif (France) pie chart of the kinematic classes of rock glaciers (upper part), horizontal bar of reliability of classified rock glaciers (central part), and horizontal bar of the spatial representativeness of classified rock glaciers (lower part).

2.2.4 Troms, (Northern Norway)

The Troms study area (Fig. 2.2.4.1) is located in Kåfjord, Lyngen, Storfjord and Tromsø municipalities in the County of Troms og Finnmark in Northern Norway and covers ca. 7614 km^2. The alpine topography is characterized by a high altitudinal gradient with deep narrow fjords and high mountain peaks up to ca 1800 m a.s.l. in the central part of the area (Lyngen Alps). This subarctic region is at the transition between discontinuous/sporadic permafrost zones and seasonal frost.

The morphological rock glacier inventory covering the study area has been made in 2010 by the University of Oslo (UiO) (Lilleøren and Etzelmüller, 2011). The inventory has been updated following the IPA rock glacier action group recommendations and exploiting higher resolution orthophotos and findings from InSAR.

Interferograms from Sentinel-1 were computed from both Track 58 ASC and 95 DSC, between 2015 and 2019. Only the images acquired between June and October (i.e. in the unfrozen summer periods) were used, in order to avoid the presence of snow cover. 1221 and 1308 interferograms, respectively for the Track 58 ASC and 95 DSC, were initially selected based on coherence. Several averaged InSAR maps (stacking) were processed using different temporal intervals (within the season and interannually). Short time intervals (e.g. 6 days: 56–57 interferograms after sorting) allow for higher detectable maximal velocities. Longer time intervals (e.g. one year: 299–326 interferograms after sorting) provide better sensitivity to low displacement rates.

We additionally used a 10 m resolution DTM from the Norwegian Mapping Authority (2016, available on kartkatalog.geonorge.no) and 2016-08-18, 2011-08-16 and 2006-08-16 orthoimages (0.25–0.5 m resolution) (norgeibilde.no, WMS service available on kartkatalog.geonorge.no). The unstable rock slope and glacier inventories from the Norwegian Geological Survey (NGU) and the Norwegian Water Resources and Energy Directorate (NVE) have also been exploited. The Norwegian Ground Motion Mapping service InSAR Norway (insar.ngu.no) has been used to doublecheck the results at specific locations.

Multiple temporal baseline stacking InSAR products document 29086 40x40 m pixels on rock glaciers, corresponding to a total area of 46.5 km^2. 36.0 km^2 are in class 1 (< 0.3 cm/yr). 2.9 km^2 are in class 0 (undefined, i.e. decorrelated in 6 days). For the remaining 7.6 km^2, velocity between 0.3–1 cm/yr (class 8: others) and 1–100 cm/yr (classes 2–5) are detected. Figure 2.2.4.2 shows the fraction of the documented areas for each velocity class. Figure 2.2.4.1 shows the entire investigated region, with a focus on selected representative areas.

The inventory consists of 414 units for a total of 340 systems (290 single units and 124 units in 50 composite systems). Among these, 21 remain kinematically undefined and 240 are < mm/yr to cm/yr (no detected movement). 153 units have mm/yr to m/yr kinematic attribute. Figure 2.2.4.3 shows the number of the classified rock glacier units for each kinematic class.

The study area is characterized by a large set of – often combined – periglacial processes, that leads to challenges both for geomorphological characterization (e.g. unit division, upslope unit connection), as well as for associating the detected InSAR movement to an actual process (e.g. impact of superficial solifluction processes on relict rock glaciers). Discussions related to inclusion/exclusion of specific landforms of the inventory have started between the different project partners and already led to corrections/updates. This work will possibly continue in the future and may lead to a new version of the dataset. No specific InSAR problem has been identified.

The work on this climatic region was conducted by Line Rouyet, with contributions from Karianne S. Lilleøren, Bernd Etzelmüller and Reynald Delaloye.

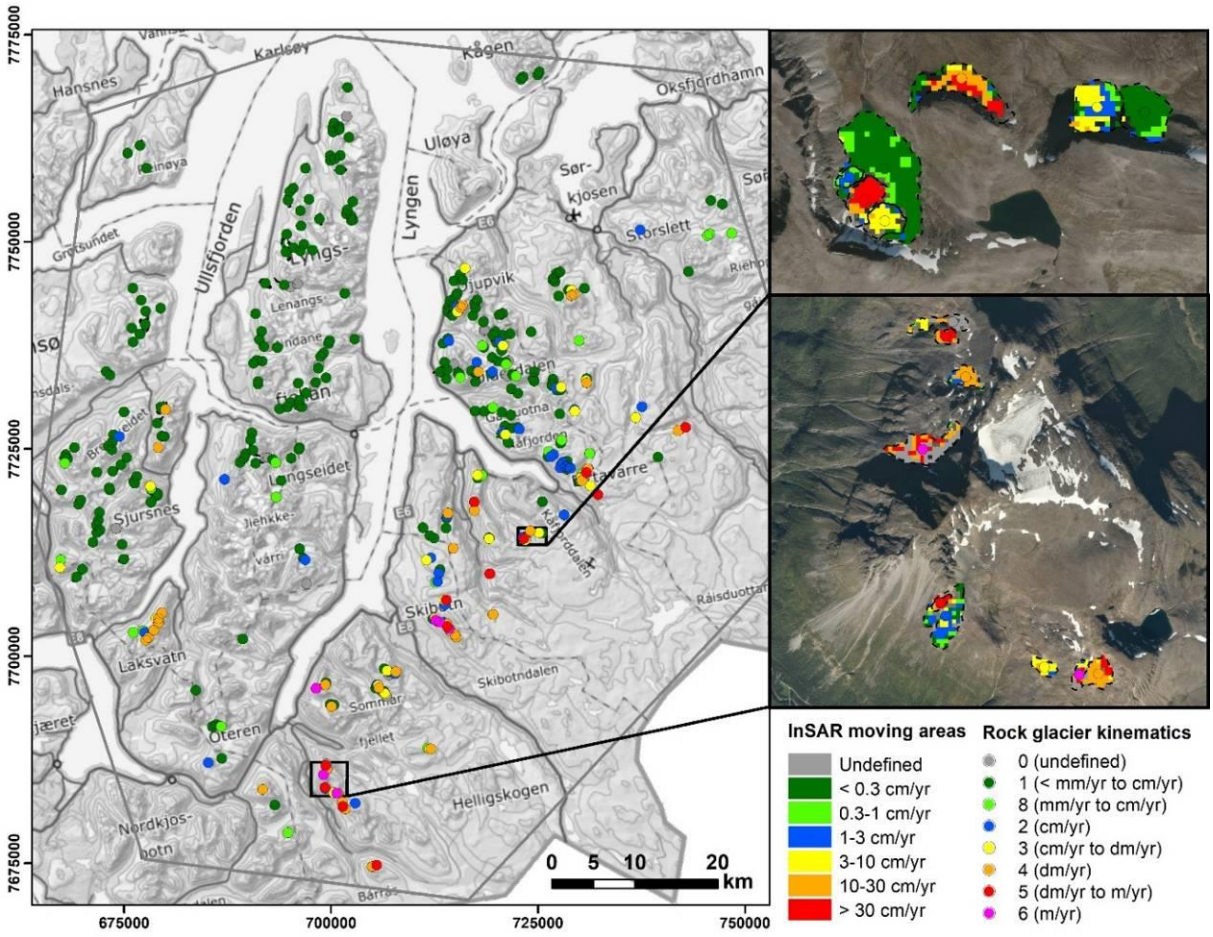

Figure 2.2.4.1: Troms, (Northern Norway) example of inventory, with focus on two representative areas. The grey lines on the main map show the limits of the area of interest. Dashed black lines on detailed maps are the indicative geomorphological outlines (extended definition) primarily used to extract the moving areas.

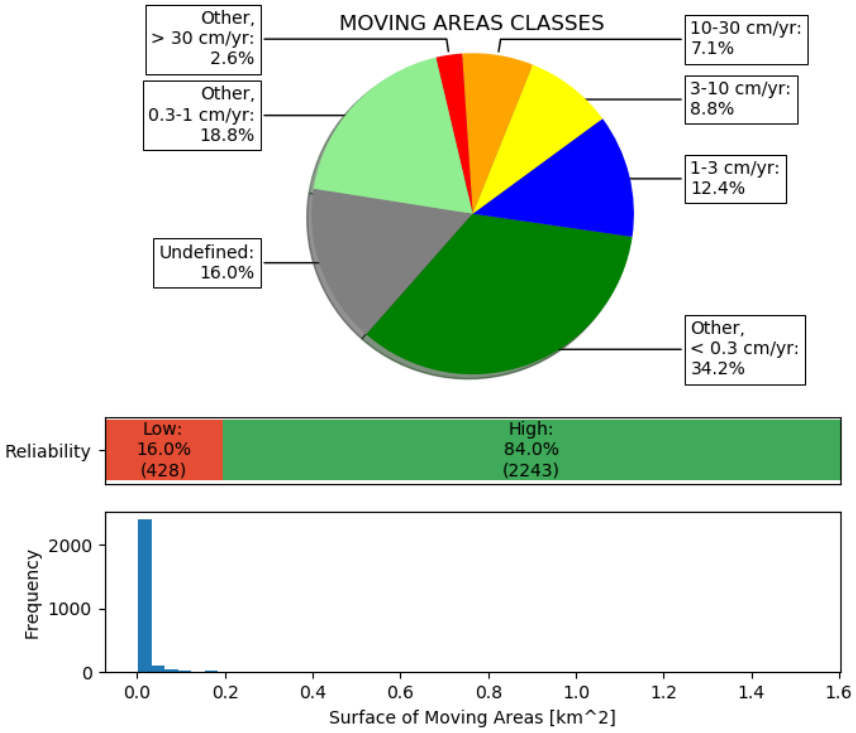

Figure. 2.2.4.2: Troms, (Northern Norway) pie chart of the velocity classes of moving areas (upper part), horizontal bar of reliability of classified moving areas (central part), and histogram of the surface covered by moving areas extracted from the 40x40 m pixels raster (lower part).

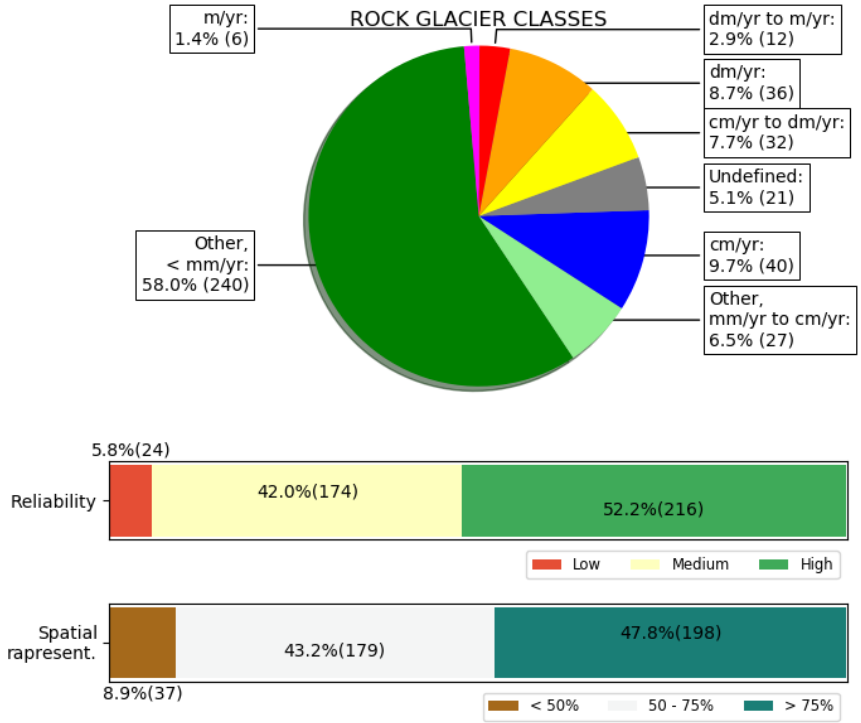

Figure 2.2.4.3: Troms, (Northern Norway) pie chart of the kinematic classes of rock glaciers (upper part), horizontal bar of reliability of classified rock glaciers (central part), and horizontal bar of the spatial representativeness of classified rock glaciers (lower part).

2.2.5 Finnmark (Northern Norway)

The Finnmark study area (Fig. 2.2.5.1) is located in Gamvik, Berlevåg and Tana municipalities in the County of Troms and Finnmark in Northern Norway and covers ca 2920 km^2. The topography consists of a series of mountains reaching 724 m a.s.l., distributed around the large Tana fjord. This subarctic region is at the transition between discontinuous/sporadic permafrost zones and seasonal frost.

The morphological rock glacier inventory covering the study area has been made in 2010 by the University of Oslo (UiO) (Lilleøren and Etzelmüller, 2011). Following the IPA rock glacier action group recommendations and exploiting higher resolution orthophotos and findings from InSAR, the inventory has been updated.

Interferograms from Sentinel-1 were computed from both Track 43 ASC and 51 DSC, between 2015 and 2020. Only the images acquired between June and October (in the unfrozen summer periods) were used, in order to avoid the presence of snow cover. 2168 and 1754 interferograms, respectively for the Track 43 ASC and 51 DSC, were initially selected based on coherence. The area has been divided into two subsets for the processing to avoid unwrapping errors (due to data gaps on fjords). Several averaged InSAR maps (stacking) were processed using different temporal intervals (within the season and interannually). Short time intervals (e.g. 6 days: 61–67 interferograms after sorting) allow for higher detectable maximal velocities. Longer time intervals (e.g. one year: 388–486 interferograms after sorting) provide better sensitivity to low displacement rate.

We additionally used a 10 m resolution DTM from the Norwegian Mapping Authority (2016, available on kartkatalog.geonorge.no) and 2018-07-18 and 2008-08-19 orthoimages (0.25–0.5 m resolution) (norgeibilde.no, WMS service available on kartkatalog.geonorge.no). The Norwegian Ground Motion Mapping service InSAR Norway (insar.ngu.no) has been used to doublecheck the results at specific locations.

Multiple temporal baseline stacking InSAR products documented 2479 40x40 m pixels on rock glaciers, corresponding to a total area of 4.0 km^2. 2.0 km^2 are in class 1 (< 0.3 cm/yr). 0.1 km^2 are in class 0 (undefined). For the remaining 1.9 km^2, velocity between 0.3–1 cm/yr (class 8: others) and 1–100 cm/yr (classes 2–5) are detected. Figure 2.2.5.2 shows the fraction of the documented areas for each velocity class.

The inventory consists of 57 units for a total of 19 systems (11 single units and 46 units in 8 composite systems). Among these, 7 remain kinematically undefined and 32 are < mm/yr to cm/yr (no detected movement). 18 units have mm/yr to m/yr kinematic attribute. Figure 2.2.5.3 shows the number of the classified rock glacier units for each kinematic class. Figure 2.2.5.1 shows the entire investigated region, with a focus on selected representative areas.

Strong atmospheric/ionospheric effects affect several interferograms. The quality of the InSAR stacking products is variable and led to uncertainty in terms of reliability, especially for the velocity class 1–3 cm/yr. This issue is mentioned in the field “Remarks” of the products and the “Reliability” adjusted accordingly. In case of low reliability and spatial representativeness, the category “Undefined” has been used.

Most of the landforms are relict or transitional. However, for the major systems in the Western part of the study area, we detect a gradient from no movement at the bottom of the slope to mostly 1-10 cm/yr (up to 30 cm/yr at some locations) in the upper part. The challenge is that the detected velocity may not be related to permafrost creep even in presence of rock glacier morphological features (e.g. superficial over relict). Discussions related to removal of uncertain units and changes of units’ division are at early stage for this area. It is therefore likely that corrections lead to a new version of the dataset.

The work on this climatic region was conducted by Line Rouyet, with contributions from Karianne S. Lilleøren and Bernd Etzelmüller.

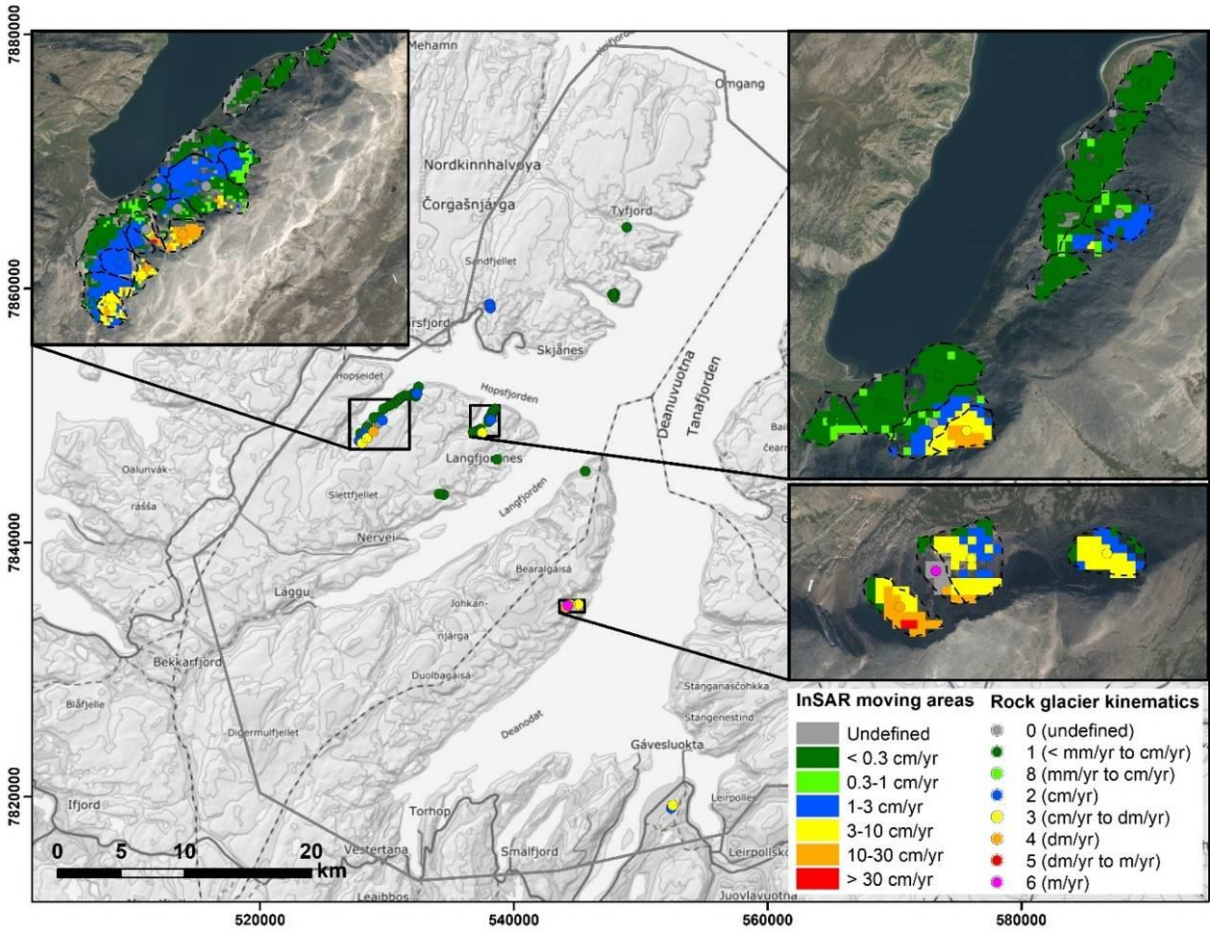

Figure 2.2.5.1: Example of Finnmark (Northern Norway) inventory, with focus on three representative areas. The grey lines on the main map show the limits of the area of interest. Dashed black lines on detailed maps are the indicative geomorphological outlines (extended definition) primarily used to extract the moving areas.

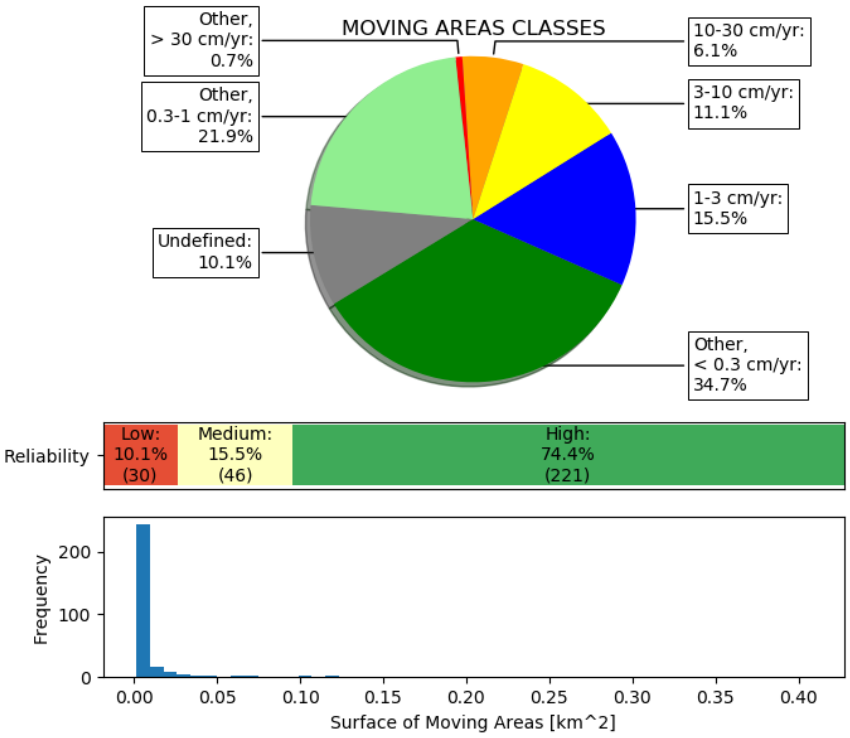

Figure 2.2.5.2: Finnmark (Northern Norway) pie chart of the velocity classes of moving areas (upper part), horizontal bar of reliability of classified moving areas (central part), and histogram of the surface covered by moving areas extracted from the 40x40 m pixels raster (lower part).

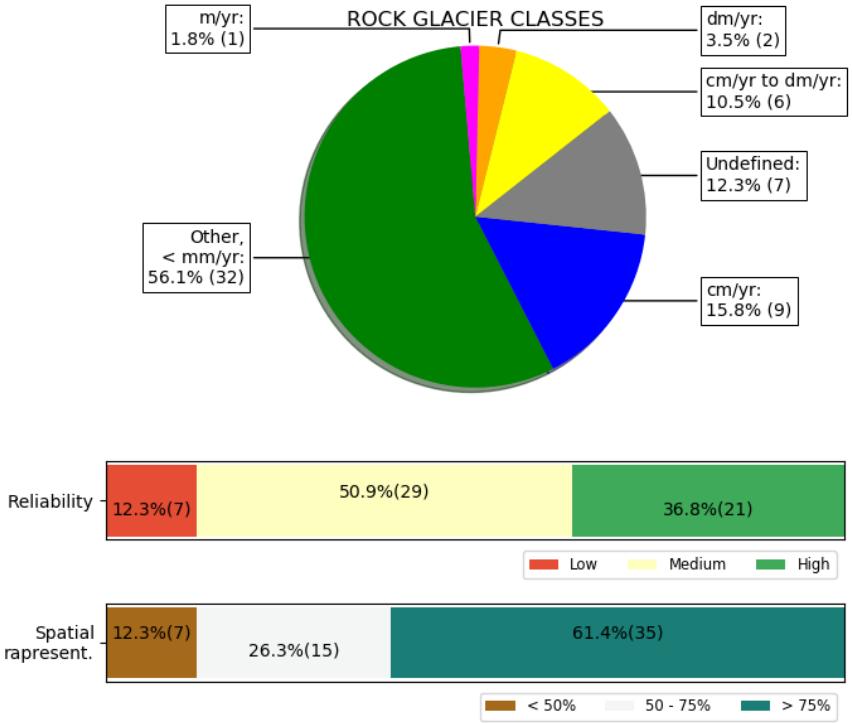

Figure 2.2.5.3: Finnmark (Northern Norway) pie chart of the kinematic classes of rock glaciers (upper part), horizontal bar of reliability of classified rock glaciers (central part), and horizontal bar of the spatial representativeness of classified rock glaciers (lower part).

2.2.6 Nordenskiöld Land (Svalbard)

The Svalbard study area includes most of Nordenskiöld Land on Spitsbergen (Svalbard archipelago) and covers ca 3726 km^2 (Fig. 2.2.6.1). Nordenskiöld is delimited by Isfjorden in the North-West and Van Mijenfjorden in the South-East. Mountain peaks are up to ca 900 m a.s.l. in the western part, ca. 1000 m a.s.l. in the North and ca. 1200 m a.s.l. in the South-East. This arctic region is characterized by continuous permafrost and significant glacial influence.

The rock glacier locations are based on a new morphological inventory made by the University Centre in Svalbard (UNIS) in Spring–Summer 2020. The work, led by Hanne H. Christiansen, benefited from major contributions from Ole Humlum and Ashton B. McDonald. Following the IPA rock glacier action group recommendations and exploiting findings from InSAR, the inventory has been further adjusted by Line Rouyet.

Interferograms from Sentinel-1 were computed from both Track 14 ASC and 154 DSC, between 2015 and 2020. Note that data from the descending track were not available before 2018. Only the images acquired between June and October (in the unfrozen summer periods) were used, in order to avoid the presence of snow cover. 266 and 189 interferograms, respectively for the Track 43 ASC and 51 DSC, were initially selected based on coherence. The area has been divided into four subsets for the processing to avoid unwrapping errors (due to data gaps on fjords and glaciers). Several averaged InSAR maps (stacking) were processed using different temporal intervals (within the summer seasons only, interannual pairs being largely affected by coherence loss). Short time intervals (e.g. 6 days: 41–60 interferograms after sorting) allow for higher detectable maximal velocities. Longer time intervals (e.g. 150 days: 166–266 interferograms after sorting) provide better sensitivity to low displacement rate.

We additionally used a 20 m resolution DTM from the Norwegian Polar Institute (2016, available on kartkatalog.geonorge.no) and a mosaic orthoimage product based on Mid-July to Mid-August 2008 to 2011 orthoimages (10–40 cm resolution) (toposvalbard.npolar.no, WMS service available on kartkatalog.geonorge.no).

Multiple temporal baseline stacking InSAR products documented 11690 40x40 m pixels on rock glaciers, corresponding to a total area of 18.7 km^2. 0.8 km^2 are in class 1 (< 1 cm/yr), 0.9 km^2 are in class 0 (undefined, i.e. decorrelated in 6 days). For the remaining 17 km^2, velocity between 1–100 cm/yr (classes 2–5) are detected. Figure 2.2.6.2 shows the fraction of the documented areas for each velocity class.

The inventory consists of 260 units for a total of 232 systems (209 single units and 51 units in 23 composite systems). Among these, 37 remain kinematically undefined and 4 are < mm/yr (no detected movement). 219 units have cm/yr to m/yr kinematic attributes. Figure 2.2.6.3 shows the number of the classified rock glacier units for each kinematic class. Figure 2.2.6.1 shows the entire investigated region, with a focus on selected representative areas.

Svalbard is a highly dynamic environment. Seasonal thawing of the active layer leads to subsidence during the unfrozen summer periods and solifluction processes are extensively affecting the slopes. These processes typically have a cm/yr or cm/yr to dm/yr order of magnitude. In many cases, the detected velocity on rock glaciers does not significantly differ from the background signal along the slope. When occurring, this issue is mentioned in the field “Remarks” of the products and the “Reliability” adjusted accordingly.

There is overall a significant difference of kinematics between rock glaciers categorized as glacier-connected (typically dm/yr or dm/yr to m/yr) and those that are talus- or debris-mantle-connected

(typically cm/yr or cm/yr to dm/yr). This may indicate that the current inventory is potentially including landforms driven by glacial flow or affected by subsidence on ice-cored moraine, which should be removed in a second version of the inventory. At this stage, the issue is simply mentioned in the field "Remarks" of the products. In general, this shows the challenge of glacial-periglacial continuum in an Arctic context, but also indicates that InSAR may be valuably exploited to differentiate specific processes.

The work on this climatic region was conducted by Line Rouyet, with contributions from Hanne H. Christiansen, Ole Humlum and Ashton B. McDonald.

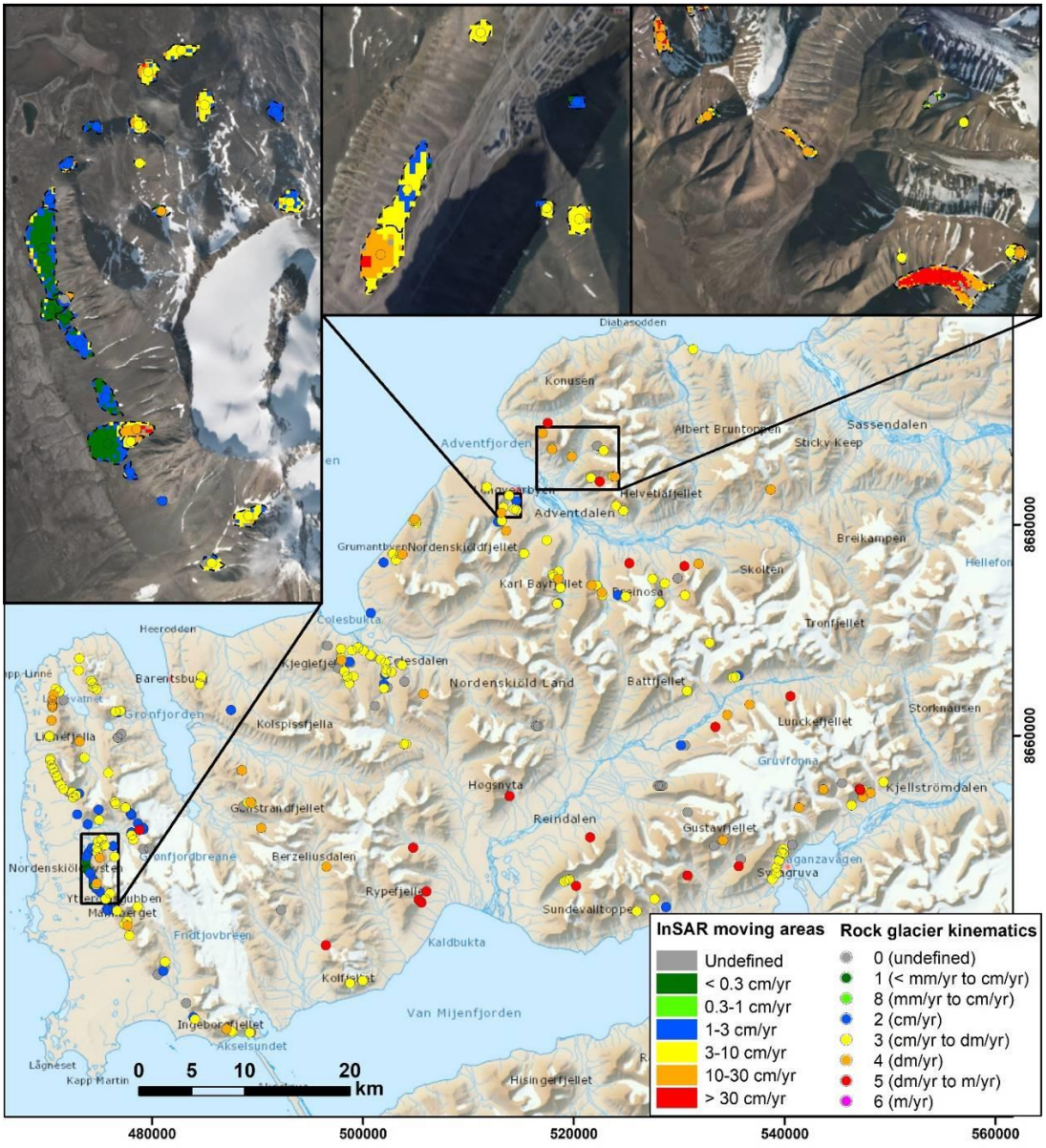

Figure 2.2.6.1: Example of Nordenskiöld Land (Svalbard) inventory, with focus on three representative areas. The grey lines on the main map show the limits of the area of interest. Dashed black lines on detailed maps are the indicative geomorphological outlines (extended definition) primarily used to extract the moving areas.

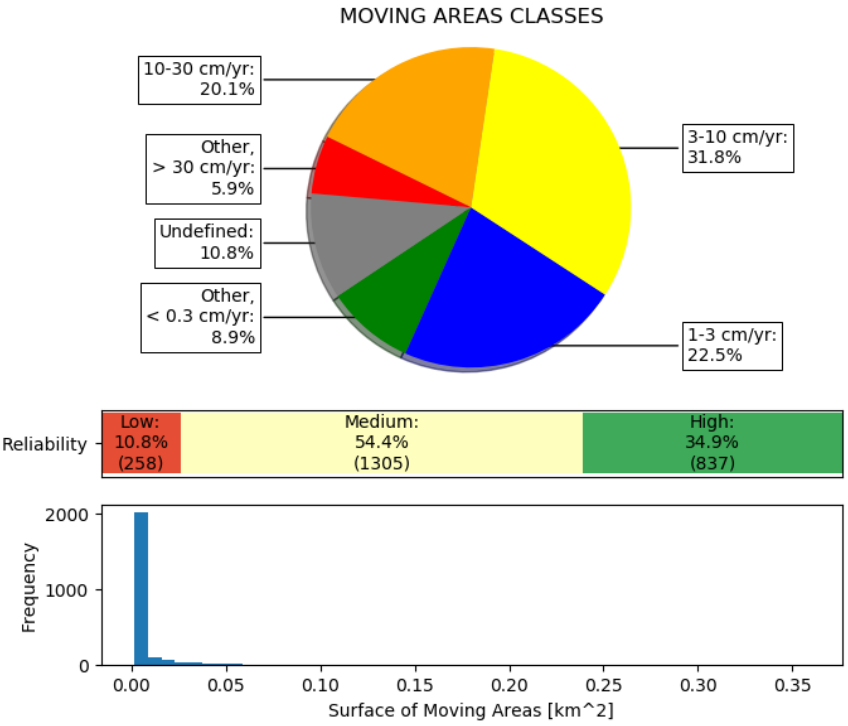

Figure 2.2.6.2: Nordenskiöld Land (Svalbard) pie chart of the velocity classes of moving areas (upper part), horizontal bar of reliability of classified moving areas (central part), and histogram of the surface covered by moving areas extracted from the 40x40 m pixels raster (lower part).

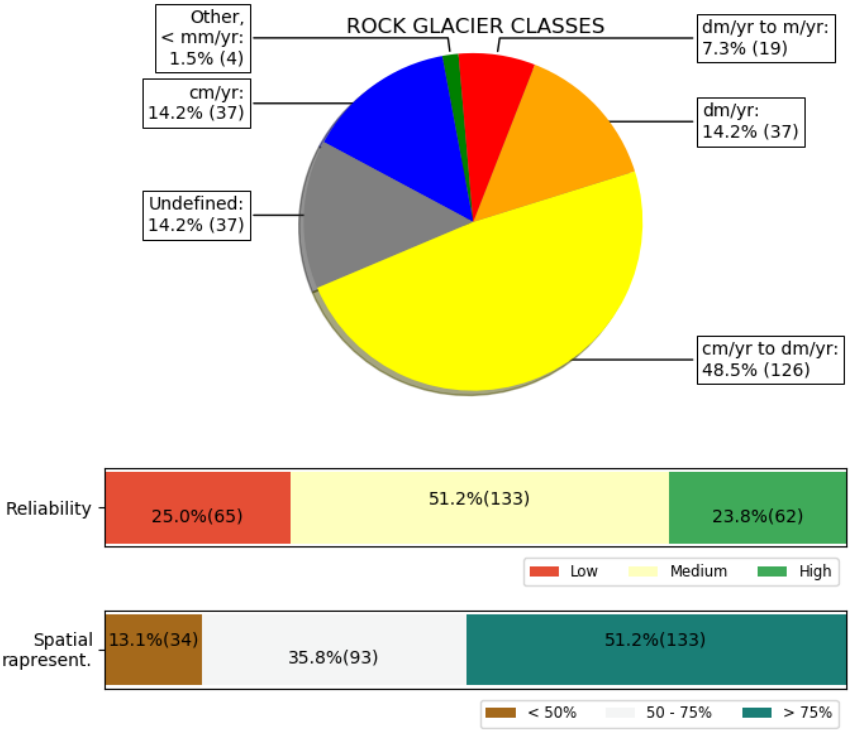

Figure 2.2.6.3: Nordenskiöld Land (Svalbard) pie chart of the kinematic classes of rock glaciers (upper part), horizontal bar of reliability of classified rock glaciers (central part), and horizontal bar of the spatial representativeness of classified rock glaciers (lower part).

2.2.7 Disko Island (Greenland)

Disko Island (Qeqertarsuaq) is a roughly 8500 km^2 large island offshore in Western Greenland. It begins at a geographical altitude equal to Ilulissat, the neighbouring city on the mainland of Greenland. Towards the North, the Vaigat Strait (Sullorsuaq) separates Disko from the mainland. The topography from Disko spans from sea-level up to 1920 m a.s.l. The climatic conditions favour the formation of a small ice cap and several valley glaciers.

An InSAR based inventory of moving areas for a large part of Disko and the slope north of the Vaigat Strait is compiled from different InSAR sources. The main datasets used to determine outlines of the moving areas and classify the annual velocity for the identified rock glacier features are ALOS-2 PALSAR-2 and Sentinel-1 Interferograms, both ascending and descending. Their coverage is shown in figure 2.2.7.1.

588 moving areas and 570 rock glacier features were identified (Figure 2.2.7.2 and 2.2.7.3). An overview map and a subdivision into the rock glacier classes is shown in figure 2.2.7.1.

In general, especially for the faster moving rock glaciers, the motion signature is sometimes very clear visible in the short-termSentinel-1 interferograms. For 2018-2019, a large number of mostly coherent interferograms were available. However, local effects (remaining snow, local acceleration) hinder the clear quantification of the velocity classes. Therefore, for most objects, only a single set of interferograms could be used to define the velocity class. This velocity might not be representative for rock glaciers that show strong variability in velocity throughout a year.

On the other hand, L-band interferograms from Palsar-2 are better suited to map and quantify motion over an entire year, also for slower features. However, here only a very limited data set with mainly one single interferogram for an area was available.

Another problem was related to the availability of optical data. The rock glaciers were identified with help of optical satellite imagery. As source dataset for the optical images, mainly the Google Map Satellite overlay was used. Partly Sentinel-2 cloud-free data from EOX::Maps was used. No high-resolution optical data were available on the investigated area. Therefore, it was not possible to provide reliable information about the geomorphological characteristics of the rock glaciers. Attribute fields as the unit morphology, the type of spatial connection to the upslope unit, the degree of destabilization and the spatial representativeness were not provided.

The work on this climatic region was conducted by Rafael Caduff and Margaret Darrow.

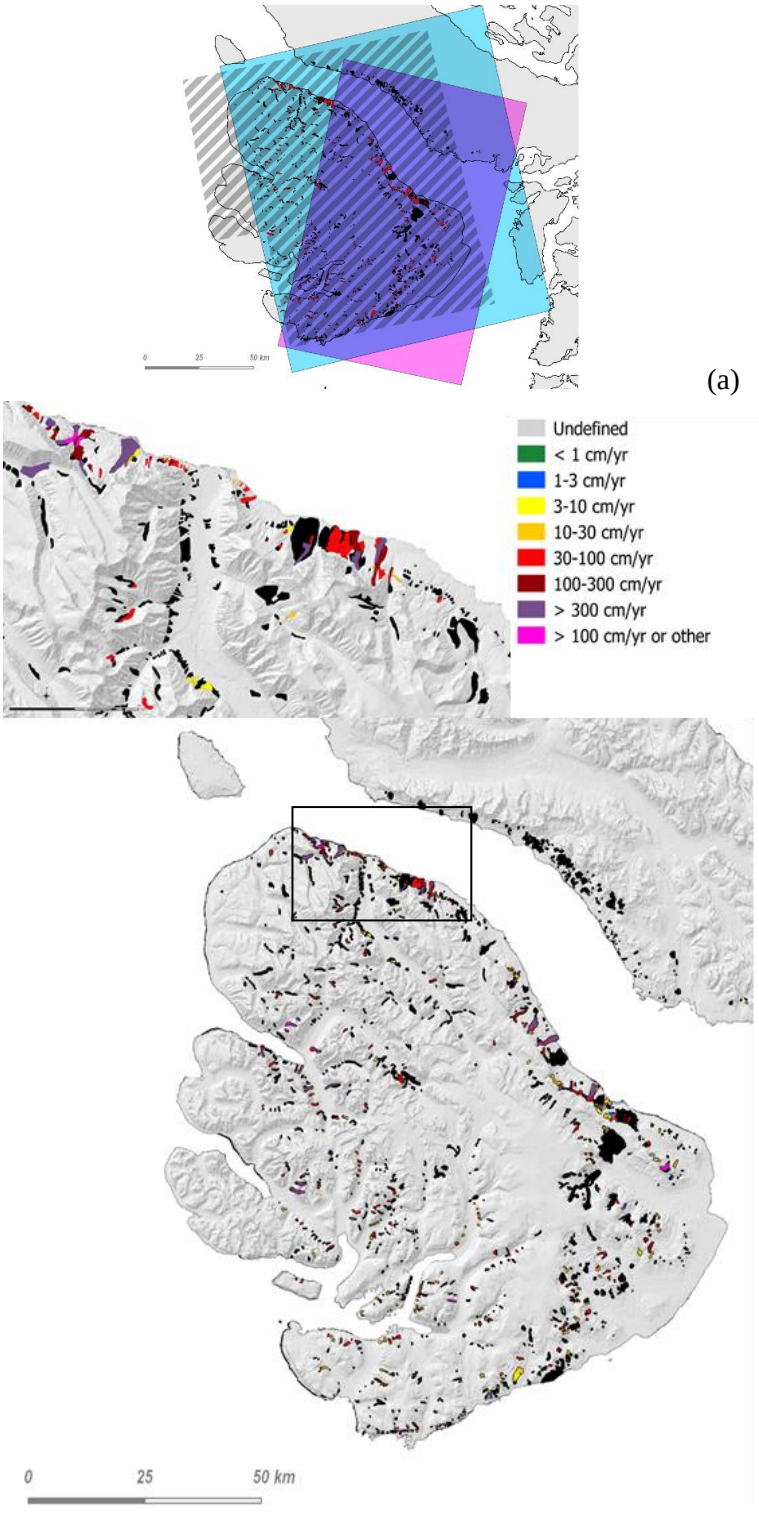

Figure 2.2.7.1: (a) Overview of the Disko Island test-site. The satellite coverage is indicated as color pattern overlays: Magenta: Sentinel-1 Descending; Cyan: Sentinel-1 Ascending. Grey hatched: ALOS-2 PALSAR-2 (compilation of several frames). Red areas indicate the areas of motion related to rock glacier; black areas indicate the areas of motion not related to rock glacier. (b) Overview and detail overview of the map indicating rock glacier motion. The classification follows the scheme as shown in the legend section. The black rectangle in the lower panel indicates the position of the upper detail. Black areas indicate the areas of motion not related to rock glacier.

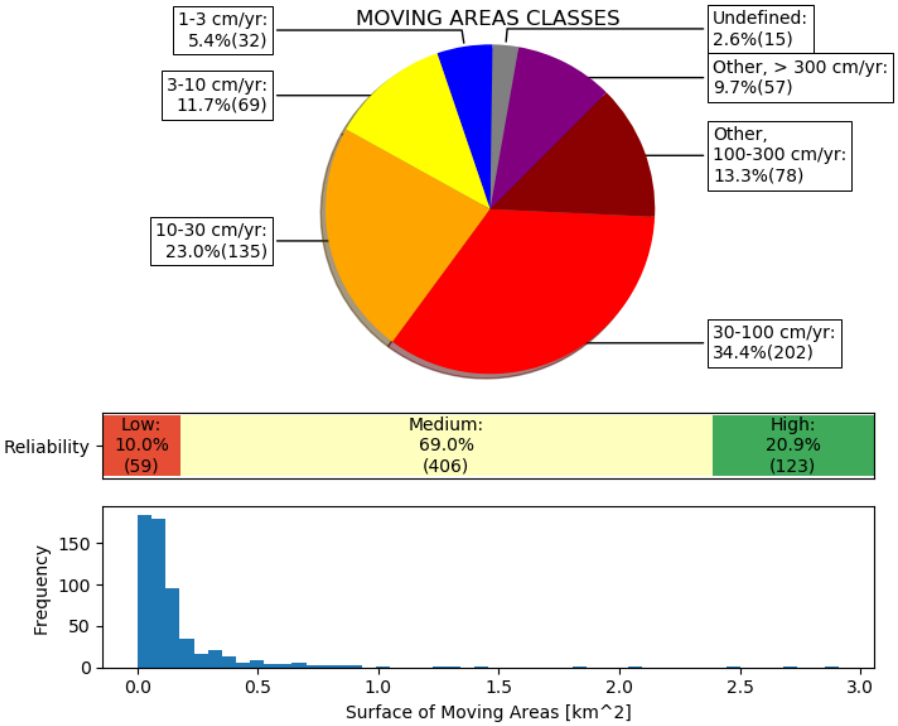

Figure 2.2.7.2: Disko Island (Greenland) pie chart of the velocity classes of moving areas (upper part), horizontal bar of reliability of classified moving areas (central part), and histogram of the surface covered by moving areas (lower part).

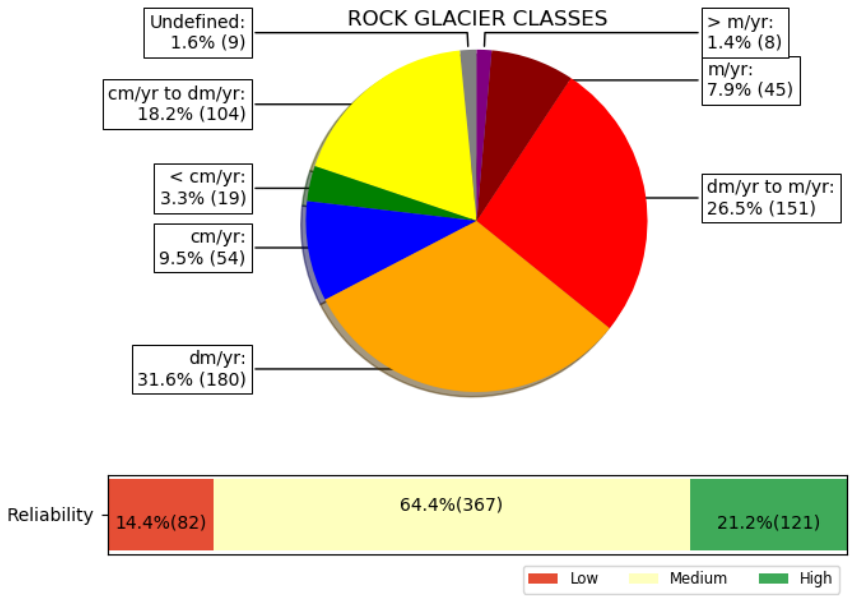

Figure 2.2.7.3: Disko Island (Greenland) pie chart of the kinematic classes of rock glaciers (upper part), and horizontal bar of reliability of classified rock glaciers (lower part).

2.2.8 Tien Shan (Kazakhstan-Kyrgyzstan)

The investigated area is located in the central part of Ile Alatau (Northern Tien Shan) in Kazakhstan, it covers about 350 km² and includes the Small Almaty, Big Almaty and Left Talgar valleys (Figure 2.2.8.1). Several mountain peaks are higher than 4000 m a.s.l.. with the highest being Pik Talgar 4973 (m a.s.l.).

Geomorphological inventories were conducted during Soviet time based on aerial images, but is only available in tabular format. A further inventory for a similar area was published in 2014 (Bolch and Gorbunov, 2014), but generated based on much lower resolution Landsat data with the visual aid of aerial photos. A preliminary inventory for a similar region was generated using a Pléiades optical image acquired on 27th August 2016 by A. Strel. An inventory of moving areas was generated within the GlobPermafrost project (Kääb et al. 2020). It includes several kinds of moving areas including landslides, solifluction, areas with subsidence and rock glaciers. These previous data sets were used as baseline information to locate rock glaciers and to detect moving areas related to rock glaciers.

The interferograms used were carefully selected by visual analysis from all the available ones generated from ALOS-1 PALSAR-1, ERS and Sentinel-1 data. The main interferograms used stem from Sentinel-1 Track 34 DSC acquired in August 2018, June and August 2019 using time intervals of 12, 48 and 272 days. Additional interferograms used stem from Sentinel-1 Track 56 ASC acquired June till September 2019 using time intervals of 12, 24, 48 and 60 days. For selected rock glaciers the interferograms from ALOS-1 PALSAR-1 acquired in August and October 2008 (time interval 46 days) and ALOS-2 PALSAR-2 acquired in October 2016 and June 2016 were used as additional information.

The geomorphological boundaries of rock glaciers were identified based on a digital terrain model (DTM) with a spatial resolution of 1m generated from tri-stereo Pléiades data acquired 09/09/2020 and the according Pléiades orthoimage with a spatial resolution of 0.5m. The compilation of the inventory of rock glaciers was limited to the extent of the Pléiades image.

Based on InSAR 93 moving areas related to rock glaciers were detected. The majority of the areas moved in range of few decimetres to one meter per year and about one quarter moved in the one to three decimetres per year (Figure 2.2.8.2). The distribution of the kinematic classes of rock glaciers is similar with almost 50% creeping in the range of few decimetres to one meter per year (Figure 2.2.8.3).

38% of the rock glaciers were talus-connected and 43% are glacier forefield-connected and 16% are poly-connected. Figure 2.2.8.1 shows the entire investigated area of Ile Alatau with the identified moving areas and rock glaciers classes.

The overall quality of the selected interferograms was suitable to detect the movement level of most rock glaciers. For most objects the data from descending orbits were used. In case of radar layover and shadow the ascending orbit was used so that for all rock glaciers suitable coverage was available. However, for some rock glaciers no clear signal was found or the movement was too low for a signal. These were classified as “undefined”. The upper boundary is often not clearly visible. The morphological indicators and the interferograms were used as basis for the delineation. Some areas specifically in the glacier forefields in the Upper Left Talgar Valley are characterised by ice-cored moraines and debris-covered ice showing movement and subsidence. Those areas were not included.

The work on this climatic region was conducted by Tobias Bolch.

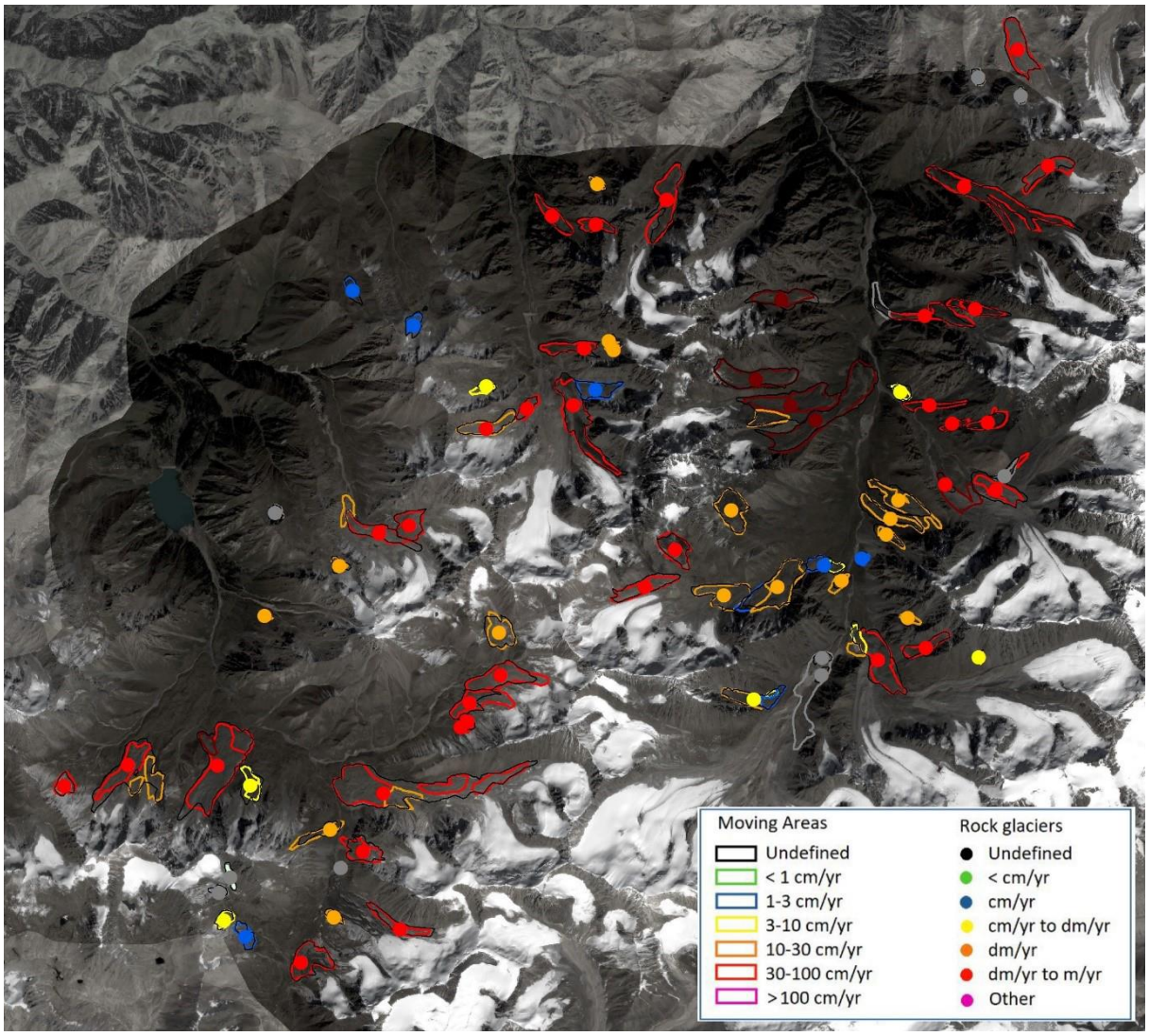

Figure 2.2.8.1: Tien Shan (Kazakhstan-Kyrgyzstan) study area showing the inventory of moving areas and rock glaciers.

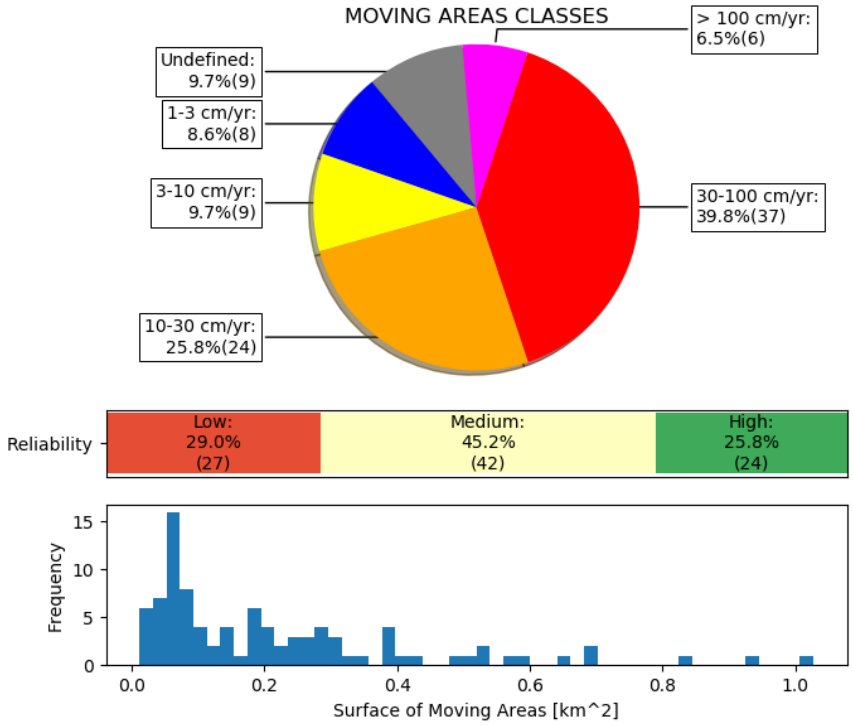

Figure 2.2.8.2: Tien Shan (Kazakhstan-Kyrgyzstan) pie chart of the velocity classes of moving areas (upper part), horizontal bar of reliability of classified moving areas (central part), and histogram of the surface covered by moving areas (lower part).

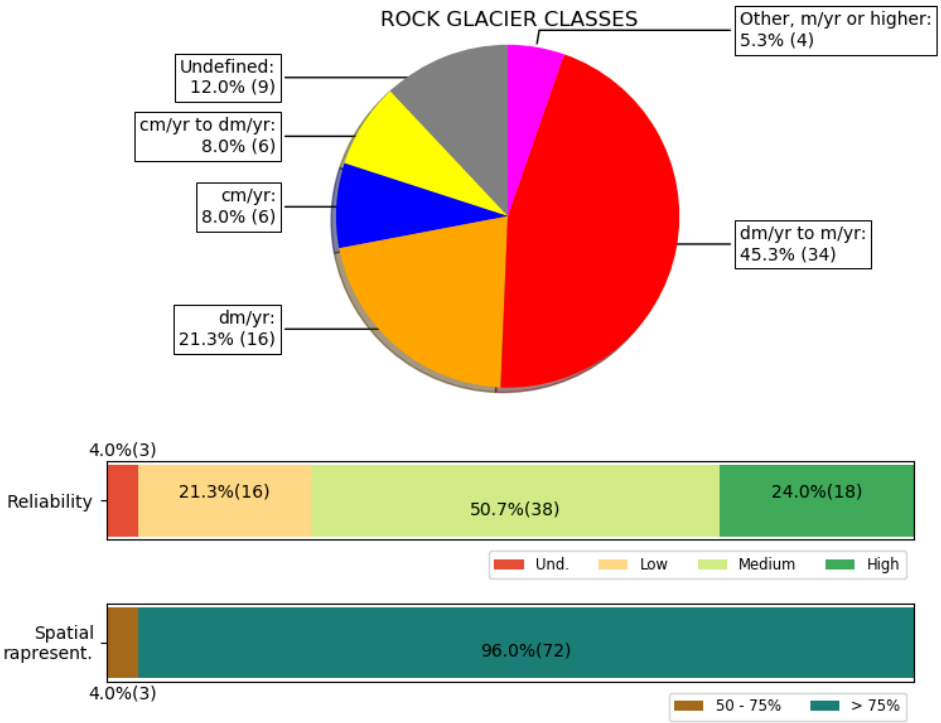

Figure 2.2.8.3: Tien Shan (Kazakhstan-Kyrgyzstan) pie chart of the kinematic classes of rock glaciers (upper part), horizontal bar of reliability of classified rock glaciers (central part), and horizontal bar of the spatial representativeness of classified rock glaciers (lower part).

2.2.9 Brookes Range (Alaska)

Brooks Range is a roughly 1000 km wide mountain range spanning E-W through northern Alaska at a latitude of about 67°N. As test-site, a 1230 km^2 large rectangular shaped area was selected in the midst of the mountain range (Figure 2.2.9.1), including a 50 km long section of the Dalton Highway, connecting Fairbanks and Deadhorse that partly suffers impact from slope motion.

The topography of the test-site is characterized by the main N-S elongated valley along which the Dalton Highway runs in parallel. Its lowest point in the south lies at around 470 m. The point with the highest elevation of about 2100 m is marked by a peak in the northeast of the test-site. Apart from the main valley, several tributary valleys that run N-S as well as a few E-W running valleys are included in the test-site.

An InSAR based inventory of moving areas for the test-site is compiled from different InSAR sources. The main datasets used to determine outlines of the moving areas and the annual velocity for the identified rock glacier features are ALOS-2 PALSAR-2 and Sentinel-1 Interferograms for which a complete coverage in both ascending and descending geometry is available.

The general workflow for the determination of the motion areas started with the identification of motion signatures in the geocoded interferograms and the drawing of the outlines. In a second step, rock glacier type features related to the moving areas inventory were identified with help of optical satellite imagery. As source dataset for the optical images, mainly ESRI World Image (as WMS / Sept. 2020) was consulted. GeoNorth imagery was partly consulted as well. Finally, the kinematics (classified velocity) were determined for each moving area and for each rock-glacier type feature based on the InSAR signature. For this, a characteristic and clear motion pattern was localized within the set of different temporal base lines hence different motion sensitivity. Faster motion was covered mainly in 6- or 12-days Sentinel-1 interferograms.

Based on this approach, of the initially mapped 538 moving areas for the Brooks Range test-site 434 rock glaciers were identified. An overview map and a subdivision into the RG classes is shown in Figures 2.2.9.1, 2.2.9.2 and 2.2.9.3.

In general, especially for the faster moving rock glaciers, the motion signature is sometimes very clear visible in the short-term Sentinel-1 interferograms. For 2018-2019, a large number of mostly coherent interferograms were available. However, local effects (remaining snow, local acceleration) hinder the clear quantification of the velocity classes. Therefore, for most objects, only a single set of interferograms could be used to define the velocity class. This velocity might not be representative for rock glaciers that show strong variability in velocity throughout a year.

On the other hand, L-Band interferograms from ALOS-2 PALSAR-2 are better suited to map and quantify motion over an entire year and in densely vegetated areas, including slower features. However, here only a very limited data set with mainly one single interferogram for an area was available.

Another problem was related to the availability of optical data. The rock glaciers were identified with help of optical satellite imagery. As source dataset for the optical images, mainly ESRI World Image (as WMS / Sept. 2020) and GeoNorth imagery were used. No high-resolution optical data were available on the investigated area. Therefore, it was not possible to provide reliable information about the geomorphological characteristics of the rock glaciers. Attribute fields as the unit morphology, the type of spatial connection to the upslope unit, the degree of destabilization and the spatial representativeness were not provided.

The work on this climatic region was conducted by Rafael Caduff and Magaret Darrow.

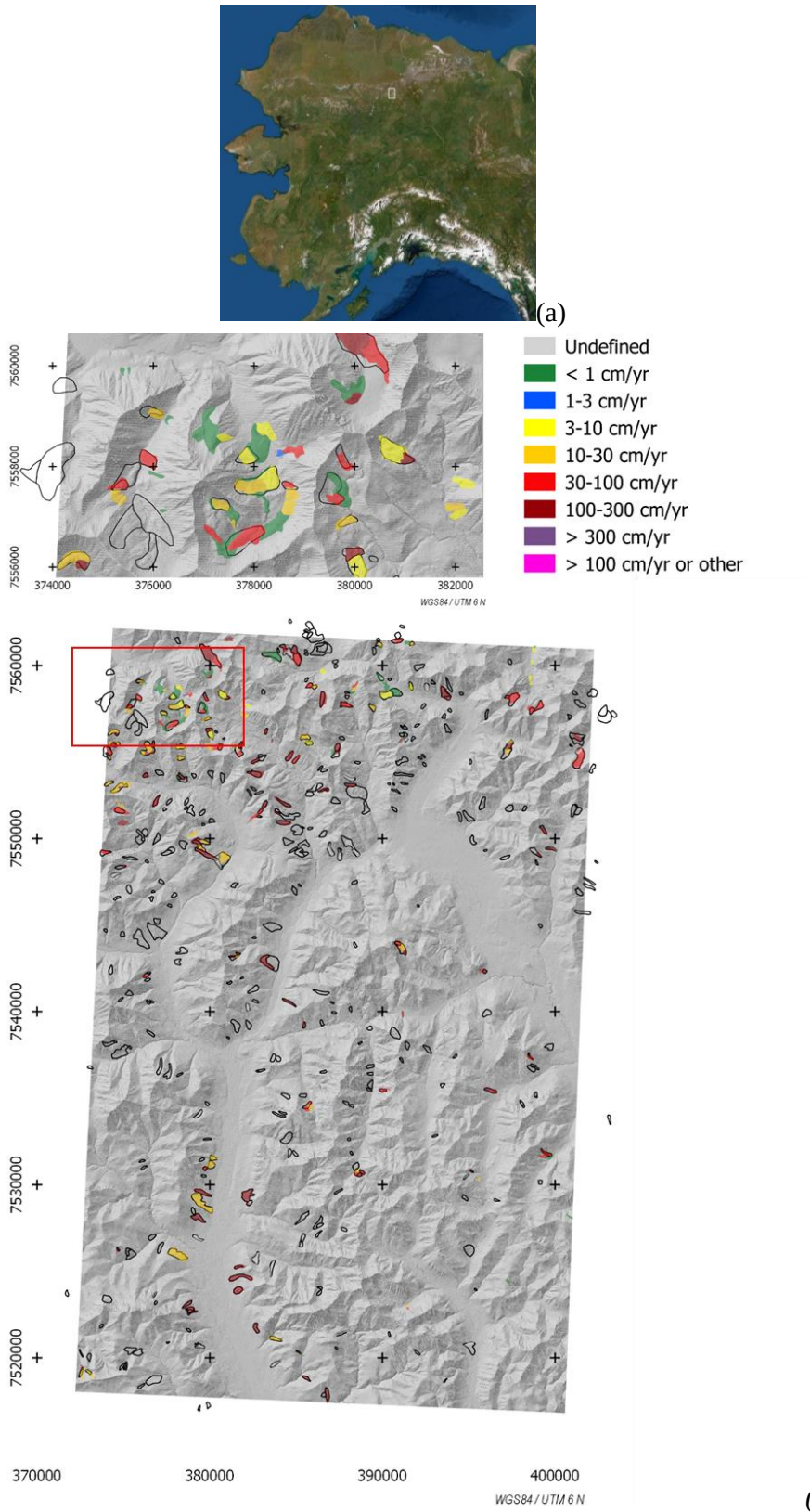

Figure 2.2.9.1: (a) Overview on the Alaska Peninsula and the location of the test-Site (white Rectangle). Background Image: ESRI World Image, accessed: Nov. 2020. (b) Overview and detail overview of the map indicating rock glacier motion. The classification follows the scheme as shown in the legend section. Black outlines indicate the areas of motion not related to rock glacier.

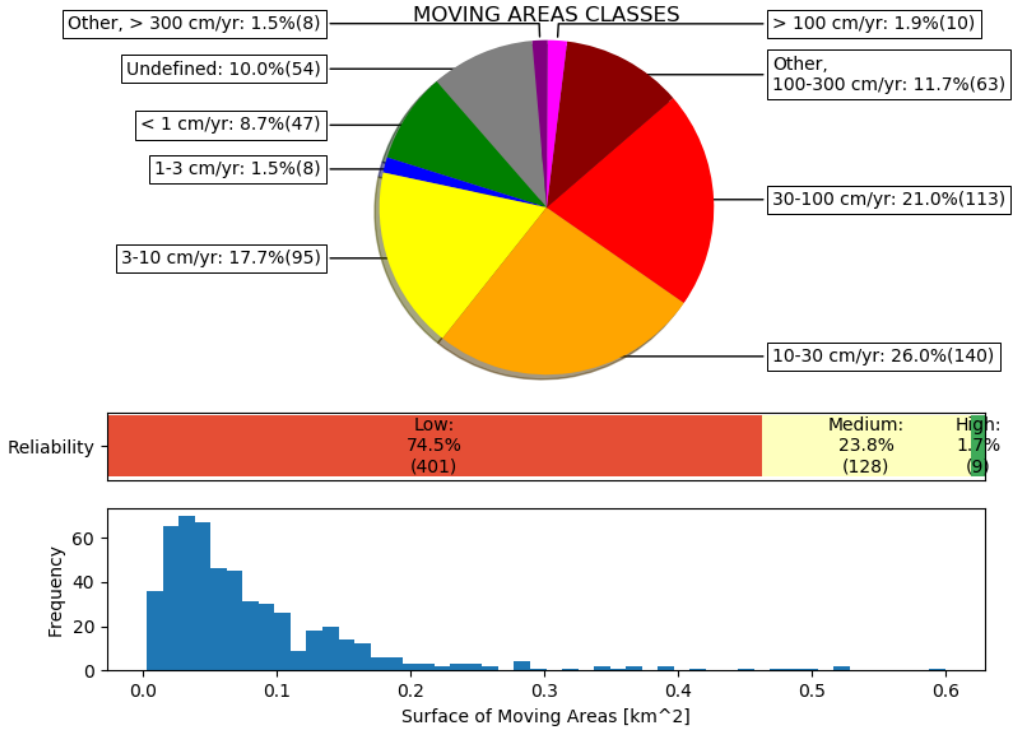

Figure 2.2.3.2: Brookes Range (Alaska) pie chart of the velocity classes of moving areas (upper part), horizontal bar of reliability of classified moving areas (central part), and histogram of the surface covered by moving areas (lower part).

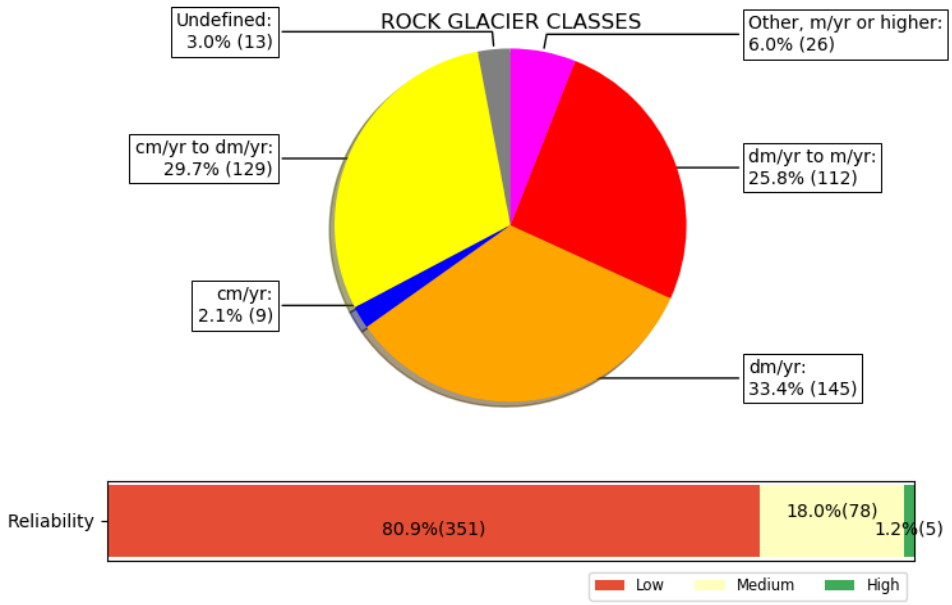

Figure 2.2.3.3: Brookes Range (Alaska) pie chart of the kinematic classes of rock glaciers (upper part), horizontal bar of reliability of classified rock glaciers (central part), and horizontal bar of the spatial representativeness of classified rock glaciers (lower part).

2.2.10 Central Andes (Argentina)

The investigated area (Figure 2.2.10.1) is situated in the Central Andes of Mendoza, Argentina. The region corresponds to the most southern part of the Dry Andes, where extensive areas with permafrost conditions are found. Most of the selected area consists of the Cordón del Plata mountain range, Cordillera Frontal, where the maximum height surpasses 6000 m, and the minimum altitude is approx. 2000 m. Furthermore, over this region, permafrost occurs from ~3600 m on upwards (Trombotto Liaudat, 2000; Ruiz and Trombotto Liaudat, 2012).

Here an area of 2940 km^2, with centre in Cordón del Plata of the Central Andes of Argentina, was selected to analyse the data. This region is the home of the most extended active-layer monitoring record in Argentina (continuously since 1999). It is where one of the most studied rock glaciers of the Southern Andes, Morenas Coloradas rock glacier, is located and where some of the unique surface velocity measurements have been performed (Trombotto and Borzotta, 2009; Trombotto, 2014; Bodin et al., 2015; Trombotto-Liaudat and Bottegal, 2019). Inside the study area, there is one of the real-time automatic weather stations of the IANIGLA Network (http://estaciones.ianigla.mendoza-conicet.gob.ar/). The automatic weather station (AWS) called Morenas Coloradas (3400 m) is located at the front of the well-known rock glacier, and it has been operated since February of 2018. There are seven other AWS complementing the network in the region. Some of them, like Toscas or Horcones, have been operated for almost 20 years. Previous and discontinuous weather data indicates that, in this region, at around 2500 m a.s.l., the mean annual air temperature is around 6-7°C and total annual precipitation is around 400-500 mm.

The selected area is one of the Central Andes regions, where most rock-glaciers and debris-covered-rock glaciers are located. Almost 25% of the debris-covered and rock glaciers identified in the National Glacier Inventory of Argentina (IANIGLA and MAyDS, 2018) are located inside the selected area and due to the North-South orientation of Cordon the Plata, glaciers, rock-glaciers and transitional landforms area oriented to the East or West.

For the Central Andes of Argentina rock glacier inventory, the recently published glacier and rock glacier inventory of Argentina (Zalazar et al., 2020) was used. All ice masses larger than 0.01 km^2 were included in the inventory. Rock glaciers and sections of debris-covered glaciers were manually digitized using a combination of medium to very-high spatial resolution images (ASTER, ALOS, SPOT, CBERS-2). Along the Southern Andes of Argentina, rock glacier units were mapped using a limited footprint (i.e., the frontal and lateral talus were not included). The extent of the rock glaciers was limited to where permafrost creep was evident considering the surface morphology (i.e., the talus was not included). Where there was no clear boundary between rock glaciers and debris-covered glaciers (upper unit), they were mapped together and described as “debris-covered ice with rock glaciers”. In those cases, the upper clean ice and the following debris-covered ice with rock glaciers were grouped and assigned the larger unit's IDs but differentiated by their morphological characteristics in the database.

For the Central Andes, interferograms from Sentinel-1 and ALOS-1 PALSAR-1 were available to interpret surface displacement between 2018 and 2020, with both ascending and descending geometries. Also, there were delivered displacement maps along the LOS in m/yr obtained by stacking 6- or 12-days Sentinel-1 interferograms for this site.

The most useful data source was Sentinel-1 interferograms, with time intervals between 6 to 48 days. For more extended periods and the ALOS-1 PALSAR-1 interferograms, the data was too noisy. The displacement maps look very promising to assess the surface velocity of rock glaciers. Still, they seem

to have a threshold for surface velocity above 1 m/yr, which inhibits assessing the maximum surface velocity in most of the most massive rock glaciers. The displacement maps were also made from interferograms of medium to late summer (February to May). So, they only provide summer surface velocities. However, the kinematic information can be deduced from all available interferograms, thus including the autumn, winter and spring periods.

Based on the InSAR data, a total of 837 moving areas related to glaciers, debris-covered, and rock glaciers were detected (Figure 2.2.10.1, 2.2.10.2, 2.2.10.3 and 2.2.10.4). For those moving areas that are related to glaciers or which partially included debris-covered ice, it was highlighted in the remarks that these polygons "contain glacier or debris-covered glacier". When possible, over these complex landforms, the areas with different surface velocities were identified. For some of them, like in Morenas Coloradas o Vertiente glaciers, it is possible to separate the clean ice and debris-covered ice from the rock glacier based one using the surface velocity. Most of the time, clean ice and debris-covered glaciers are characterized as moving areas with surface displacement higher than 1 m/yr. However, for most of them, high velocity was interpreted from decorrelated interferograms with time steps of 6 or 12 days, which could also be related to ablation and changing surface morphology. But for others, the 6 day time step interferograms from late autumn of winter seasons provide coherent fringe cycles that allow more confidence in the surface velocity estimation. Meanwhile, most rock glaciers are characterized by surface velocities of 30 to100 cm/yr.

It was also possible to identify well-defined moving areas, related to the creep of mountain permafrost, that were not included in the Glacier Inventory of Argentina.

A total of 580 rock glaciers and 95 debris-covered glaciers with rock glaciers were identified in the study area (Figure 2.2.10.1, 2.2.10.2, 2.2.10.3 and 2.2.10.4). Those classified by the National glacier inventory of Argentina as "debris-covered glaciers with rock glacier" were identified in the remarks field with the legend "Complex form connected to the debris-covered glacier". For most of the rock glaciers, it was possible to characterize the kinematics. Nevertheless, for some small rock glaciers or those oriented North-South, it was impossible to assess the surface velocity. Most of the rock glaciers characterized from the surface morphology as inactive rock glaciers by the National Glacier Inventory of Argentina have undefined surface velocity.

Interferograms with time steps larger than 48 days were too noisy to detect moving areas. Some small rock glaciers could not be identified as moving areas. The coarse spatial resolution of the DEM (10 m) used to build the interferograms, and the location of some of these small rock glaciers could be a source of these problems in classification. Some rock glaciers are in areas with radar foreshortening, layover or shadow for both ascending and descending geometries. The interferograms from ALOS-1 PALSAR-1 and -2 were not used for interpretation. They were noisier than Sentinel-1 interferograms.

In some cases, the rock glaciers are connected with a debris-covered glacier in the upper part. The boundary between rock glaciers and debris-covered glaciers (upper unit) is sometimes unclear. This limitation was reduced by combining rock glaciers and the connected debris-covered glacier in the map. For these cases, the remark “debris-covered ice with rock glaciers” within the rock glaciers attribute table was added.

The work on this climatic region was conducted by Lucas Ruiz.

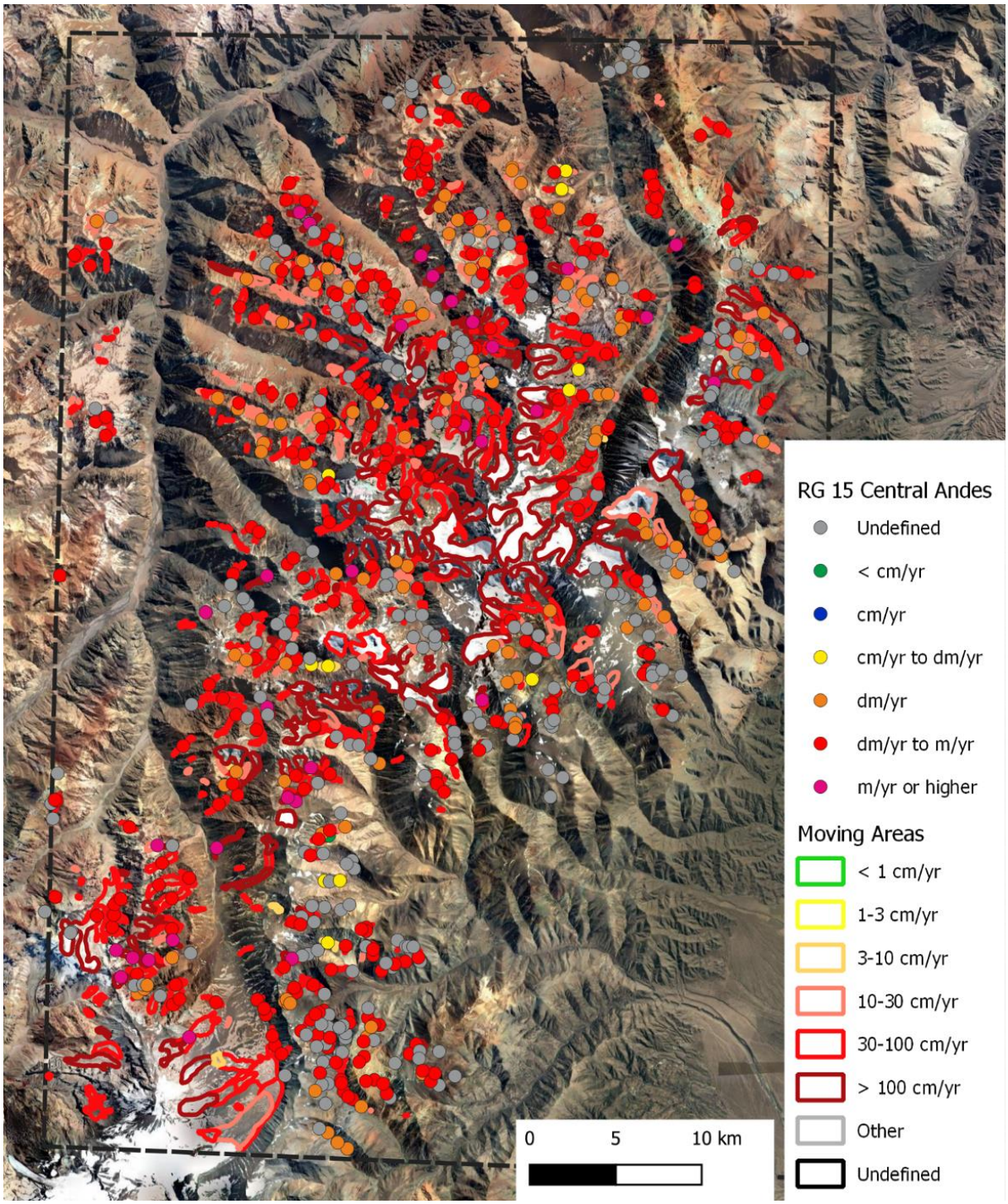

Figure 2.2.10.1: The overview map of the selected study area in the Central Andes of Argentina.

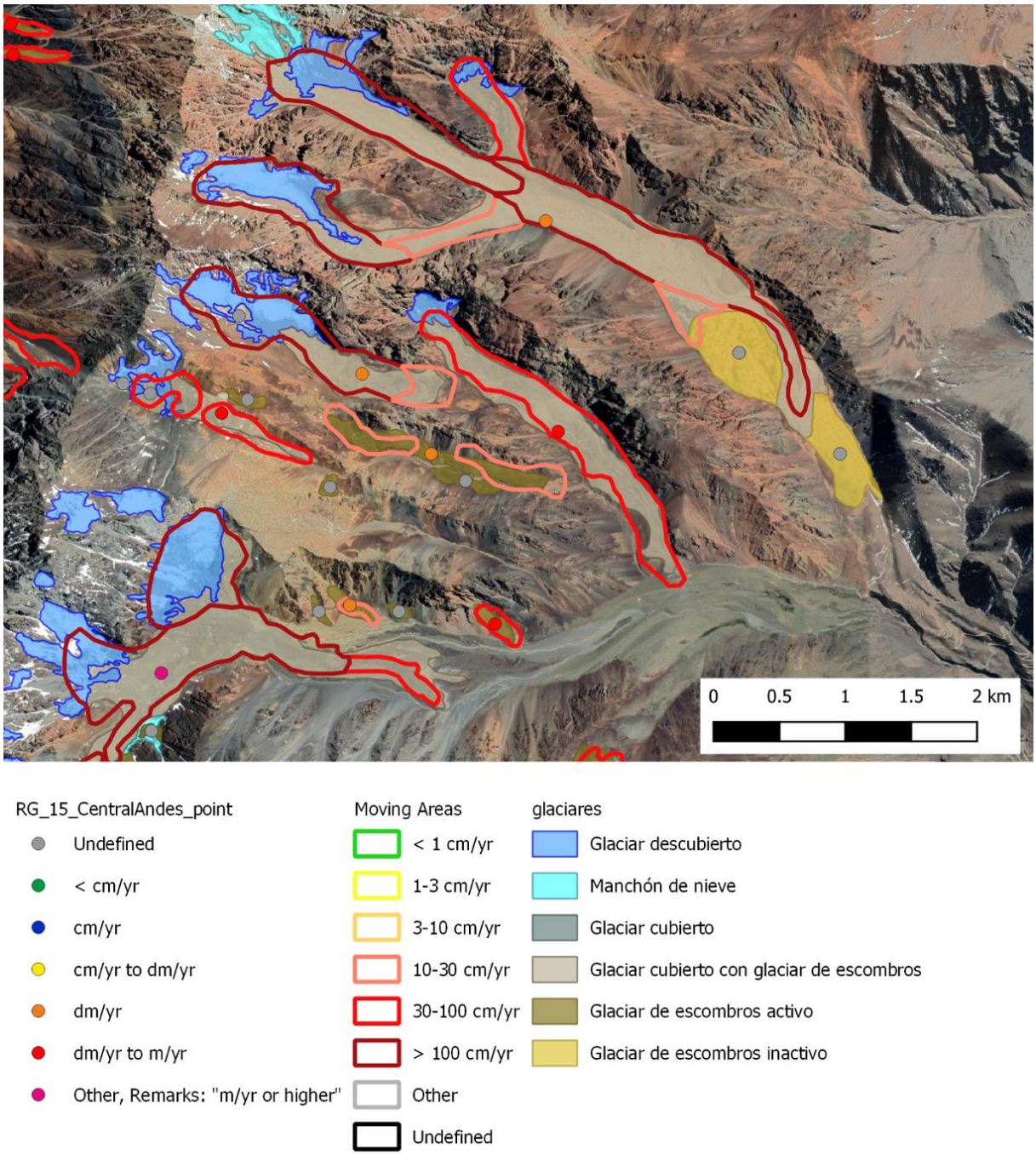

Figure 2.2.10.2: Example of the moving area and rock glacier identification for complex debris-covered and rock glaciers identified in the National Glacier Inventory of Argentina.

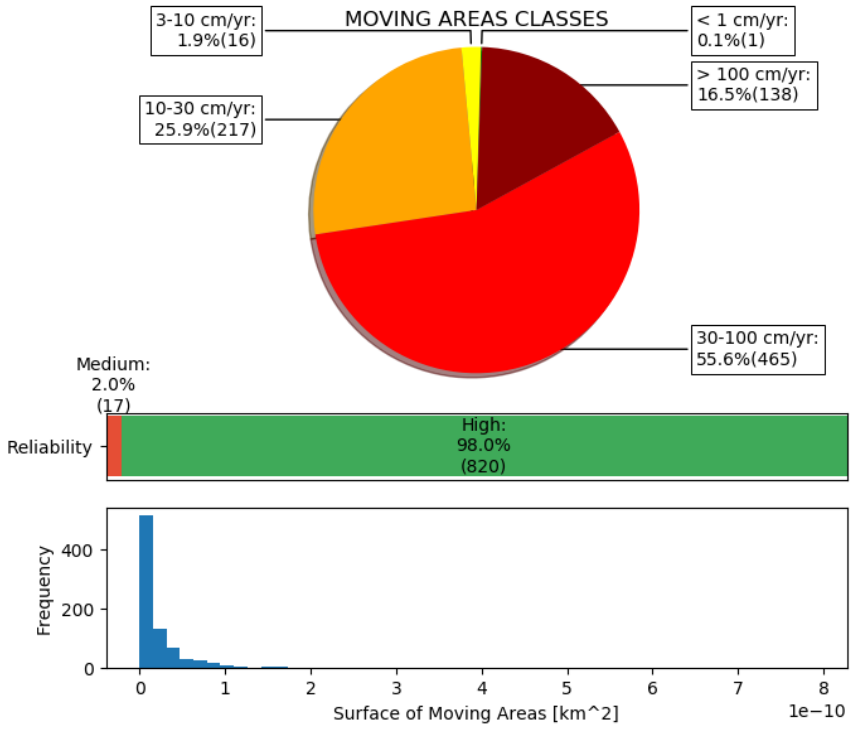

Figure 2.2.10.3: Central Andes (Argentina) pie chart of the velocity classes of moving areas (upper part), horizontal bar of reliability of classified moving areas (central part), and histogram of the surface covered by moving areas (lower part).

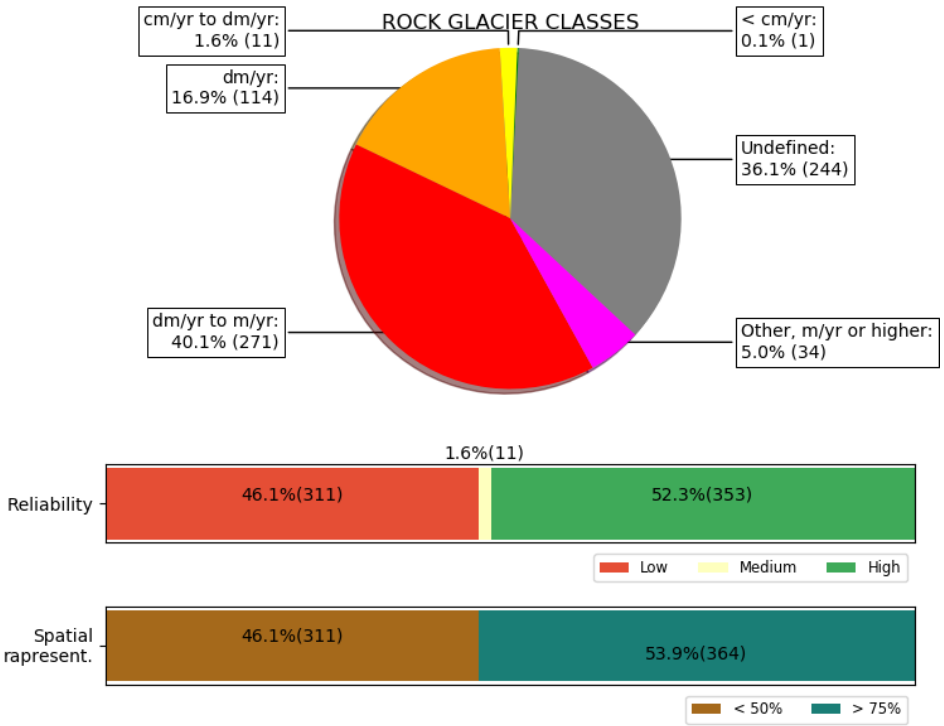

Figure 2.2.10.4: Central Andes (Argentina) pie chart of the kinematic classes of rock glaciers (upper part), horizontal bar of reliability of classified rock glaciers (central part), and horizontal bar of the spatial representativeness of classified rock glaciers (lower part).

2.2.11 Southern Alps (New Zealand)

The Southern Alps of New Zealand are an elongated mountain range of ~800 km length and ~60 km width crossing nearly the entire Southern Island from north-east to south-west. The highest elevation is reached at Mount Cook (3724 m a.s.l.). The orientation of the Southern Alps perpendicular to the main oceanic perturbations coming from the west provokes a strong precipitation gradient from west to east. Precipitations are intense in the west and around the Main Divide (i.e. the main crest) and decrease strongly towards the east. As a consequence, glaciers are numerous around the highest areas close to the Main Divide, hindering the presence of rock glaciers.

An inventory of rock glaciers in the Southern Alps performed by Sattler et al. (2016) showed that all the rock glaciers are located in the south-east side of the Main Divide, where glaciers are reduced in area, and that the active landforms are concentrated in the central part of the range, where elevations higher than 2000 m a.s.l. are present. According to this study permafrost is possible above 1850 m a.s.l. in south-exposed slopes.

Interferograms from Sentinel-1 were computed from both Track 23 ASC and Track 146 DSC. Because of the location of the Southern Alps in the southern hemisphere, only images acquired between January and October (in the unfrozen summer periods) were used, in order to avoid the presence of snow cover. We used two sets of data processed by Gamma Remote Sensing for the years 2015-2018 and the years 2018-2019. The first set contained 12 interferograms from the ascending orbit and 11 interferograms from the descending one. The second set contained 10 interferograms from each orbit. Time intervals were of 6, 12, 24, 48, 72, 360, 366, 372, 726, 732 days. Interferograms from ALOS-2 PALSAR-2 were also available but generally too noisy for being used.

The analysis of the moving areas and of the rock glaciers was made using orthoimages downloaded from the LINZ (Land Information New Zealand) data service as well as Google Earth images.

The interferograms available for this study were generally relatively noisy, probably because of the humid climate provoking signal perturbation. They were especially noisy in steep areas, like in talus slopes, showing many signals without any geomorphic significance. In addition, many rock glaciers are south-north oriented, thus not in an optimal configuration for InSAR analyses. Signal identification was thus challenging. To ensure the highest degree of reliability, the analyses were performed independently by two operators. The computed velocities were also validated on two specified rock glaciers in the Irishman Stream valley - Ben Ohau range - with GNSS surveys.

A total of 112 active rock glaciers were identified with InSAR (Figures 2.2.11.1 - 2.2.11.3). The large majority of them is present in three mountain ranges: the Ben Ohau Range (west of Lake Pukaki), the Liebig range (north-west of Lake Tekapo) and the Two-Thumb range (east of Lake Tekapo) (Figure 2.2.11.1). A few rock glaciers are also present in the west of Lake Ohau and in the area of Lake Heron and Lake Coleridge. Regarding the size of the Central Southern Alps, the number of active rock glaciers is relatively low. Two reasons for this can be identified. First, the vertical extension of the periglacial belt is limited due to the humidity of the climate, which implies low glacier equilibrium line altitudes. Second, many areas present steep and well-developed valley slopes, a topography not suitable for rock glaciers. On the other hand, relict rock glaciers are widespread and reach great dimensions.

Generally speaking, rock glacier velocities in the Southern Alps are very low. About half of the detected rock glaciers have velocities in the order of cm/yr and only 10% of the rock glaciers have velocities higher than the class dm/yr (Figures 2.2.11.2 and 2.2.11.3). The highest velocities are generally found in the northern parts of the ranges. The reasons for such low velocities have still to be

investigated but are probably linked to relatively cold summer air temperatures due to the oceanic climate.

The work on this climatic region was conducted by Christophe Lambiel.

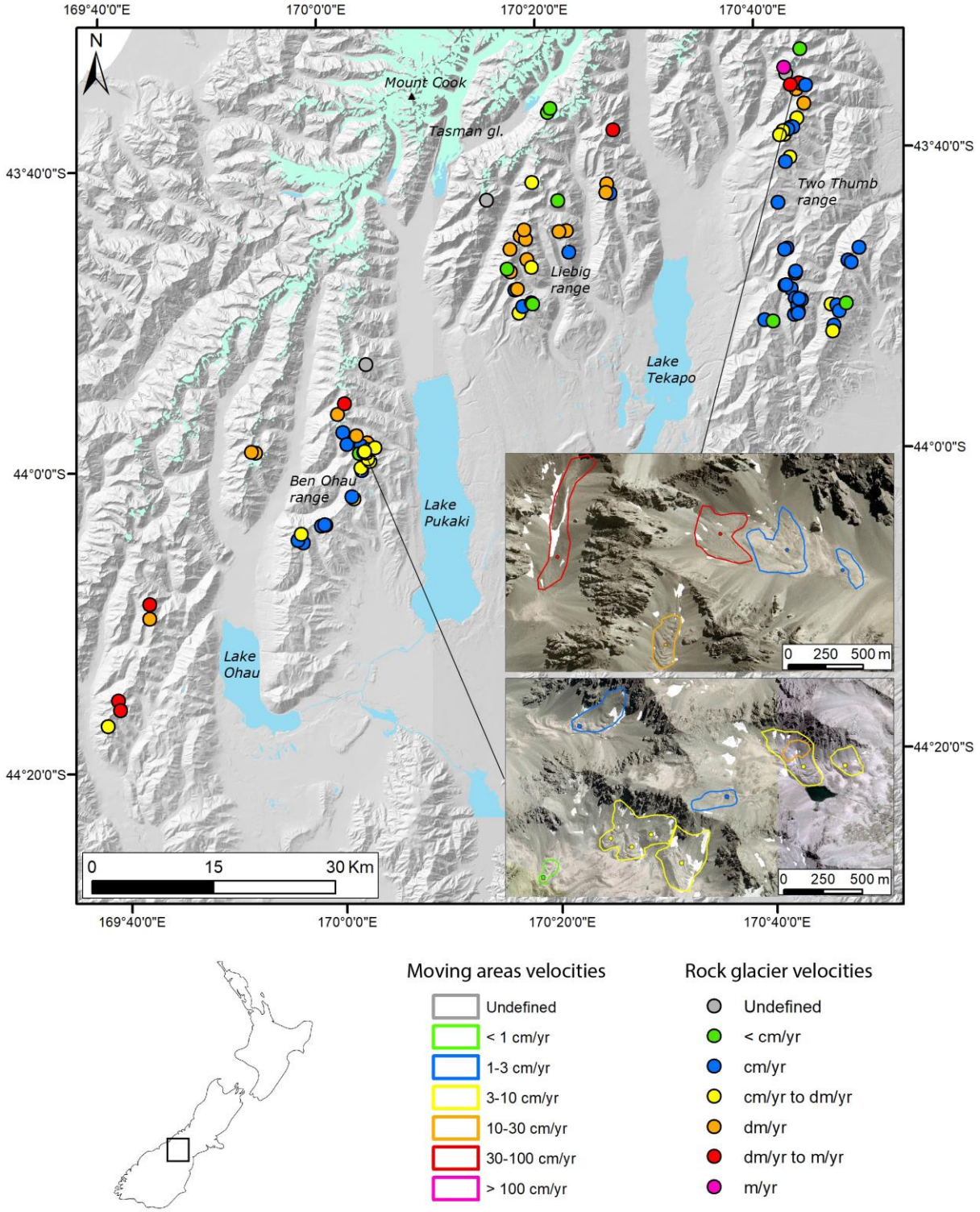

Figure. 2.2.11.1: Rock glacier inventory in the Central Southern Alps, with 2 examples of sectors from the Ben Ohau range and the Two Thumb range. The few rock glaciers of Lake Heron and Lake Coleridge areas are not shown here.

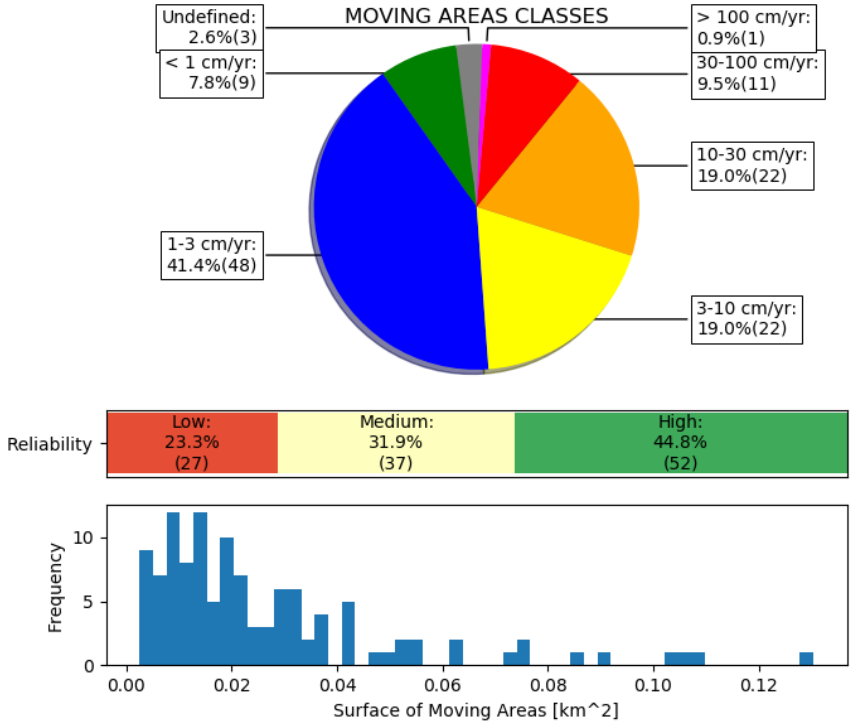

Figure 2.2.11.2: Southern Alps (New Zealand) pie chart of the velocity classes of moving areas (upper part), horizontal bar of reliability of classified moving areas (central part), and histogram of the surface covered by moving areas (lower part).

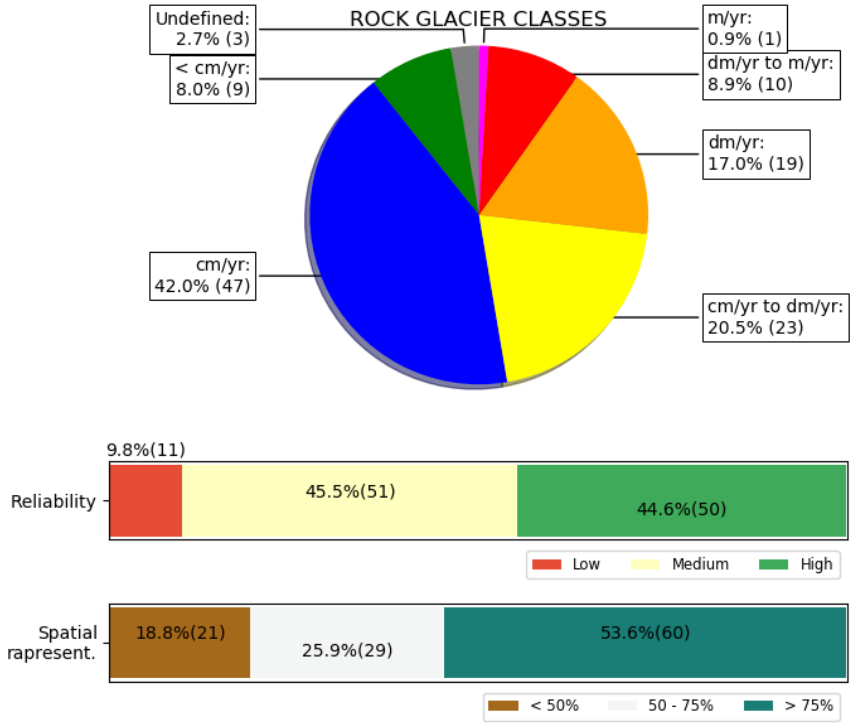

Figure 2.2.11.3: Southern Alps (New Zealand) pie chart of the kinematic classes of rock glaciers (upper part), horizontal bar of reliability of classified rock glaciers (central part), and horizontal bar of the spatial representativeness of classified rock glaciers (lower part).

2.3 Data availability and release

The product will be made available through the IPA action group webpage on the website of University of Fribourg.

3 Rock glacier kinematic time series (RGK)

3.1 Introduction

On a global scale, the evolution of mountain permafrost is scarcely observed, predominantly by temperature monitoring in a few boreholes, whose long-term maintenance is particularly challenging. A large majority of periglacial mountain areas worldwide are thus lacking permafrost monitoring data. Therefore, the response of mountain permafrost to ongoing climate evolution cannot be depicted in most regions on Earth. Several studies conducted in the European Alps for the last two decades have shown that there is a dependency of rock glacier interannual behaviour on permafrost temperature, the latter particularly impacting the rheological and hydrological properties of the frozen ground (Ikeda et al., 2020; Kääb et al., 2007). It has been observed that rock glaciers tend to accelerate on an interannual basis under warmer conditions as long as the permafrost degradation has not become too severe to counter it (Delaloye et al., 2010; Eriksen et al., 2018; Roer et al., 2008). In addition, rock glaciers tend to display a concomitant regional behaviour: namely, interannual acceleration and deceleration are occurring at almost the same time and in the same proportion in a given region, independently of the activity rate and the morphological characteristics of the rock glaciers (Delaloye et al., 2010). Finally, continuous or seasonal monitoring has shown that the observed rock glaciers develop a landform-specific but repetitive intra-annual behaviour, whose inter-annual variations do not significantly alter the pluri-annual trends. Between the 1980s and the 2010s, most rock glaciers in the European Alps have increased their annual velocity rate by a factor 2 to 10. A similar evolution can be expected to have occurred or to occur in the future in many other mountain ranges depending on their specific climatic settings.

Remote sensing data allow the production of kinematical information on many widespread rock glaciers. The increasing emergence of open-access and high-resolution satellite imagery (e.g. optical, SAR) facilitates the set-up of regional surveys worldwide, making it possible to compute rock glacier kinematics time series, to investigate the occurrence of concomitant regional behaviours, and to evaluate their climatic significance. Exploiting the availability of remote sensing data on tens of thousands of rock glaciers, and even more, to explore the concomitance of their kinematical behaviour and to develop a regional index (or parameter) evidencing the evolution of mountain permafrost based on rock glacier kinematics is the challenge raised by the IPA (International Permafrost Association) Action Group Rock glacier inventories and kinematics (2018-2022) in its Task 2. This task aims to explore the feasibility of preparing products that could serve the monitoring of rock glacier kinematics as an associated parameter of the ECV (Essential Climate Variable) Permafrost in a climate-oriented perspective. Rock Glacier Kinematics (RGK) has been also submitted by GTN-P in December 2019 as a new associated parameter (product) to the variable ECV Permafrost to GCOS (Global Climate Observing System) regarding its new implementation plan. The product definition sheet was put out for public consultation in mid-January 2020.

The IPA Action Group Rock glacier inventories and kinematics document “Rock glaciers kinematics as an associated parameter of ECV Permafrost” [RD-31] released in January 2020, provisionally set the necessary concepts for standardizing the production and exploitation of rock glacier kinematic time series in a climate-oriented perspective. RGK would consist of collected individual kinematical time series, which are fulfilling standardized requirements (to be defined), in order to provide the basis for producing regional indices. More specifically, 1st-level data would consist of individual kinematic

time series having an annual or pluri-annual resolution expressing a velocity. 2nd-level data would consist of individual kinematic time series having an annual or pluri-annual resolution expressing a relative velocity to a reference time. A regional index (or parameter) would then be an assemblage (e.g. mean) of selected 2nd-level time series. The document has been discussed during a dedicated workshop in February 2020 in Fribourg (Switzerland). However, because of the COVID-19 outbreak crisis since early 2020, the final version of the guidelines, intended to be made available in June 2020 will only be ready in winter 2021 at earliest.

With the aim of producing a regional RGK index, individual kinematic time series are requested. Therefore, within CCN2 of the ESA CCI+ Permafrost project we concentrated so far on the implementation of remote sensing methods to automatically produce annual or pluri-annual velocity values on specific rock glaciers (1st-level data). Rock glaciers on which a climate-oriented monitoring is feasible strongly dependent on site-specific favourable configurations. For the selection of the correct rock glaciers and locations, the availability of a rock glacier inventory is obviously needed. As these products were just released within this project, the number of sites currently analysed is scarce, but can be steadily increased in the future.

3.2 RGK examples

Sentinel-1 InSAR time series processing chains have been set up according to the specifications described in the ATBD [RD-24] and following the methodology published by Strozzi et al. (2020). Examples of time series are shown thereafter for the Swiss Alps, Norway, Svalbard and Disko Island. Further refinements are required to be able to monitor many more rock glaciers, with the objective to provide 2nd-level products and regional indexes. Processing lines to compute the displacement fields of rock glaciers using offset tracking on repeat SAR data and feature tracking on repeat optical airphotos were also set up according the specifications described in the ATBD [RD-24]. Examples of such displacement maps and time series are shown thereafter for the Swiss Alps and Norway (Region IDs 06, 08, 09 and 12, see also PSD [RD-21]).

The initial results shown below enable already a number of important conclusions, among others: The proposed methodology turns out very well feasible and promises a large step forward in global monitoring of rock glacier movement. The success of the method opens up a completely new field for the application of SAR (i.e. worldwide rock glacier monitoring). The examples exhibit a large variation of seasonal and interannual rock glacier velocity variations. The examples given cover already the full range of high to low overall velocities, large and small velocity variations, and increasing and stable interannual evolution of velocities. Some rock glaciers seem to have large velocities throughout much of the year, some seem to become almost inactive over winter.

06-Swiss Alps

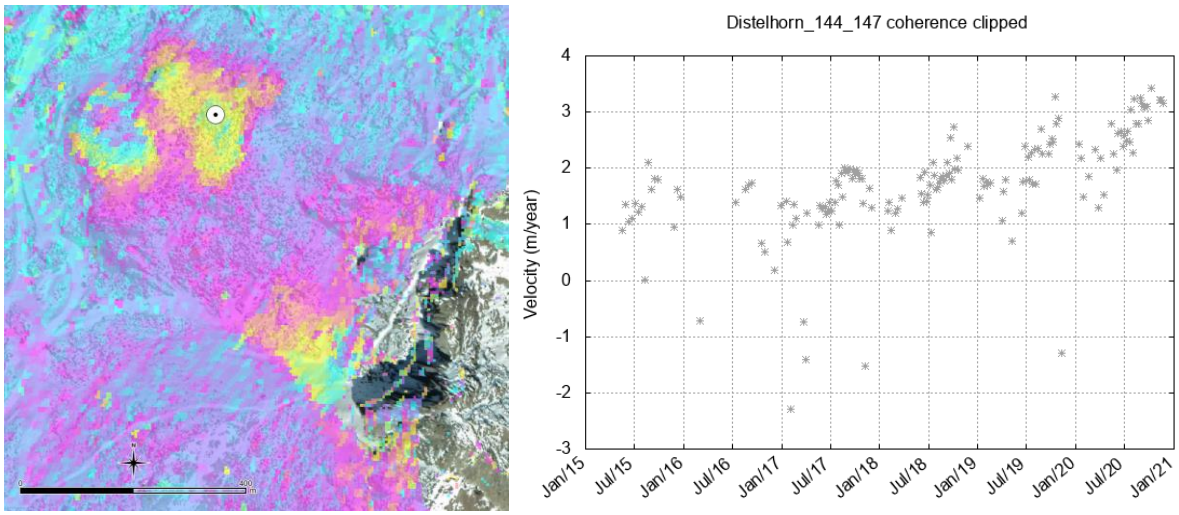

Pt1-Swiss Alps-Distelhorn (VS), 632935 E / 115615 N
(http://www.google.com/maps/place/46.19119,7.86524), differential Sentinel-1 interferogram (left) and velocity projected along slope (right)

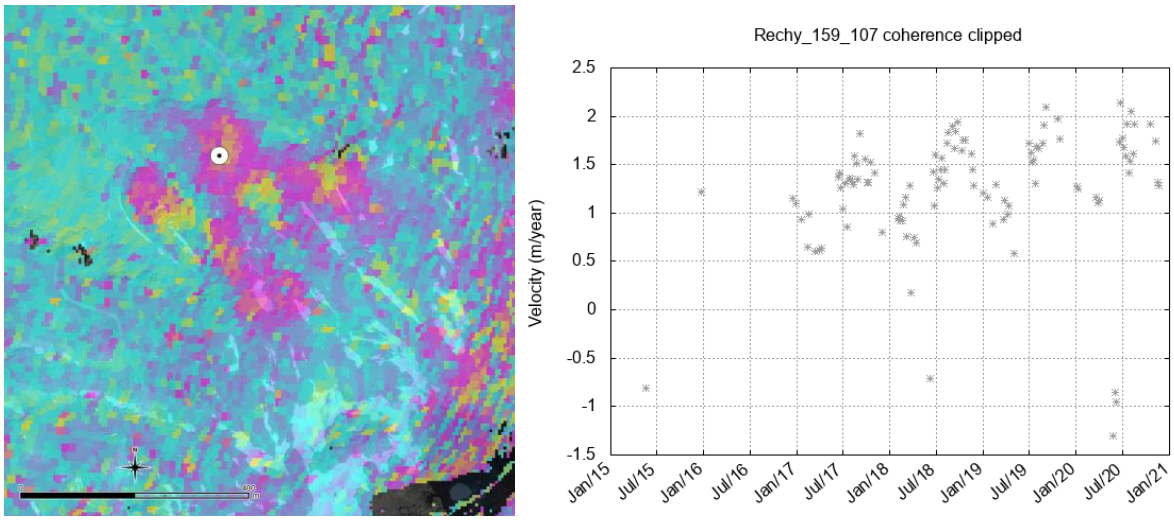

Pt2-Swiss Alps-Rechy (VS), 605615 E / 113560 N
(http://www.google.com/maps/place/46.17349,7.51134),
differential Sentinel-1 interferogram (left) and velocity projected along slope (right)

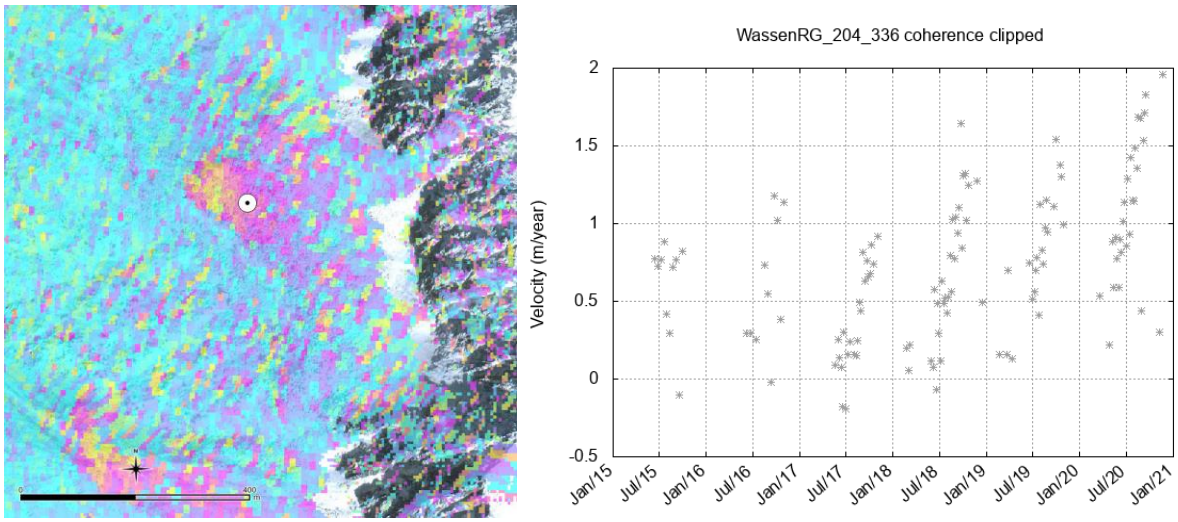

Pt3-Swiss Alps-Wassen (UR), 691100 E / 172000 N (http://www.google.com/maps/place/46.69299,8.62966), differential Sentinel-1 interferogram (left) and velocity projected along slope (right)

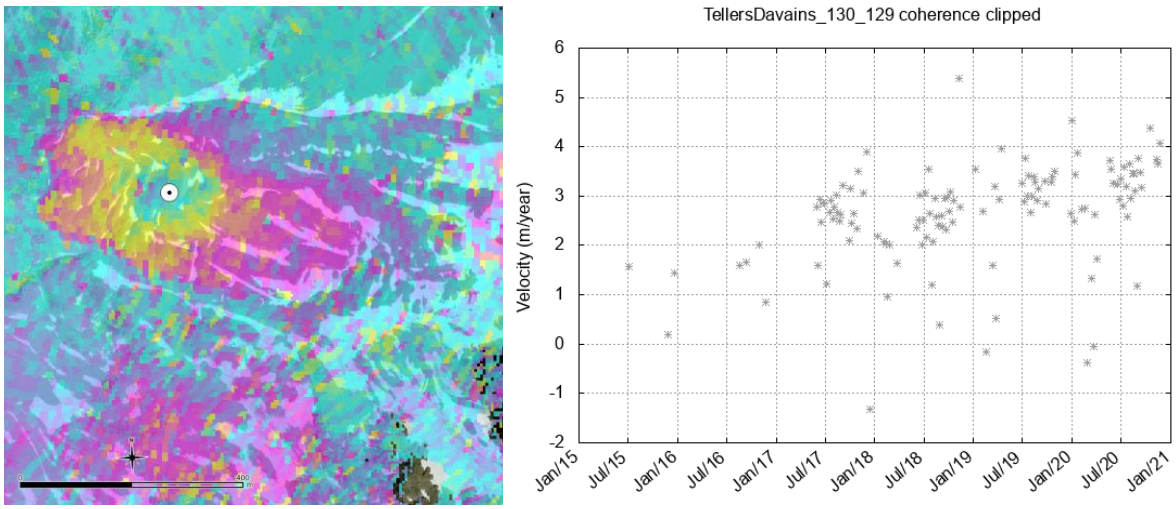

Pt4-Swiss Alps-Tellers Davains (GR), 771815 E / 156555 N (http://www.google.com/maps/place/46.53821,9.6787), differential Sentinel-1 interferogram (left) and velocity projected along slope (right)

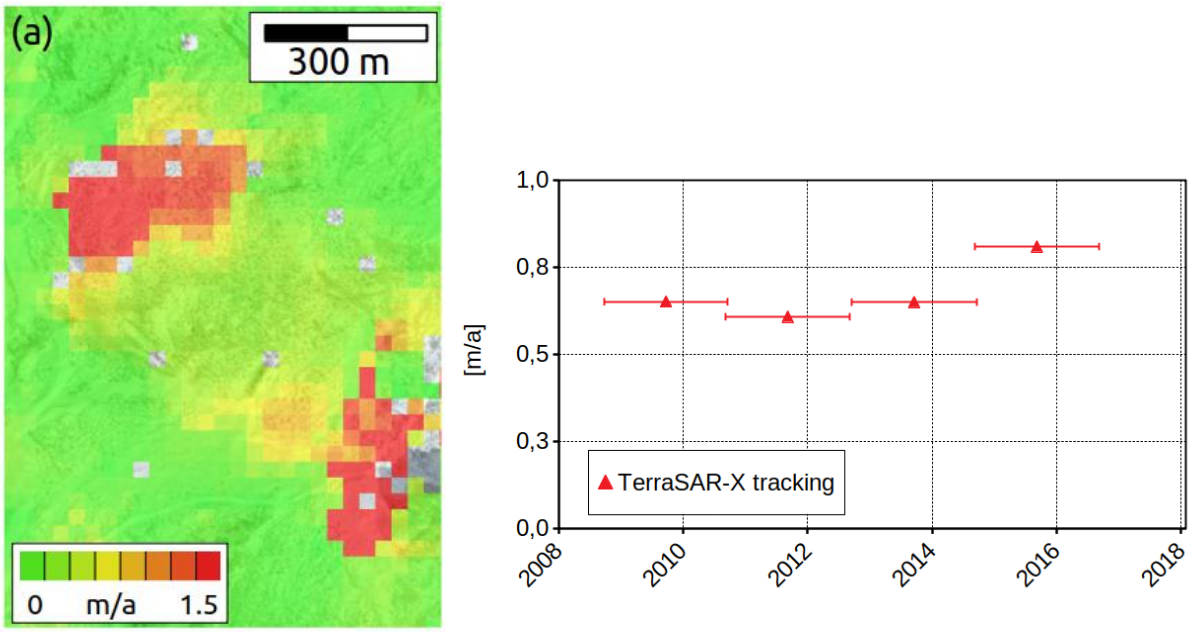

Pt5-Swiss Alps-Distelhorn (VS), 632935 E / 115615 N (http://www.google.com/maps/place/46.19119,7.86524), horizontal velocity map from TerraSAR-X offset tracking between 11.09.2014 and 06.09.2016 (left) and velocity projected along the terrain surface (right), modified after Strozzi et al., 2020

07-Troms

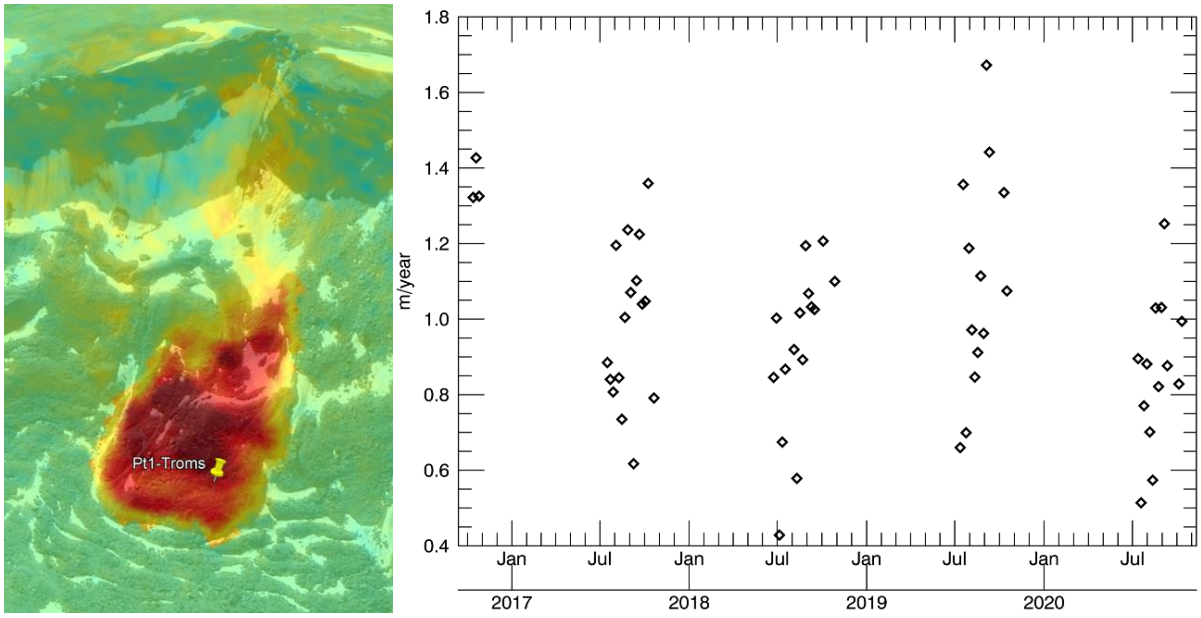

Pt1-Troms-Moldojohka. Left: average of 6 days interferograms along LOS. Right: 6 days InSAR time series projected along the local slope (angle: 24.2°, aspect: 40.8). Point location: 69°26’38.62’’N 20°42’23.54’’E / CCI-07-0172 rock glacier system in RGI

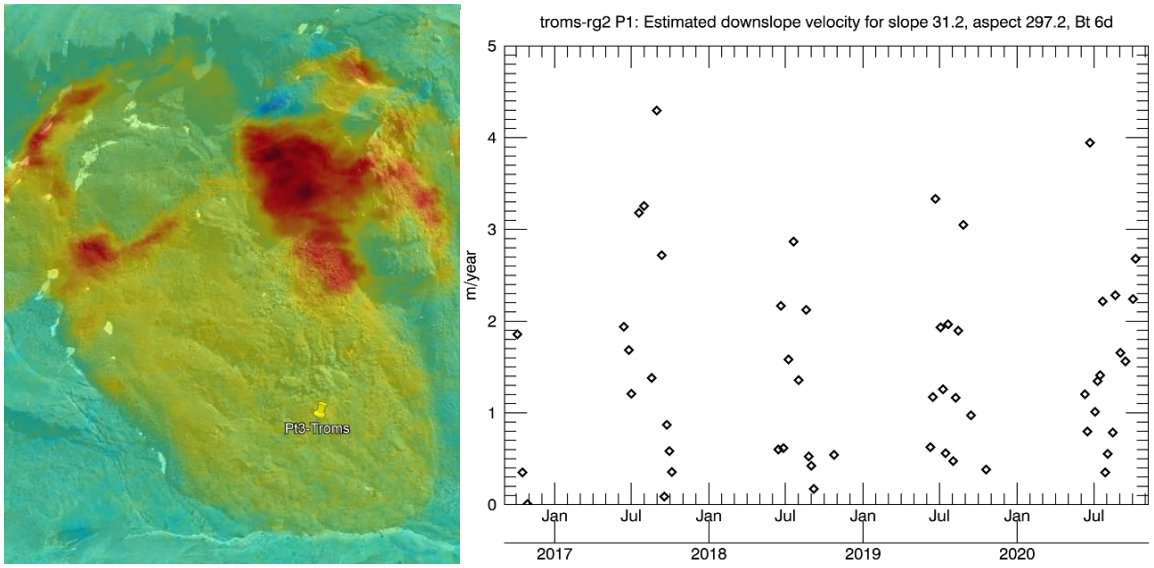

Pt2-Troms-Njárgavárri. Left: average of 6 days interferograms along LOS. Right: 6 days InSAR time series projected along the local slope (angle: 31.2°, aspect: 297.2). Point location: 69°30’42.91’’N 20°54’48.28’’E / CCI-07-0176 rock glacier system in RGI

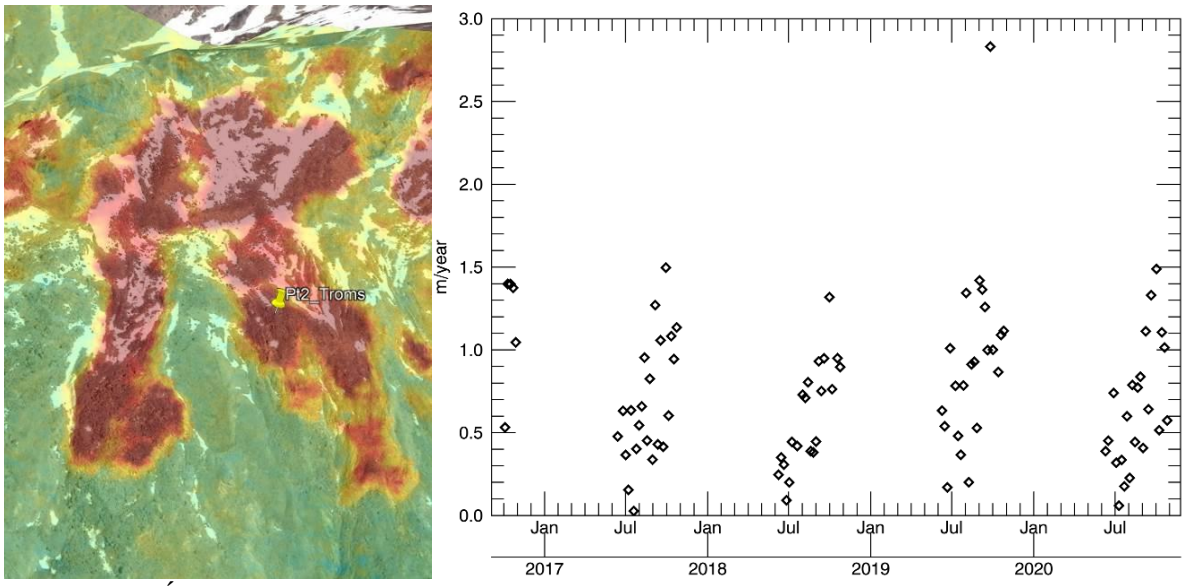

Pt3-Troms-ÁdjetEast. Left: average of 6 days interferograms along LOS. Right: 6 days InSAR time series projected along the local slope (angle: 29.2°, aspect: 213.3). Point location: 69°21’20.92’’N 20°27’03.132’’E / CCI-07-0294 rock glacier system in RGI

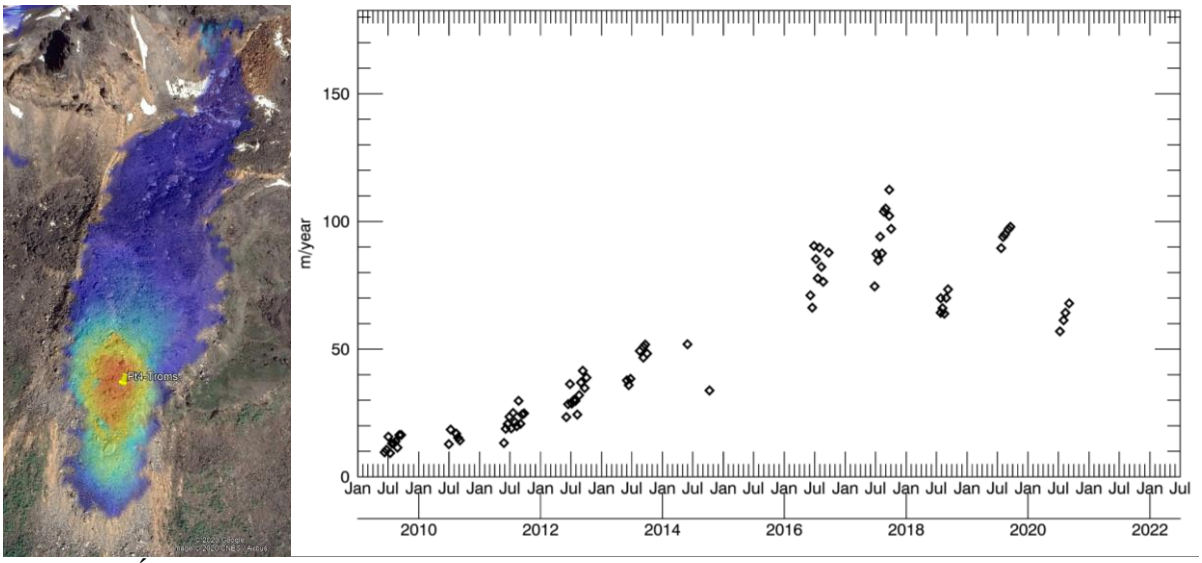

Pt4-Troms-ÁdjetWest. Destabilized rock glacier previously studied by Eriksen et al., 2018. SAR offset tracking based on TerraSAR-X Stripmap images (6 days pairs, in rane/azimuth plane). Left: SAR offset tracking average 2009-2020. Right: Updated SAR offset tracking time series until 2020. Point location: 69°21’46.04’’N 20°24’22.95’’E / CCI-07-0158 rock glacier system in RGI

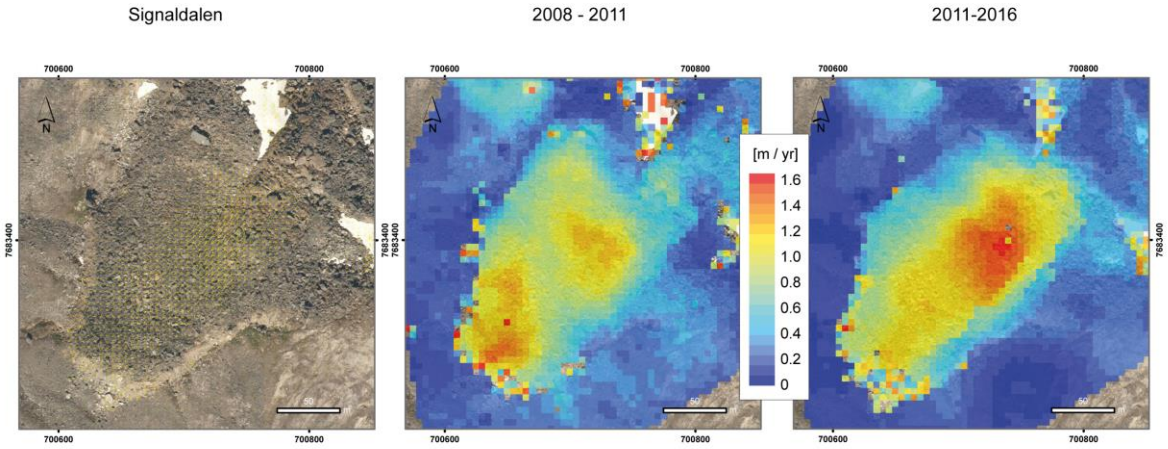

Pt5-Troms-Signaldalen, 69°11'09"N / 20°03'58"E, horizontal velocity maps from feature tracking on repeat optical airphotos for 2008-2011 (middle) and 2011-2016 (right). Rock glacier inventory number CCI-07-0316. Maximum speeds are 1.6 m/yr over 17.8.2011-18.8.2016, average speeds around 1 m/yr. Speeds 14.9.2008 – 17.8.2011 are on average slightly lower (90%) than the 2011-2016 ones. A more distinct increase in speeds by 30% is observed in fastest-flowing middle section of the rock glacier.

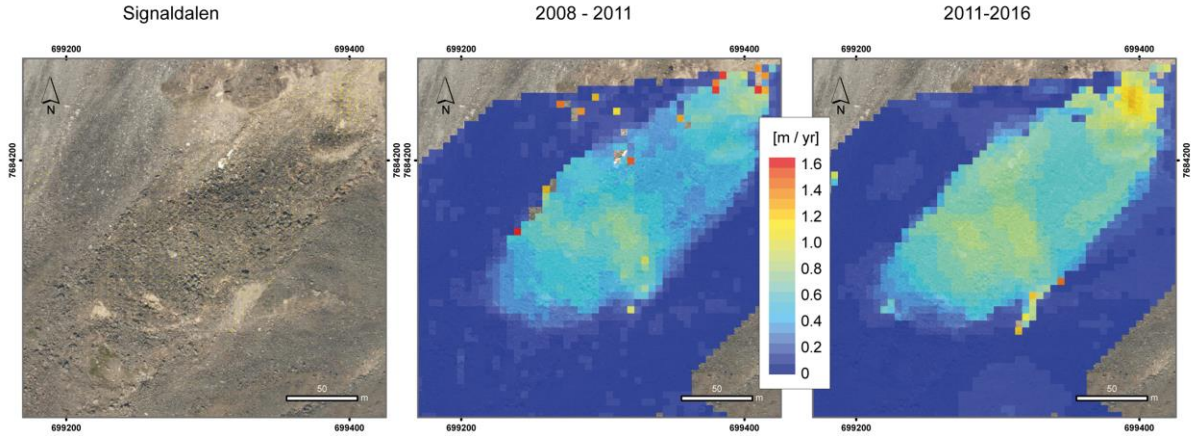

Pt6-Troms-Signaldalen, 69°11'36"N / 20°01'55"E, horizontal velocity maps from feature tracking on repeat optical airphotos for 2008-2011 (middle) and 2011-2016 (right). Rock glacier inventory number CCI-07-0330. Maximum speeds are up to 1.2 m/yr in the uppermost part, average speeds around 0.65 m/yr. Speeds for 2011-2016 are on average 27% faster than for 2008-2011.

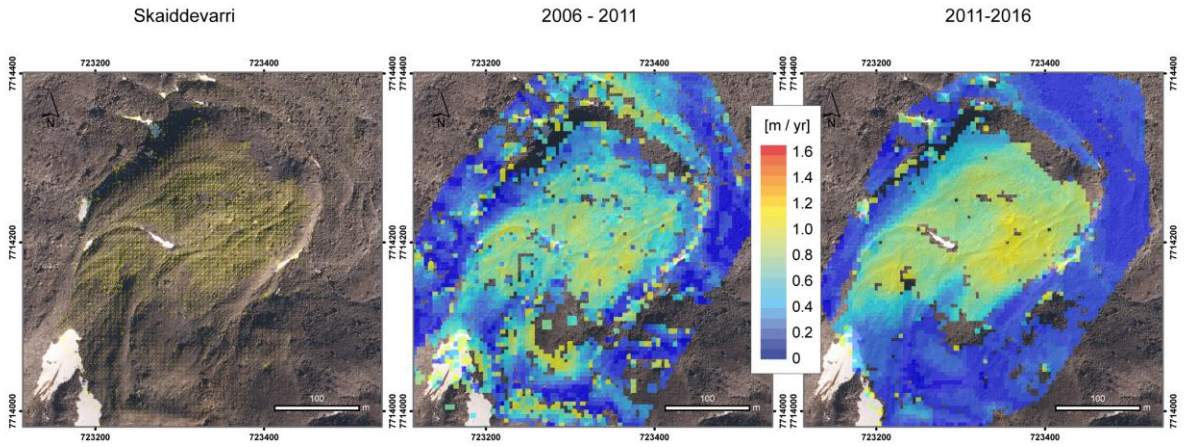

Pt7-Troms-Skaiddevarri, 69°26'36"N / 20°42'25"E, horizontal velocity maps from feature tracking on repeat optical airphotos for 2008-2011 (middle) and 2011-2016 (right). Rock glacier inventory number CCI-07-0172. Maximum speeds are around 1 m/yr, average speeds around 0.75 m/yr. 2011-2016 speeds are around 25% faster than 2006-2011 speeds.

08-Finnmark

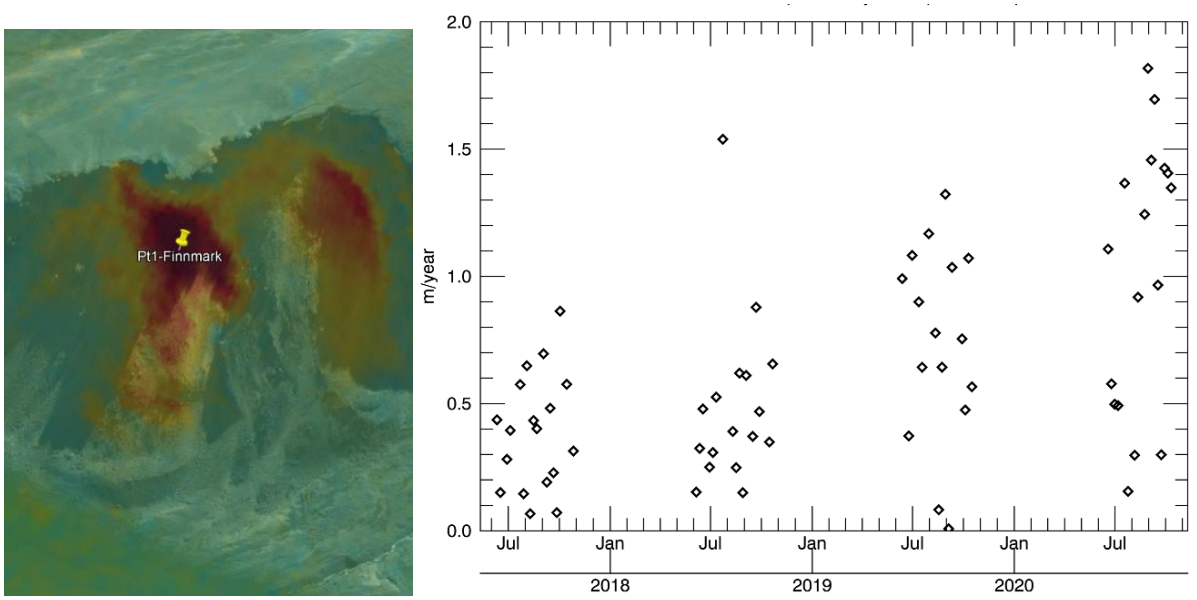

Pt1-Finnmark-Govdaluovttcohkka. Left: average of 6 days interferograms along LOS. Right: 6 days InSAR time series projected along the local slope (angle: 30.9°, aspect: 347.0). Point location: 70°36’54.65’’N 28°11’51.04’’E / CCI-08-0019 rock glacier system in RGI

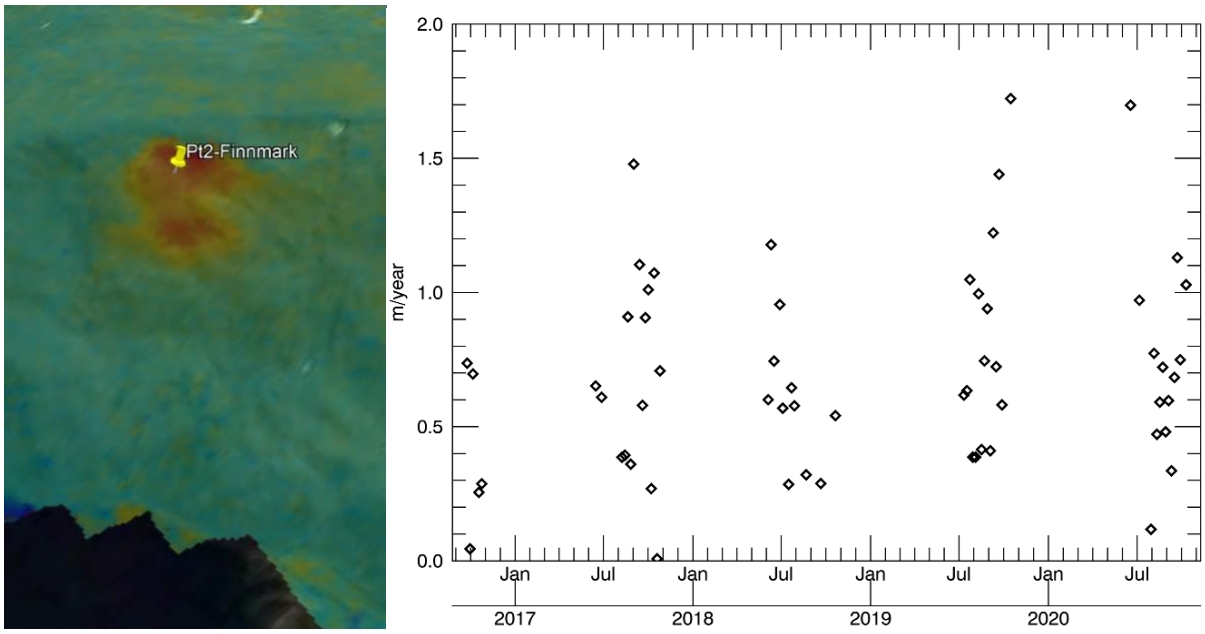

Pt2-Finnmark-LilleSkogfjorden. Left: average of 6 days interferograms along LOS. Right: 6 days InSAR time series projected along the local slope (angle: 26.5°, aspect: 295.1). Point location: 70°44’19.32’’N 28°01’11.93’’E / CCI-08-0001 rock glacier system in RGI

09-Svalbard

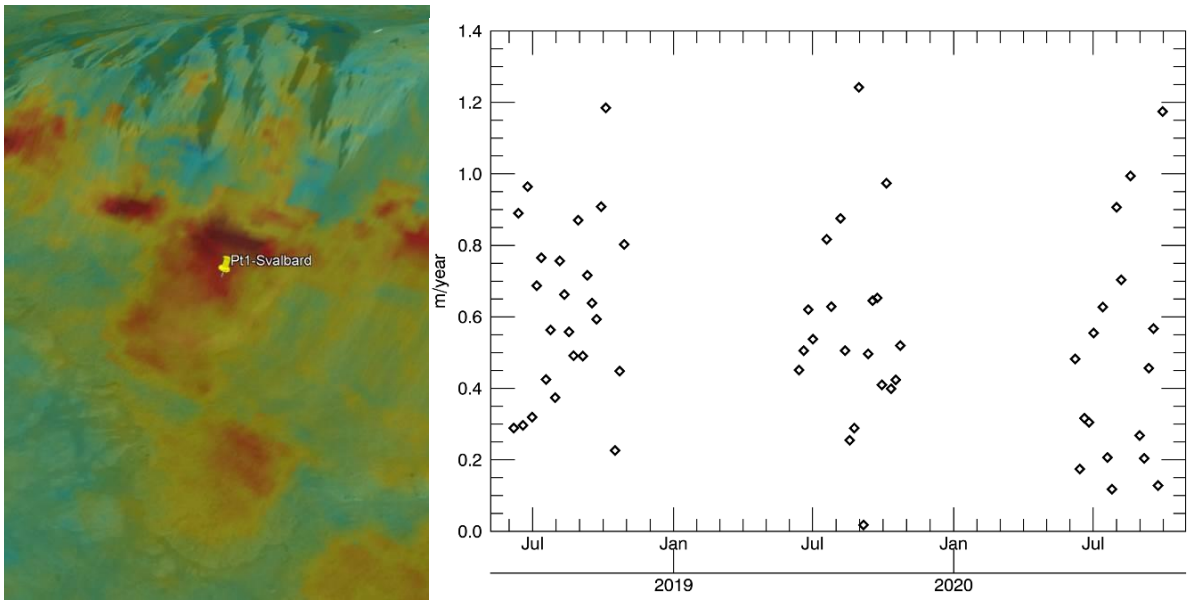

Pt1-Svalbard-KappLinné. Left: average of 6 days interferograms along LOS. Right: 6 days InSAR time series projected along the local slope (angle: 33.3°, aspect: 274.0). Point location: 78°02’46.07’’N 13°43’55.52’’E / CCI-09-0107 rock glacier system in RGI

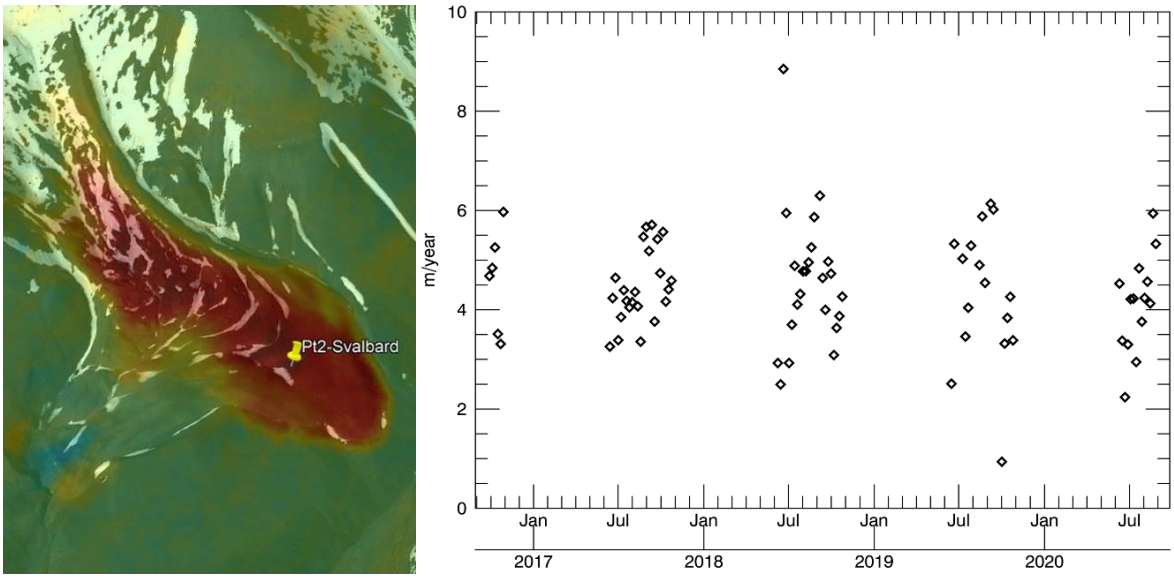

Pt2-Svalbard-Høgsnyta. Left: average of 6 days interferograms along LOS. Right: 6 days InSAR time series projected along the local slope (angle: 20.3°, aspect: 100.5). Point location: 78°57’47.63’’N 15°36’20.95’’E / CCI-09-0010 rock glacier system in RGI

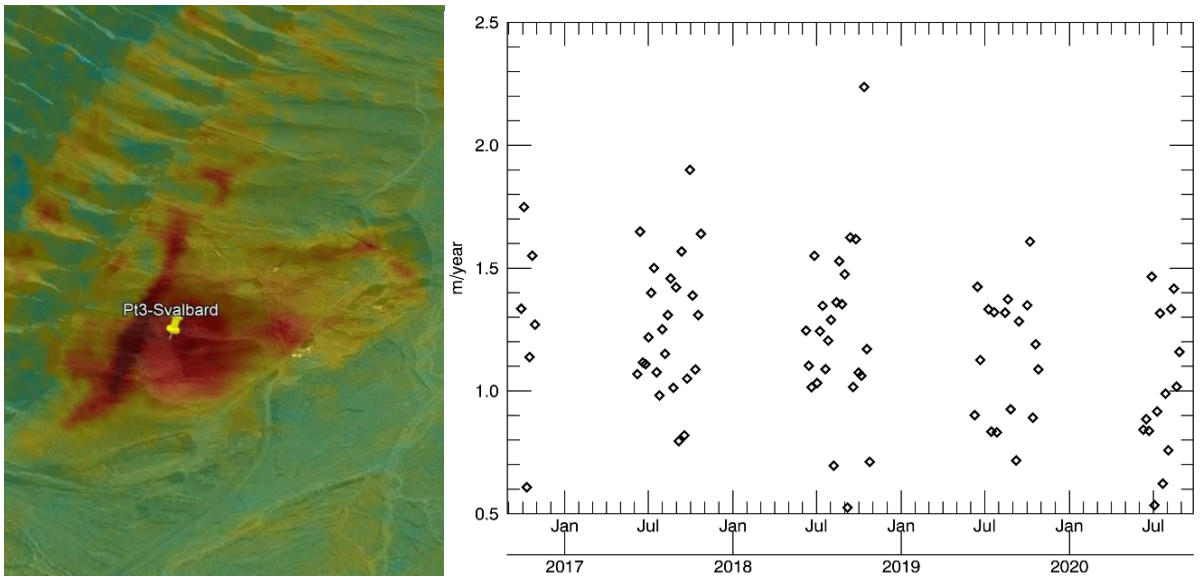

Pt3-Svalbard-Longyeardalen. Left: average of 6 days interferograms along LOS. Right: 6 days InSAR time series projected along the local slope (angle: 22.4°, aspect: 107.3). Point location: 78°12’09.65’’N 15°34’12.11’’E / CCI-09-0004 rock glacier system in RGI

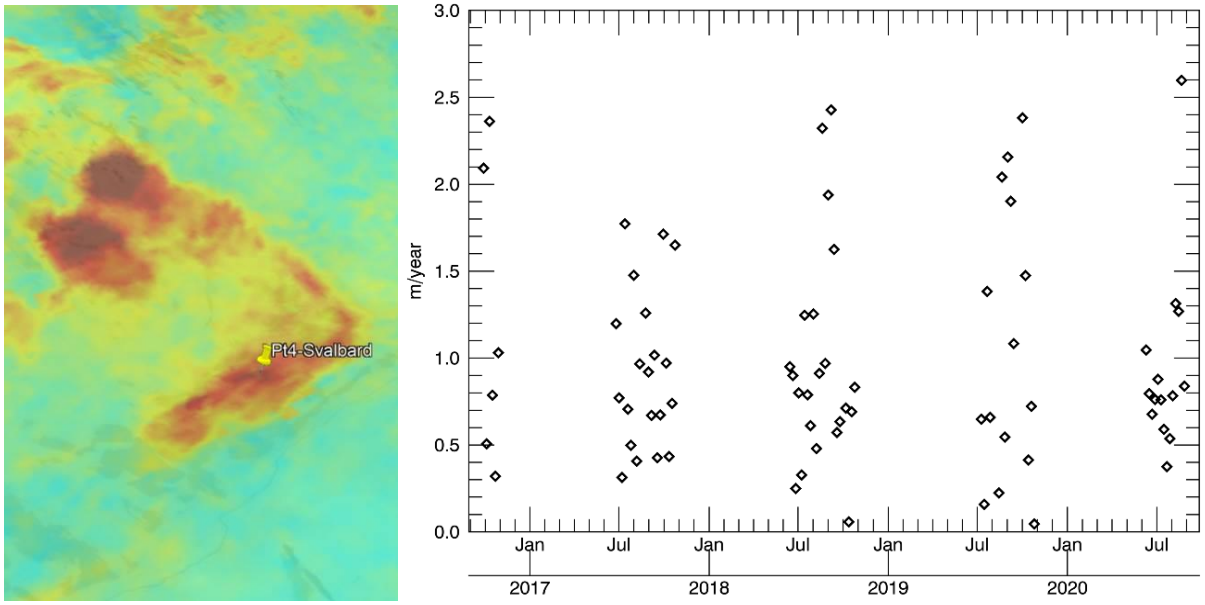

Pt4-Svalbard-Bolterdalen. Left: average of 6 days interferograms along LOS. Right: 6 days InSAR time series projected along the local slope (angle: 30.9°, aspect: 74.4). Point location: 78°08’02.44’’N 15°59’22.2’’E / CCI-09-0166 rock glacier system in RGI

12-Disko Island

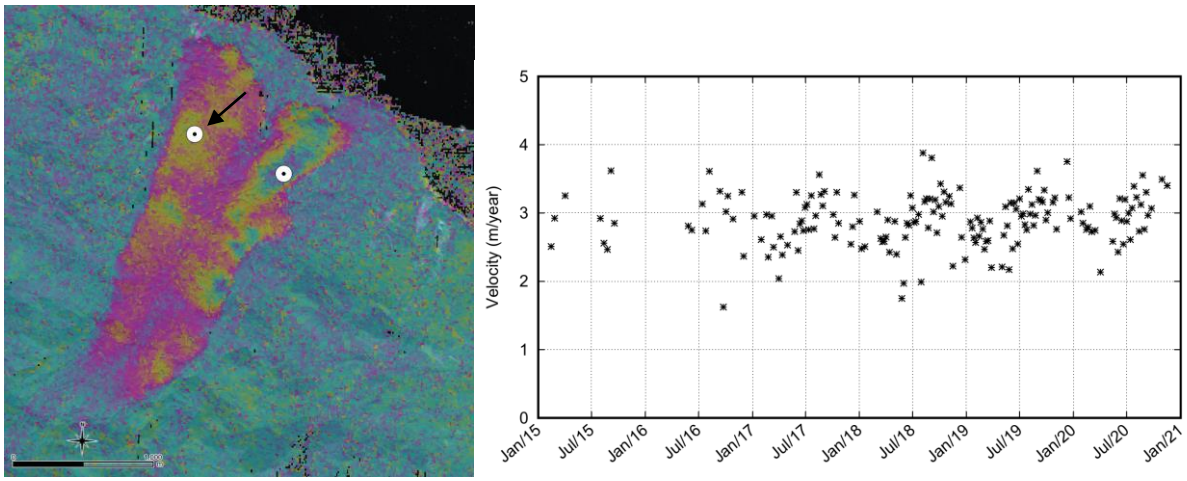

Pt1-Disko Island-A Differential Sentinel-1 interferogram (left) and velocity projected along slope (right) for the left point (in the interferogram) at UTM zone 22 coordinate 438084.907 E / 7754554.148 N (http://www.google.com/maps/place/69.89116,-52.61378)

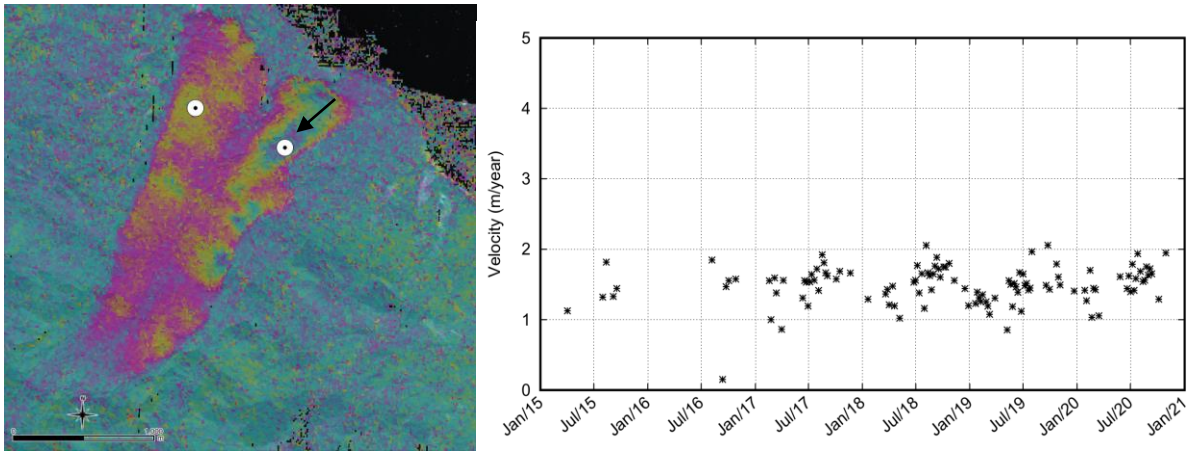

Pt2-Disko Island-B Differential Sentinel-1 interferogram (left) and velocity projected along slope (right) for the right point (in the interferogram) at UTM zone 22 coordinate 438720.105 E / 7754272.032 N (http://www.google.com/maps/place/69.88878,-52.59704)

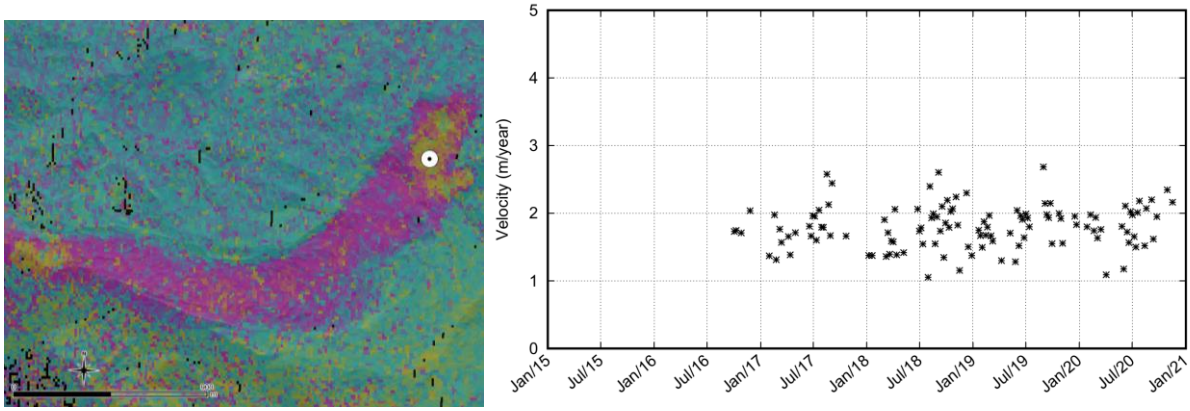

Pt3-Disko Island-C Differential Sentinel-1 interferogram (left) and velocity projected along slope (right) at UTM zone 22 coordinate 440559.595 E / 7751197.532 N (http://www.google.com/maps/place/69.86164,-52.54710)

3.3 Trends in rock glaciers velocity in Southern Carpathians (Romania)

Sentinel-1 data was downloaded from both Track 29 ASC and Track 80 DSC. For each track, around 240 acquisition dates were available, with around 430 SLC files downloaded from each track. The area of interest is located at the edge of the SLC scenes. The edge of the scenes tends to shift, thus approximately two scenes per acquisition dates were downloaded to ensure that the area of interest will be contained, regardless of the shift.

Size of the downloaded data was around 3.6 Tb (both tracks). A single burst was extracted from each Track. Track 29 ASC was abandoned because of a slightly disadvantageous illumination geometry.

115 dates (May to October, 2015-2019) from Track 80 DSC were retained.

261 interferometric combinations were formed (max. perpendicular baseline of 10 [m] and minimum temporal separation of 30 [days]).

56 low atmosphere interferograms were selected for multi-baseline analysis and displacement profiles extraction.

The result of the interferometric stacking using the low atmosphere interferograms is illustrated for Retezat mountains in Figure 3.3.1 in displacement units, in radar slant-range direction. Figure 3.3.2 illustrates a displacement profile between the 7th of July 2016 and the 29th of July 2019 relative to a stable area in the vicinity of the displacement (the closer the stable reference area, the less atmospheric disturbance is present in the measurements).

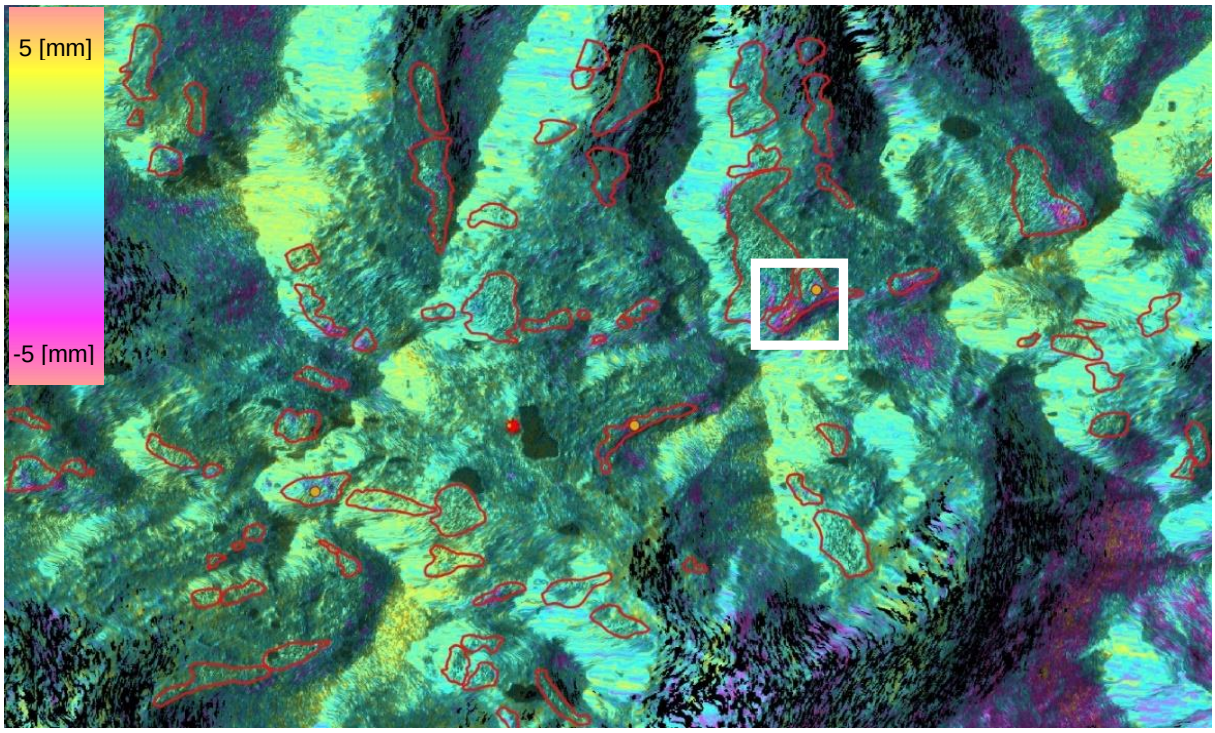

Figure 3.3.1 Displacement rate map in Retezat mountains, Romania. Source: Sentinel-1

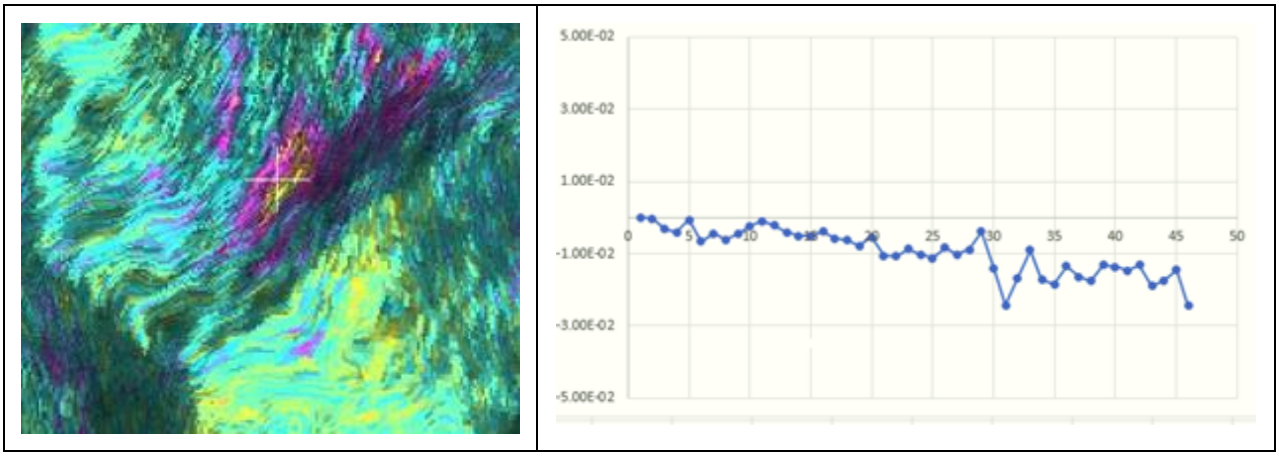

Figure 3.3.2. Example of a temporal displacement profile, Retezat mountains, Romania. Source: Sentinel-1 (on the X axis the time between the 7th of July 2016 and the 29th of July 2019, on the Y axis the displacement in mm).

3.4 Data availability and release

RGK examples currently consists in a couple of sites per study area (05-Romanian Carpathians, 06-Swiss Alps, 07-Troms, Norway, 08-Finnmark, Norway, 09-Nordenskiöld Land, Svalbard, 12-Disko Island, Greenland). The number of documented rock glaciers is meant to increase in the future. Because the current processing chain still requires to be refined, RGK examples are only recorded in this document but not yet made available through an open data portal.

4 Mountain Permafrost Distribution Model in the Carpathians

4.1 Introduction

The Permafrost_cci project is focused on the product ground temperature and relevant derivatives (active layer thickness and permafrost zones). This implies the production of consistent, stable, and error-characterised products, covering the period with available EO data from 1981 to date. Algorithms have been identified which can provide these parameters ingesting a set of global satellite data products (Land Surface Temperature LST, Snow Water Equivalent SWE, and landcover) in a permafrost model scheme that computes the ground thermal regime [RD-4].

The Southern Carpathians in Romania are located in a marginal periglacial mountain environment, where the permafrost occurrence is patchy and the preservation of permafrost is controlled by site-specific conditions. Specific user requirements for the case study that includes mountain permafrost in Southern Carpathians for ground temperature and active layer thickness have been compiled in [RD-16]. They demand a regional geographical coverage (regional permafrost extent Southern Carpathians, 14000 km²), high temporal resolution (monthly data), high spatial resolution (target resolution 0.1 km) including representation of sub-grid variability, and long temporal coverage (one to several decades back in time). These requirements go considerably beyond the state-of-the-art in remote permafrost ECV assessment, based on published studies and recently demonstrated progress [RD-4].

For the specific mountain permafrost sites located in the Southern Carpathians other permafrost products were thus determined and specified in [RD-16]: (i) permafrost distribution model, (ii) trends in velocity of selected rock glaciers, and (iii) rock glaciers inventory. Algorithms to create permafrost distribution models and to derive trends in velocity of selected rock glaciers are part of the processing system implemented in CCN1. Algorithms to compile rock glacier inventories, on the other hand, were not considered, because the aim of the work specified for CCN 1 was only to enrich an existing rock glacier inventory consisting of 306 landforms (Onaca et al., 2017) with information about the activity status of rock glaciers and the permafrost occurrence. The Climate Research Data Package of CCN1 comprises therefore a permafrost distribution model at regional scale using a random forest algorithm and trends in rock glaciers velocity from ALOS-2 PALSAR-2 and Sentinel-1 SAR interferometry (see Section 3.4).

4.2 Permafrost distribution model at regional scale

Permafrost in the Southern Carpathians is patchy, being able to exist only under certain topographical conditions. The mountain permafrost distribution model shows that permafrost has an extent of, most likely, 3km^2 (possibly between 0.1 km^2 to 7.74 km^2). The model shows that most areas with a high probability of permafrost occurrence are located in the highest mountain's groups (Retezat, Parâng, Făgăraș and Bucegi). Also, small patches of permafrost are predicted to exist in Iezer, Țarcu and Godeanu Mountains.

The central part of Retezat Mountains is a representative area for the permafrost distribution in the South Carpathians and this is also the most studied area regarding mountain permafrost in the Romanian Carpathians. The permafrost patches are found on glacial cirques with steep walls and

mostly northern exposition where shading is pronounced. There is a good correlation between the permafrost occurrence and rock glacier existence (Figure 4.2.1), with the exception of the Bucegi Mountains where there are no rock glaciers mapped.

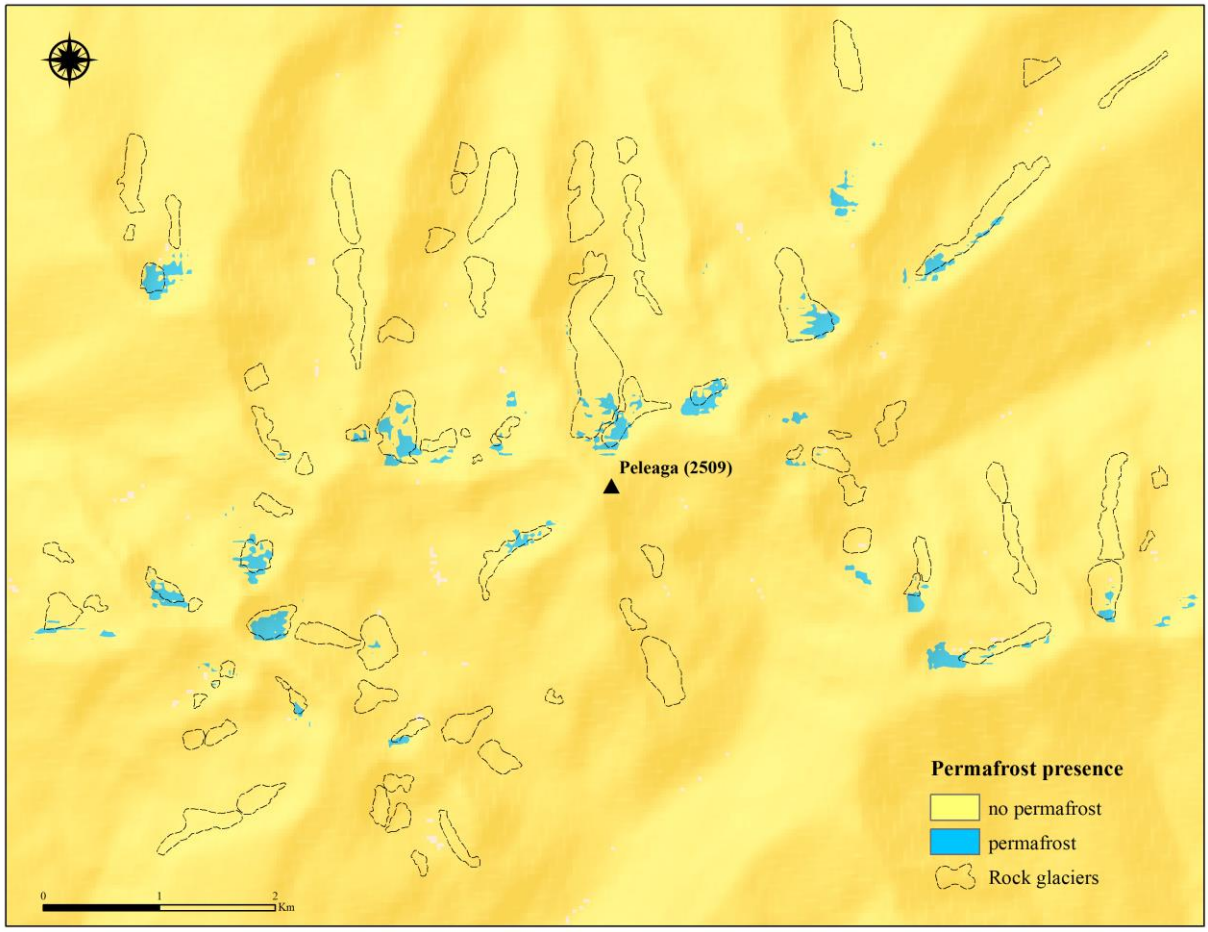

Figure 4.2.1 Permafrost possible distribution in Retezat mountains, Romania.

4.3 Data availability and release

The permafrost distribution map for the Southern Carpathians, together with the training and validation data used for modelling, will be made available for download by WUT through the Department of Geography and the ESA Open Data Portal at http://cci.esa.int/data. The R script that was used for creating the model will also be made available for download. The Permafrost distribution model for the Southern Carpathians and its impact on the use of machine learning for regional permafrost mapping, local geomorphologic importance and scientific relevance in the context of climate research are the main issues that will be addressed in a peer review paper that will be published in the framework of the project, covering current findings.

5 References

5.1 Bibliography

Ardelean, A.C., Onaca, A.L., Urdea, P., Șerban, R.D., Sîrbu, F., 2015. A first estimate of permafrost distribution from BTS measurements in the Romanian Carpathians (Retezat Mountains). Géomorphologie: relief, processus, environnement, 2, 4, 297–312.

Bartsch, A., Grosse, G., Kääb, A., Westermann, S., Strozzi, T., Wiesmann, A., Duguay, C., Seifert, F. M., Obu, J., Goler, R., GlobPermafrost – How space-based earth observation supports understanding of permafrost. Proc. 'Living Planet Symposium 2016', Prague, Czech Republic, 9–13 May 2016 (ESA SP-7 40, August 2016), pp. 6.

Boeckli, L., Brenning, A., Gruber, S., Noetzli, J., 2012. A statistical approach to modelling permafrost distribution in the European Alps or similar mountain ranges. Cryosphere 6 (1), 125–140.

Bodin X, Trombotto Liaudat and Soruco A (2015) Evaluation of a terrestrial photogrammetry method for the study of high mountain dynamics. Quebrada del Medio rock glacier, Mendoza, Argentina. Geomorphometry for Geosciences. Bogucki Wydawnictwo Naukowe, Adam Mickiewicz University in Poznań - Institute of Geoecology and Geoinformation, Poznań, Poland, 189–192

Bolch, T., Gorbunov, A.P. (2014): Characteristics and origin of the rock glaciers in northern Tien Shan (Kazakhstan/Kyrgyzstan). Permafrost and Periglacial Processes 25(4): 320-332. doi: 10.1002/ppp.1825.

Christiansen, H.H, Etzelmüller, B., Isaksen, K., Juliussen, H., Farbrot, H., Humlum, O., Johansson, M., Ingeman-Nielsen, T., Kristensen, L., Hjort, J, Holmlund, P., Sannel, A.B.K., Sigsgaard, C., Åkerman, H.J., Foged, N., Blikra, L.H., Pernosky, M.A. and Ødegård, R., 2010. The Thermal State of Permafrost in the Nordic area during the International Polar Year 2007-2009. Permafrost and Periglacial Processes, 21, 156–181.

Delaloye, R., Lambiel, C. and Gärtner-Roer, I., 2010. Overview of rock glacier kinematics research in the Swiss Alps: seasonal rhythm, interannual variations and trends over several decades. Geographica Helvetica, 65(2), 135–145.

Eriksen, H.Ø., Rouyet, L., Lauknes, T.R., Berthling, I., Isaksen, K., Hindberg, H., Larsen, Y. and Corner, G.D., 2018. Recent acceleration of a rock glacier complex, Ádjet, Norway, documented by 62 years of remote sensing observations. Geophysical Research Letters, 45(16), pp.8314–8323.

Gardent, M., Rabatel, A., Dedieu, J.-P., Deline, P., 2014. Multitemporal glacier inventory of the French Alps from the late 1960s to the late 2000s. Global and Planetary Change 120, 24–37. https://doi.org/10.1016/j.gloplacha.2014.05.004

Ianigla and Mayds (2018) Resumen ejecutivo de los resultados del Inventario Nacional de Glaciares. IANIGLA-CONICET, Mendoza

Ikeda, A., Matsuoka, N. and Kääb, A, 2008. Fast deformation of perennially frozen debris in a warm rock glacier in the Swiss Alps: An effect of liquid water. J. Geophys. Res.-Earth, 113(F1), https://doi.org/10.1029/2007JF000859.

Kääb, A., Strozzi, T., Bolch, T., Caduff, R., Trefall, H., Stoffel, M., & Kokarev, A. (2020). Inventory, motion and acceleration of rock glaciers in Ile Alatau and Kungöy Ala-Too, northern Tien Shan, since the 1950s. The Cryosphere Discussions, 1-37. doi: 10.5194/tc-2020-109

Kääb, A. and Vollmer M., 2000. Surface geometry, thickness changes and flow fields on creeping mountain permafrost: automatic extraction by digital image analysis.
Permafrost and Periglacial Processes,11, 315–326

Kääb, A., Isaksen, K., Eiken T. and Farbrot. H., 2002. Geometry and dynamics of two lobe-shaped rock glaciers in the permafrost of Svalbard. Norwegian Journal of Geography, 56, 152-160

Kääb, A., Frauenfelder, R. and Roer, I, 2007. On the response of rockglacier creep to surface temperature increase. Global Planet. Change, 56(1-2), 172–187, https://doi.org/10.1016/j.gloplacha.2006.07.005.

Lilleøren, K. S. and Etzelmüller, B. 2011. A regional inventory of rock glaciers and ice-cored moraines in Norway. Geografiska Annaler: Series A, Physical Geography, 93(3), 175–191. https://doi.org/10.1111/j.1468-0459.2011.00430.x

Marcer, M., Bodin, X., Brenning, A., Schoeneich, P., Charvet, R., Gottardi, F., 2017. Permafrost Favorability Index: Spatial Modeling in the French Alps Using a Rock Glacier Inventory. Frontiers in Earth Science 5. https://doi.org/10.3389/feart.2017.00105

Marcer, M., Serrano, C., Brenning, A., Bodin, X., Goetz, J., Schoeneich, P., 2019. Evaluating the destabilization susceptibility of active rock glaciers in the French Alps. The Cryosphere 13, 141–155. https://doi.org/10.5194/tc- 13-141-2019

Monnier, S., 2004. Identification, caractérisation et distribution spatiale des glaciers-rocheux dans la haute vallée de l'Arc (Alpes françaises du Nord)/Identification, characterisation and spatial distribution of rockglaciers in the upper Arc Valley (northern French Alps). Géomorphologie: relief, processus, environnement 10, 139–155.

Onaca, A., Ardelean, F., Urdea, P., Magori, B., 2017. Southern Carpathian rock glaciers: inventory, distribution and environmental controlling factors, Geomorphology. 293, 391–404.

Onaca, A., Ardelean, A. C., Urdea, P., Ardelean, F., Sîrbu, F., 2015, Detection of mountain permafrost by combining conventional geophysical methods and thermal monitoring in the Retezat Mountains, Romania, Cold Regions Science and Technology, 119, 111–123

Onaca, A., Urdea, P., Ardelean, A., Şerban, R., 2013, Assessement of internal structure of periglacial landforms from Southern Carpathians (Romania) using dc resistivity tomography, Carpathian Journal of Earth and Environmental Sciences, 8 (2), 113–122.

Roer, I., Haeberli, W., Avian, M., Kaufmann, V., Delaloye, R., Lambiel, C. and Kääb, A., 2008. Observations and considerations on destabilizing active rock glaciers in the European Alps. In: Proceedings of the 9th International Conference on Permafrost, Fairbanks, Alaska, 29 June 2008 – 3 July 2008, 1505–1510.

Roudnitska, S., Charvet, R., Ribeyre, C., Leprince-Favereaux, B., 2017. Les glaciers rocheux de Savoie : Inventaire, cartographie et risques associés (Service RTM 73). RTM - ONF, Chambéry.

Ruiz L and Trombotto Liaudat D (2012) Glaciares de escombros fósiles en el cordón Leleque, Noroeste del Chubut: significado paleoclimático y paleográfico. Rev. Asoc. Geológica Argent. 69(3), 418–435

Sattler, K., Anderson, B., Mackintosh, A., Norton, K., de Róiste, M., 2016. Estimating permafrost distribution in the maritime Southern Alps, New Zealand, based on climatic conditions at rock glacier sites. Front. Earth Sci. 4, 4.

Strozzi, T., Caduff, R., Jones, N., Barboux, C., Delaloye, R., Bodin, X., Kääb, A., Mätzler, E. and Schrott, L, 2020. Monitoring Rock Glacier Kinematics with Satellite Synthetic Aperture Radar. Remote Sensing, 12(3), 559, https://doi.org/10.3390/rs12030559.

Trombotto D (2014) nvironmental Status of the Cryogenic Permafrost Conditions in the Last Decade in the Central Andes, One Example: Morenas Coloradas Rockglacier, Mendoza, Argentina. Global chryospheric watch (GCW). Santiago de Chile, 27–29

Trombotto D and Borzotta E (2009) Indicators of present global warming through changes in active layer-thickness, estimation of thermal diffusivity and geomorphological observations in the Morenas Coloradas rockglacier, Central Andes of Mendoza, Argentina. (doi:10.1016/j.coldregions.2008.08.009)

Trombotto Liaudat D (2000) Survey of cryogenic processes, periglacial forms and permafrost conditions in South America. Rev. Inst. Geológico 21(1–2), 33–55 (doi:10.5935/0100-929X.20000004)

Trombotto-Liaudat D and Bottegal E (2019) Recent evolution of the active layer in the Morenas Coloradas rock glacier, Central Andes, Mendoza, Argentina and its relation with kinematics. Cuad. Investig. Geográfica (doi:10.18172/cig.3946)

Westermann, S., Schuler, T.V., Gisnas, K., Etzelmuller, B., 2013. Transient thermal modeling of permafrost conditions in Southern Norway. Cryosphere, 7(2), 719-739.

Zalazar L, Ferri L, Castro M, Gargantini H, Gimenez M, Pitte P, Ruiz L, Masiokas M, Costa G and Villalba R (2020) Spatial distribution and characteristics of Andean ice masses in Argentina: results from the first National Glacier Inventory. J. Glaciol., 1–12 (doi:10.1017/jog.2020.55)

5.2 Acronyms

AD	Applicable Document
ADP	Algorithm Development Plan
ASC	Ascending geometry
ATBD	Algorithm Theoretical Basis Document
AWS	Automatic Weather Station
B.GEOS	b.geos GmbH
BTS	Bottom Temperature of Snow Cover
CCI	Climate Change Initiative
CCN	Contract Change Notice
CR	Cardinal Requirement (as defined in [AD-1])
CRS	Coordinate Reference System
DARD	Data Access Requirement Document
DEM	Digital Elevation Model
DSC	Descending geometry
ECV	Essential Climate Variable
ELA	Equilibrium Line Altitude
EO	Earth Observation
ERT	Electrical Resistivity Tomography
ESA	European Space Agency
ESA DUE	ESA Data User Element
E3UB	End-to-End ECV Uncertainty Budget
GAMMA	Gamma Remote Sensing AG
GCOS	Global Climate Observing System
GNSS	Global Navigation Satellite System
GTOS	Global Terrestrial Observing System
GUIO	Department of Geosciences University of Oslo
INSAR	Synthetic Aperture Radar Interferometry
IPA	International Permafrost Association
IPCC	Intergovernmental Panel on Climate Change
L4	Level 4
LST	Land Surface Temperature
MPDM	Mountain Permafrost Distribution Model

NORCE	Norwegian Research Centre AS
NSIDC	National Snow and Ice Data Center
PE	Permafrost Extent
PS	Processing System
PSD	Product Specifications Document
PVASR	Product Validation and Algorithm Selection Report
PUG	Product User Guide
PVP	Product Validation Plan
QA4EO	Quality assurance framework for earth observation
RF	Random Forest
RD	Reference Document
RGI	Rock Glacier Inventories
RGK	Rock Glacier Kinematic Time Series
RS	Remote Sensing
SAR	Synthetic Aperture Radar
SWE	Snow Water Equivalent
T	Temperature
UNIFR	Department of Geosciences University of Fribourg
UNIS	University Centre in Svalbard
URD	Users Requirement Document
UTM	Universal Transverse Mercator
WGS	World Geodetic System
WUT	West University of Timisoara